UNIVERSITY OF CALIFORNIA - LOS ANGELES

Dynamics of Flexible Gravity-Gradient Satellites

A dissertation submitted in partial satisfaction of the requirements for the degree Doctor of Philosophy in Engineering

by

Gordon Stamm Reiter

Final Examination for the Degree Doctor of Philosophy

Tuesday, May 25, 1965, 1:30 P.M.

Room 6730, Engineering III

Committee in charge:

Professor William T. Thomson, Chairman

Professor Edwin F. Beckenbach

Professor Edgar A. Kraut

Professor Robert E. Roberson

Professor Nicholas Rott

1965

The dissertation of Gordon Stamm Reiter is approved and it is acceptable in quality and form for publication on microfilm:

Edgar A. Kraut

Robert E. Robinson

E. F. Beckenbach

Nicholas Rott

William J. Thomson

Committee Chairman

University of California, Los Angeles

1965

CONTENTS

ACKNOWLEDGMENTS

I express my profound gratitude for indispensable guidance and encouragement during a very rewarding association of more than five years to my Chairman, and advisor, Professor William T. Thomson.

My work on this dissertation has been aided greatly by the publications and advice of Professors Thomas R. Kane of Stanford University and Robert E. Roberson of the University of California, Los Angeles.

I am grateful to TRW Space Technology Laboratories both for financial support and for providing a creative atmosphere.

I appreciate the financial support of the National Aeronautics and Space Administration, under Grant NSG237-62, covering the writing of this dissertation.

VITA

February 15, 1935 - Born - Albuquerque, New Mexico

1956 - B.S., California Institute of Technology

1956-1965 - Member of the Technical Staff, TRW Space Technology Laboratories, Redondo Beach, California

1960 - M.S., University of California, Los Angeles

1961, 1964-1965 - Graduate Research Engineer, University of California, Los Angeles

1961-1963 - Space Technology Laboratories Cooperative Fellow, University of California, Los Angeles

PUBLICATIONS

"Design of a Spin-Stabilization System for the Able Space Probes." Transactions - Fourth AFBMD/STL Symposium on Ballistic Missiles and Space Technology, Los Angeles, 1959 (with W. F. Sheehan).

"Attitude Drift of Space Vehicles." Journal of the Astronautical Sciences, vol. 7, No. 2, pp. 29-34, 1960 (with W. T. Thomson).

"Testing in a Zero-G Environment." Journal of the Environmental Sciences, vol. 4, No. 2, pp. 6-8, March-April, 1961 (with D. A. Lee).

"Motion of an Asymmetric Spinning Body with Internal Dissipation." A. I. A. A. Journal, vol. 1, No. 6, pp. 1429-1430, June, 1963 (with W. T. Thomson).

"Rotational Motion of Passive Space Vehicles." Torques and Attitude Sensing in Earth Satellites, Academic Press, New York, 1964 (with W. T. Thomson).

"Zero Gravity Stability Testing of a Liquid Filled Space Vehicle." A. I. Ch. E. Symposium on Zero-Gravity, Houston, Texas, March, 1965 (with D. A. Lee).

"Jet Damping of a Solid Rocket: Theory and Flight Results." A. I. A. A. Journal, vol. 3, No. 3, pp. 413-417, March, 1965 (with W. T. Thomson).

"Magnetic Hysteresis Damping for Gravity-Gradient Stabilization." N. A. S. A. Symposium on Passive Gravity-Gradient Stabilization, N. A. S. A. - Ames Research Center, Moffett Field, California, May, 1965 (with J. P. O'Neill and J. R. Alper).

FIELDS OF STUDY

Major Field: Engineering

Studies in Dynamics. Professors William T. Thomson and Walter C. Hurty

Studies in Fluid Mechanics. Professors Nicholas Rott and Alan Powell

Studies in Applied Mathematics. Professors John W. Miles and Kurt Forster

ABSTRACT OF THE DISSERTATION

Dynamics of Flexible Gravity-Gradient Satellites
by

Gordon Stamm Reiter
Doctor of Philosophy in Engineering

University of California, Los Angeles, 1965

Professor William T. Thomson, Chairman

Three specific problems relating to flexible gravity gradient satellites in circular orbit are examined:

A. The stability of infinitesimal and noninfinitesimal amplitude angular motions for a class of flexible satellites

B. Static behavior of long wires and rods attached to satellites

C. Pitch libration of a wire satellite.

In the first problem, the linearized stability analysis of Debra and Delp for rigid satellites is extended to a class of flexible satellites. The class of satellites studied is selected for easy comparison of rigid and flexible satellite behavior over a wide range of inertia ratios. It is found that a significant range of inertia configurations which is stable for a rigid body is unstable for a flexible body with damping.

The problem of whether planar librations in the orbit plane are stable for finite amplitudes of motion, studied by Kane for the rigid satellite, is examined for a class of flexible satellites. It is found that the inertia configurations for which finite, purely planar pitch motion is unstable, found by Kane for the rigid satellite, have

counterparts in the case of a flexible satellite. The unstable inertia configurations are located through a perturbation solution of the equations of motion. Numerical studies show that addition of damping does not always remove the instability, even for very flexible satellites and small (one degree) libration amplitudes. The phenomenon found by Kane is therefore a physically realistic one and shows that linear analysis is not adequate for all cases.

In the second problem, the static behavior of flexible satellite appendages is examined on a preliminary basis. It is found that large-deflection beam theory is required if satellite appendages are sufficiently long. The nonlinear deflection of a cantilever appendage is computed for various tip masses. An analogy between the forced vibration of a beam and its static deflection under differential gravity is pointed out and discussed.

In the third problem, the planar pitching motion of a passive reflector satellite in the shape of a long wire is examined. It is found that elastic and rigid-body motion are not coupled in the linearized equations of motion. Libration damping through parametric excitation of damped elastic motion appears feasible if the wire is sufficiently long.

Chapter 1. Introduction

Gravity-gradient stabilization is the technique of using the earth's gravitational field to produce restoring moments on a satellite and give the satellite a preferred orientation. A gravity-stabilized satellite has a nominally vertical orientation, which is very desirable for such missions as communications, surveillance and weather observation. A vertically-oriented communications satellite has several times the channel capacity of a spin-stabilized satellite for the same radiated power.

Feasibility of the gravity-gradient concept has been established by several flight tests (References 1.1 and 1.2). Many more flights will take place in the next few years. The gravity-gradient effect has been studied for many years in connection with the known orientation of the moon. The first work on artificial gravity-gradient satellites, beginning about 1953, dealt principally with simple rigid-body satellites. The behavior of a rigid satellite in an inverse square force field is now fairly well understood.

Most realistic gravity-gradient satellites are structurally flexible. There are two reasons:

A. The gravity-gradient concept calls for very large moments of inertia. Large amounts of inertia are achieved by deploying space structures which are relatively flimsy by earth standards.

B. Significant flexibility is needed to provide damping. The earth's gravity field is conservative, providing a restoring moment, but no damping. Damping must be

incorporated in all practical satellite configurations, either by creating an interaction between the satellite and the earth's magnetic field (References 1.2 and 1.3) or by introducing energy dissipation in a flexible part of the satellite, a concept first suggested by Roberson and Breakwell in 1953 (Reference 1.4). Damping serves to remove energy associated with the angular motion of the satellite resulting from injection into orbit, limit steady-state oscillations produced by solar radiation pressure and other disturbance torques, and remove transients produced by disturbances, such as micrometeorite impacts.

The present discussion will exclude two important categories of gravity-gradient satellites: those which are actively damped by such means as gas jets or reaction wheels, and those which obtain damping through interaction with the earth's magnetic field.

The study of a flexible gravity-gradient satellite having given geometry, but varying inertia parameters, is a relatively complex task. A rigid body is completely characterized by three principal moments of inertia or two dimensionless inertia ratios. To describe a flexible body, one must specify not only the inertia distribution, but also the distribution of stiffness and damping within the satellite.

As shown in Chapter 3, the small motions of a rigid body about its equilibrium (vertical) orientation are described by a second-order equation and a set of two coupled second-order equations, constituting a fourth-order system. Introduction of even one flexible-body degree

of freedom in a realistic way will raise the order of the system to sixth-order, with resultant increase in complexity.

Typical current papers in the field (References 1.5 and 1.6) concern the optimization of a particular satellite configuration (preselected hinge location, planes of symmetry, etc.) by variations of the moments of inertia and hinge spring torque.

There is much work still to be done in the area. For example, the question of what is the best gravity-gradient satellite which is in the form of two rigid bodies connected by a single spring and dashpot has still not been completely resolved.

The present dissertation, then, is in a broad field in which very incomplete knowledge exists. The approach taken can be characterized by the principles:

- If general problems are too complex, try special cases and attempt inferences from them.
- Attempt extensions from topics which are better understood. Specifically, in the present case, try to see the ways a flexible body differs from a rigid body.

Three specific problems have been studied. They are described briefly and conclusions are summarized in the following section. Each problem is covered in depth in a succeeding chapter. They are connected only by being parts of the general subject area: flexible gravity-gradient satellites.

The chapters may be read independently of one another. The only convention employed is the usual one: that dots above symbols denote derivatives with respect to time.

Chapter 2. Problem Descriptions

2.1 Infinitesimal and Noninfinitesimal Amplitude Stability of a Class of Flexible Satellites (Chapter 3)

2.1.1 Problem Statement

This problem is the extension to a flexible satellite of two stability problems which have been studied for a rigid satellite in a circular orbit.

The equations of motion for a rigid satellite in a gravity field have been derived by many authors (Reference 3.2, for example). The basic equations are derived in Appendices A and B. Basically, they show that:

A. Small angular motion about an axis normal to the plane of the orbit is described by a single equation, uncoupled for small motions from the other degrees of freedom. The equations of so-called "pitch" motion is that of a simple pendulum. The body can therefore execute oscillations in pitch about the local vertical.

B. The other two degrees of freedom (roll and yaw), representing rotations about the tangent to the orbit and the vertical, respectively, are described for small angles by two coupled second-order equations forming a fourth-order system.

C. Certain inertia configurations are "stable" in the sense that the linearized equations of motion predict that small initial angular displacements do not grow indefinitely with time, but remain bounded.

The first part of this problem is the determination of the inertia configuration of a particular class of flexible bodies which result in stability in the sense of the linearized equations. The class of bodies considered is selected to allow ready comparison with rigid-body behavior.

A recent paper by Kane (Reference 3.4) has considered the combination of noninfinitesimal amplitude pitching motion and infinitesimal roll-yaw motion. By retaining the pitch angle as a large angle, he introduced additional terms in the roll-yaw equations. Numerical studies showed that the additional terms, for certain body inertia configurations, result in a roll-yaw motion which (in the linearized case) increases without bound. Thus, pure pitching motion cannot exist alone for these inertia configurations.

Since Kane found pure pitching motion to be unstable for pitch amplitudes as small as one degree, the important conclusion can be drawn that, for a rigid body, use of the linearized equations may give rise to incorrect results.

In the second part of this problem, Kane's technique is extended and used to treat the problem of stability of pure pitch motion for a flexible body which is similar to an unstable rigid body. Only by this method can it be determined whether the instability problem is practically realizable or whether it disappears when realistic flexibility and damping are introduced.

2.1.2 Conclusions

Infinitesimal-Amplitude Stability of Flexible Satellites

1. For the case where the flexible satellite has no integral damping, the stability behavior resembles that of a rigid satellite. The differences can, in general, be easily explained on a physical basis.
2. The introduction of damping causes a relatively large set of inertia configurations, stable for a rigid satellite, to become unstable.

The remaining category, stable satellites which derive damping from internal flexibility, is an important one because of the great advantages in simplicity and reliability.

Stability of Noninfinitesimal Pitching Motion

1. The inertia configurations found by Kane for which pure pitching motion is unstable can be located rather precisely by a perturbation solution of the equations of motion.
2. The technique of locating potentially unstable configurations can be extended to the case of a flexible satellite and used to limit the number of parameters which must be varied in a numerical study.
3. There is a class of undamped flexible satellites for which pure pitching motion is unstable, just as in the rigid-body case, even for pitch amplitudes of only one degree.
4. The introduction of damping into a flexible satellite for which pure pitch is unstable will remove the instability only if the satellite is very flexible. If the satellite's lowest elastic

natural frequency is even as high as the orbit frequency, some inertia configurations are still unstable in pitch. Thus, the phenomenon found by Kane is not automatically removed by introducing flexibility, but must be deliberately taken into account in design.

2.2 Static Behavior of Long Wires and Rods Attached to Vertically Stabilized Satellites (Chapter 4)

2.2.1 Problem Description

Current gravity-gradient satellites have large dimensions because the gravity-gradient moment depends on the moments of inertia of the body. There are other reasons for large satellite dimensions. The gravity-stabilized Radio Astronomy Explorer (Reference 4.3), scheduled for launch in 1967, is a giant antenna 1500 feet long (Figure 2.1).

Very large satellites need not be very strong structurally. The required strength of the structural members is determined by the technique used to deploy them from a folded position in the booster. Considering the booms of the Radio Astronomy Explorer to be cantilever beams, the static deflection under a 0.01 ounce load is several hundred feet.

The impending existence of very large, flexible satellites prompts the question: What are the in-orbit loads on the structural members of such a satellite, and what are the resulting deflections?

The problem is considered in this dissertation by examining the static behavior of a cantilever beam with tip mass, such as an inertia boom or antenna, which is extended from a rigid satellite in a circular orbit. The significant loads are produced by the orbital dynamics and

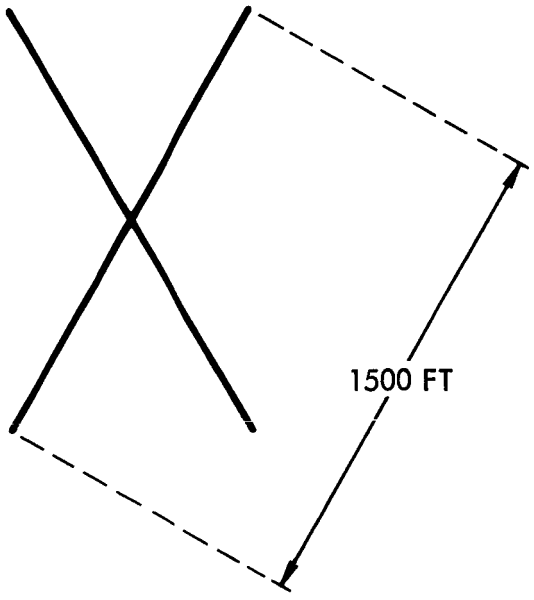

Figure 2.1. NASA Radio Astronomy Satellite Configuration (from Reference 4.3)

the gravitational gradient. Results are obtained for the important case where the beam mass is negligible in relation to the tip mass, and some conclusions are given about the case of distributed mass.

2.2.2 Conclusions

Under certain conditions, the behavior of the satellite appendages under the effect of gravitational and orbital centrifugal forces is analogous to the problem of Figure 2.2, in which the spring constant k is a negative number. The result is that, for given tip mass and beam stiffness, the equilibrium deflection is zero for beam lengths less than a given critical length. For lengths above the critical, the beam deflects drastically. The shape cannot be predicted from small-deflection beam theory; the exact equations of an elastica must be employed.

As a practical example, a beam of the type used on the Radio Astronomy Explorer, with a 5 pound tip weight, has a critical length of about 360 feet.

An analogy is found to exist between the problem of static deflection of a cantilever beam attached to a vertical satellite, having distributed mass, and the forced vibration of such a beam. The static deflection problem may be solved using the known solution for the vibrating beam.

2.3 Pitch Libration of a Rod Satellite (Chapter 5)

2.3.1 Problem Statement

Most work on the dynamics of flexible gravity-gradient satellites has dealt with satellites having, at most, two elastic degrees of freedom. The present problem treats a very special case of the motion of

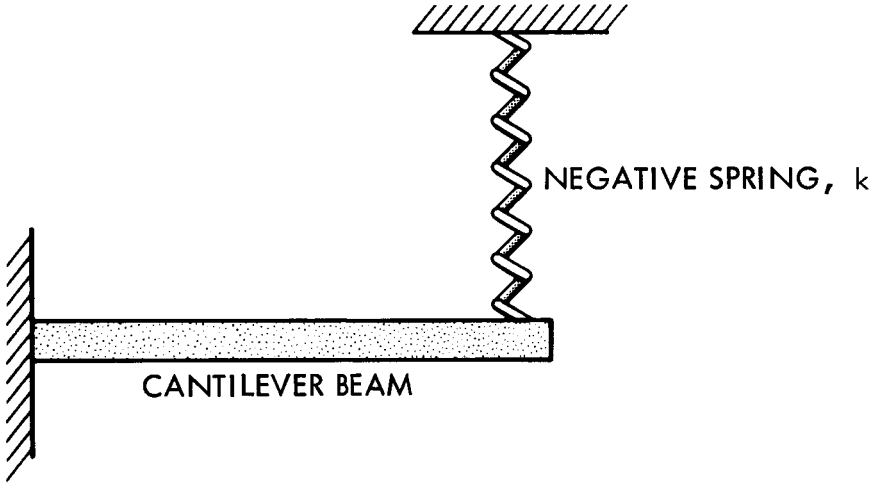

Figure 2.2. Mechanical Analog of Deflection Under Gravitational-Centrifugal Loading

a continuously flexible satellite having an infinite number of degrees of freedom. The problem is restrictive in that the satellite is idealized as a rod or beam or wire, and only planar pitch motion is considered.

Results have potential application to the so-called "long-wire satellite" (Reference 5.1), a proposed configuration for a passive communications reflector.

2.3.2 Conclusions

To a linear approximation, the long-wire satellite has uncoupled rigid and elastic motion. That is, pure pitch motion with the wire remaining in a straight line and oscillating about the vertical is possible, as is pure elastic motion with an equilibrium configuration along the vertical.

For finite amplitude pitch motion, elastic motion is excited parametrically. The equations for small elastic motion for each elastic mode reduce approximately to the Mathieu equation.

For a steel wire of 0.002 inch diameter, about 120 feet long, pitch motion will cause elastic motion to build up, transferring energy into the elastic mode. It is theorized that, if such a wire could be deployed in orbit, it might be capable of reducing its pitch amplitude to a very small value by transfer of energy into the elastic mode and subsequent structural damping.

Chapter 3. Infinitesimal and Noninfinitesimal Amplitude Stability of a Class of Flexible Satellites

This section approaches the study of flexible satellite behavior by beginning with the behavior of a rigid gravity-gradient satellite and then examining the ways flexible satellite behavior differs from rigid-body behavior. Certain conclusions on stability and instability of motion which hold for a rigid body are shown to be false for a class of flexible bodies and others are shown to hold also for the flexible body. The particular class of flexible bodies examined is chosen to permit ready comparison of rigid-body and flexible-body behavior.

3.1 Stability Behavior of a Rigid Satellite in Circular Orbit

3.1.1 Coordinate System and Small-Angle Equations

Consider a rigid satellite moving in circular orbit about the earth (Figure 3.1). The coordinate system is that of Reference 3.1.

The principal axes B_i of the rigid body are nominally aligned with a rotating, earth-pointing coordinate frame, O_i. O_1 is tangent to the orbit, O_2 normal to the orbit and O_3 points toward the earth.

The orientations of B_i differ from O_i by angles θ_i. Rotations are taken in the sequence shown in Figure 3.2; first θ_3, then θ_2, than θ_1. θ_3, θ_2 and θ_1 will be called yaw, pitch and roll, respectively.

The derivation of the equations of motion takes into account the rigid-body dynamics of the satellite, the moment of the gravitational field on the satellite, and the effects of the rotating coordinate system.

The derivation is given in Appendix B, based on the gravity torque expressions of Appendix A. The results, to first order in small θ_i are

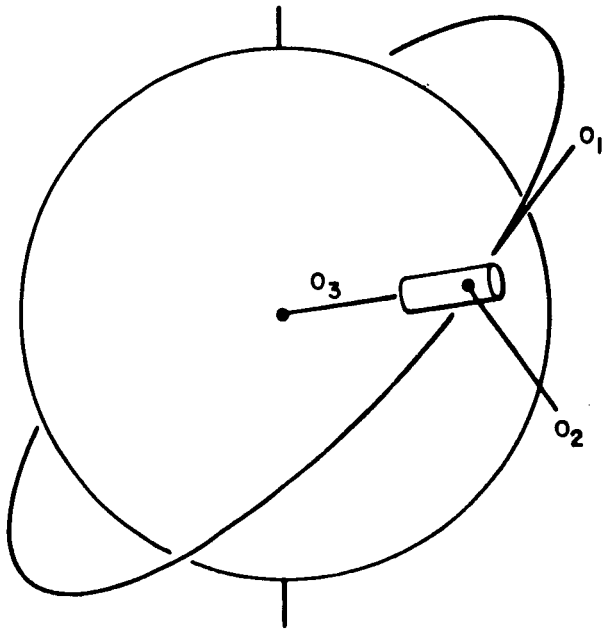

Figure 3.1. Orbit Reference Coordinate System

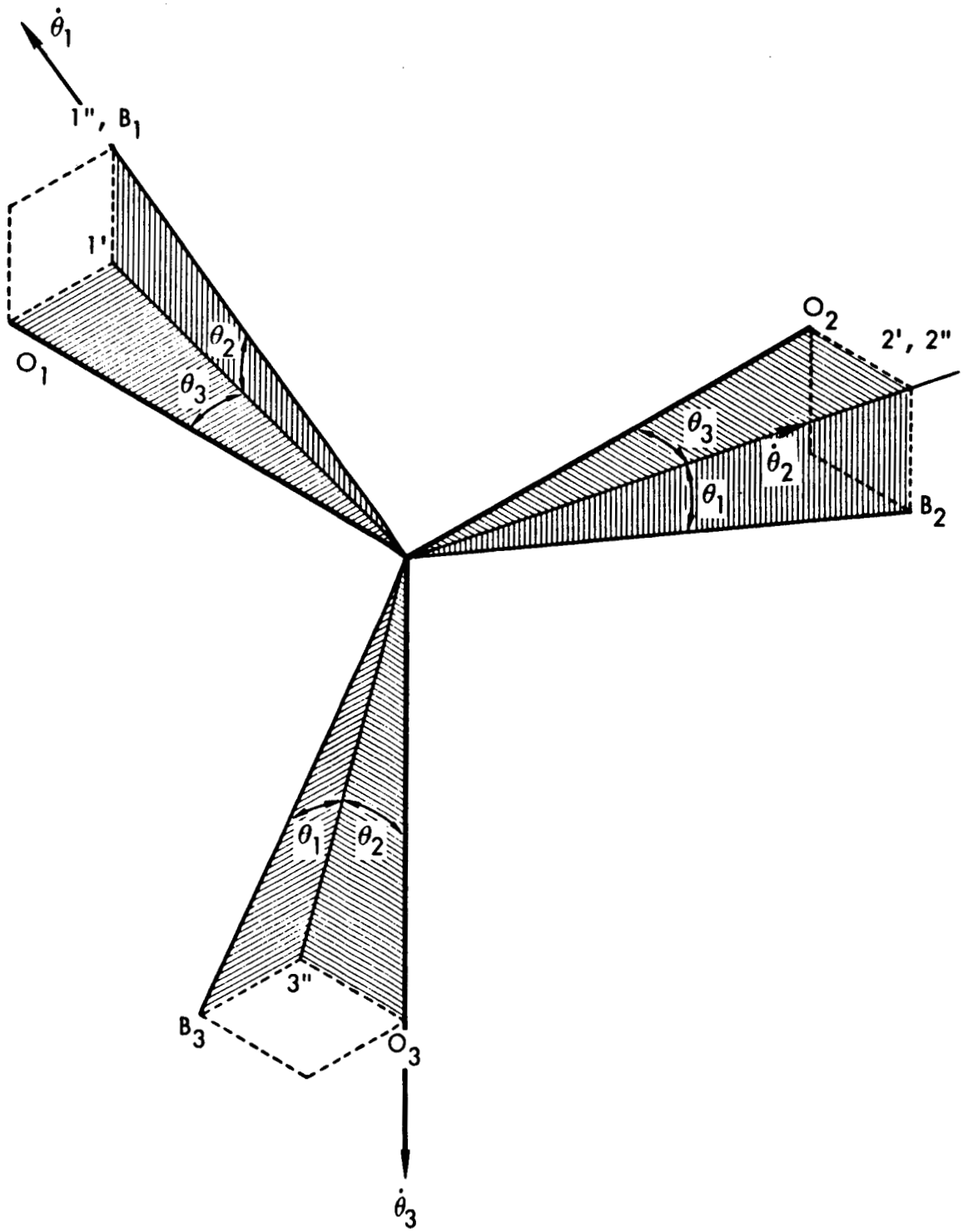

Figure 3.2. Rotations Defining Body Coordinates

$$I_1 \frac{d^2\theta_1}{dt^2} + (I_2 - I_3)\omega_o^2\theta_1 + \omega_o(I_2 - I_1 - I_3)\frac{d\theta_3}{dt} = L_1$$

$$I_2 \frac{d^2\theta_2}{dt^2} = L_2$$

$$I_3 \frac{d^2\theta_3}{dt^2} + (I_2 - I_1)\omega_o^2\theta_3 - \omega_o(I_2 - I_1 - I_3)\frac{d\theta_1}{dt} = L_3 \qquad (3.1\text{-}1)$$

where

I_i = Principal moments of inertia

ω_o = Orbital angular velocity

The gravity moments L_i are given by

$$\begin{bmatrix} L_1 \\ L_2 \\ L_3 \end{bmatrix} = \frac{3K}{R^3} \begin{bmatrix} (I_3 - I_2)\theta_1 \\ (I_3 - I_1)\theta_2 \\ 0 \end{bmatrix} \qquad (3.1\text{-}2)$$

where

R = Orbit radius

K = Earth's gravitational constant

We note that, for a circular orbit,

$$\omega_o^2 = \frac{K}{R^3}$$

and introduce the dimensionless parameters

$$K_1 = \frac{I_1 - I_2}{I_3}$$

$$K_2 = \frac{I_2 - I_3}{I_1}$$

$$\tau = \omega_o t \qquad (3.1\text{-}3)$$

So Equations (3.1-1) become

$$\ddot{\theta}_1 + (K_2 - 1)\dot{\theta}_3 + 4K_2\theta_1 = 0$$

$$\ddot{\theta}_2 + \omega_p^2\theta_2 = 0$$

$$\ddot{\theta}_3 + (K_1 + 1)\dot{\theta}_1 - K_1\theta_3 = 0 \qquad (3.1\text{-}4)$$

with

$$\omega_p^2 = \frac{3(K_1 + K_2)}{1 + K_1K_2} \qquad (3.1\text{-}5)$$

where dots denote derivatives with respect to τ.

The uncoupled θ_2 equation will be referred to as the "pitch" equation and the coupled equations for θ_1 and θ_3 are called the roll-yaw equations.

3.1.2 Stability of Infinitesimal Motion

We first summarize the attitude stability of the rigid satellite as predicted by the linearized equations of infinitesimal motion, Equation (3.1-4), recognizing the danger of assuming that the actual system behavior can be predicted from the linearized equations.

The analysis of Equations (3.1-4) is due to Debra and Delp (Reference 3.2), and may be summarized as follows.

The characteristic equation is

$$\left(s^2 + \omega_p^2\right)\left[s^4 + (1 + 3K_2 - K_1K_2)s^2 - 4K_1K_2\right] = 0 \qquad (3.1\text{-}6)$$

The equation can be factored into a linear equation and a quadratic in s^2. To avoid a divergent solution and achieve neutral stability we require that the three values of s^2 be negative. This implies:

For the linear equation

$$\omega_p^2 > 0 \quad (K_1 + K_2 > 0) \tag{3.1-7a}$$

For the quadratic, from Descartes' rule of signs

$$1 + 3K_2 - K_1K_2 > 0 \tag{3.1-7b}$$

$$K_1K_2 < 0 \tag{3.1-7c}$$

and, to assure the existence of real roots, the quadratic must have a positive discriminant:

$$(1 + 3K_2 - K_1K_2)^2 + 16K_1K_2 > 0 \tag{3.1-7d}$$

In addition, there is a physical limitation on the absolute value of K_1 and K_2. For three principal moments of inertia I_i, I_j, I_k, we have

$$I_i + I_j \geq I_k \quad , \quad i \neq j \neq k$$

which implies

$$|K_i| \leq 1$$

The stability conditions can be displayed graphically in the K_1-K_2 plane (Figure 3.3). There are two stable regions, a main region for which $K_2 > -K_1$, $(I_2 > I_1 > I_3)$ (the "long" axis of the body is nominally vertical) and a smaller one, sometimes called the Delp region, in which $I_1 > I_3 > I_2$, so that the "long" axis is normal to the orbit plane.

The physical characteristics of the bodies in various portions of the K_1-K_2 plane are indicated in Figure 3.4, adapted from Reference 3.3.

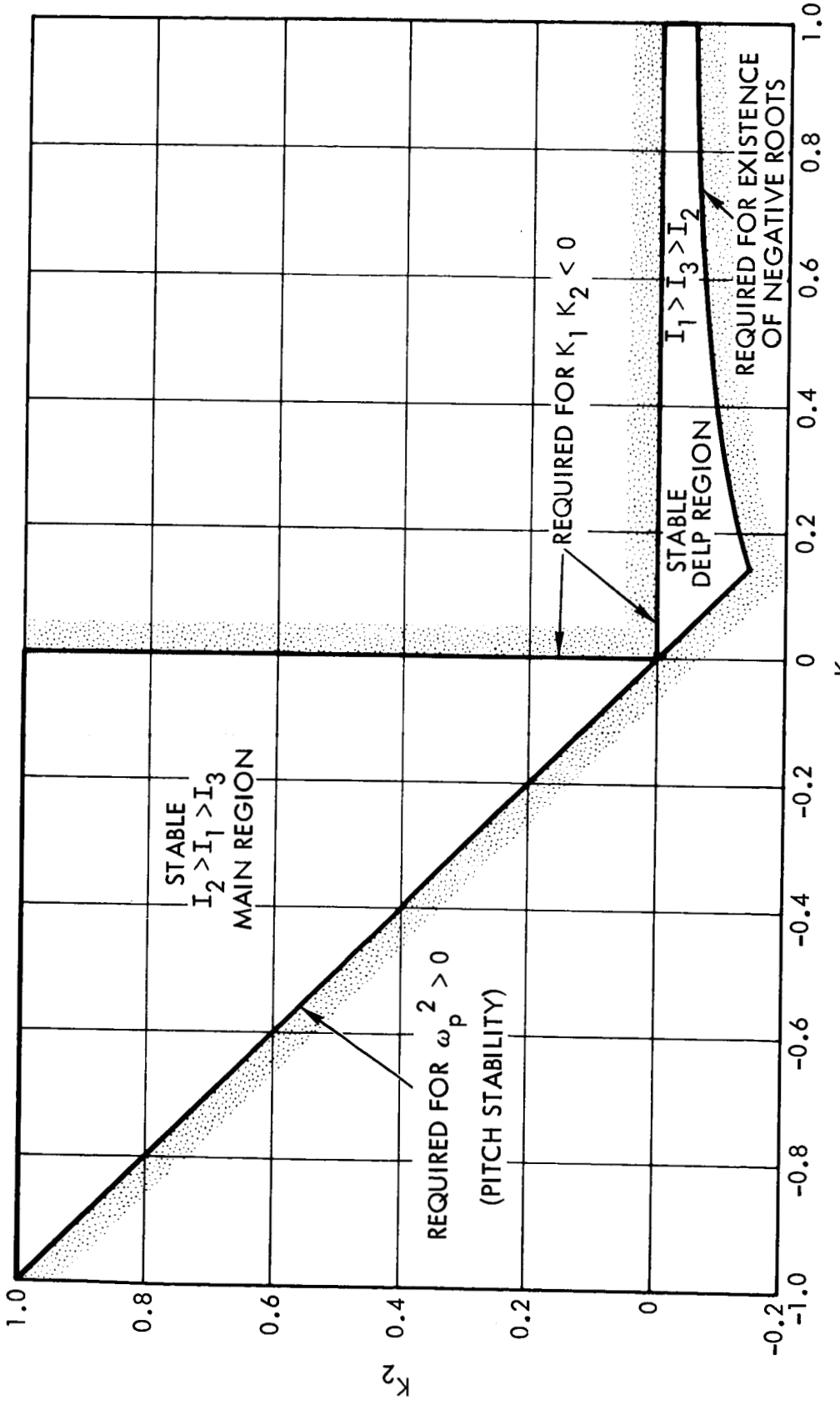

Figure 3.3. Regions of Satellite Stability in K_1-K_2 Plane, Showing Reasons for Existence of Boundaries

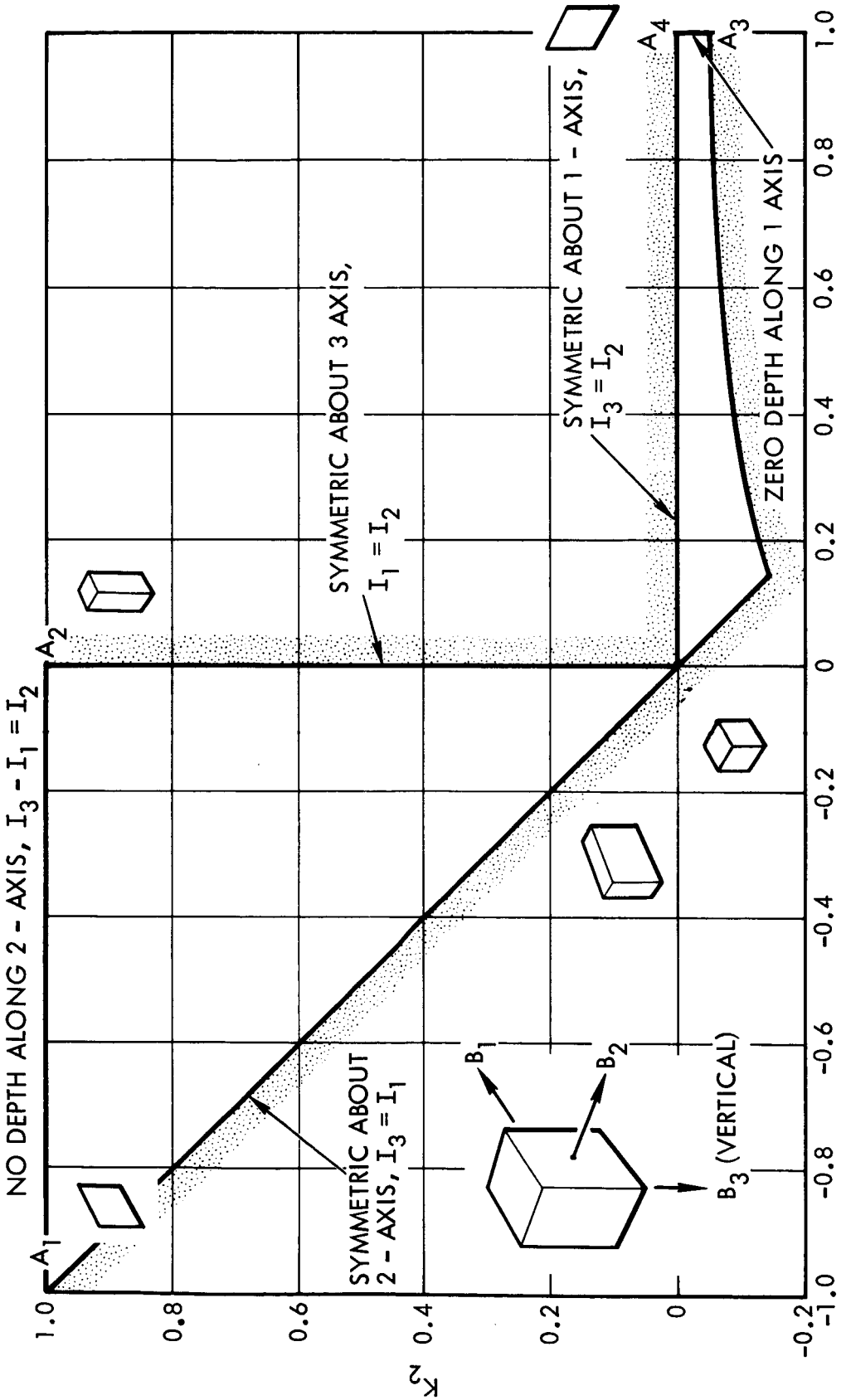

Figure 3.4. Physical Character of Satellites in Various Regions of K_1-K_2 Plane

Figure 3.3 gives a complete picture of rigid-body stability within the framework of the linearized equations.

3.1.3 Effect of Noninfinitesimal Amplitude Pitching Motion

The picture of rigid-body stability given previously can be modified considerably by the effects of nonlinear terms. A significant contribution was made recently by Kane (Reference 3.4) who considered the effect of noninfinitesimal amplitude of the pitch angle θ_2.

Kane's technique was to consider θ_1 and θ_3 as small angles, but to retain θ_2 as an arbitrary angle in the equations of motion. The pitch equation remains uncoupled from roll and yaw, but now takes the form [Appendix B, Equation (B-12b)] of the pendulum equation

$$\ddot{\theta}_2 + \frac{\omega_p^2}{2} \sin 2\theta_2 \tag{3.1-8}$$

The coefficients of the roll-yaw equations are also modified when θ_2 is retained as a large angle. The revised roll-yaw equations may be written in the symbolic form

$$\ddot{\theta}_1 + f(\theta_2, \dot{\theta}_2)\dot{\theta}_1 + f(\theta_2, \dot{\theta}_2)\theta_1 + f(\theta_2, \dot{\theta}_2)\dot{\theta}_3 + f(\theta_2, \dot{\theta}_2)\theta_3 = 0$$

$$\ddot{\theta}_3 + f(\theta_2, \dot{\theta}_2)\dot{\theta}_1 + f(\theta_2, \dot{\theta}_2)\theta_1 + f(\theta_2, \dot{\theta}_2)\dot{\theta}_3 + f(\theta_2, \dot{\theta}_2)\theta_3 = 0 \tag{3.1-9}$$

Here $f(\theta_2, \dot{\theta}_2)$ denotes various functions of θ_2 which have the limits required by Equation (3.1-4) as θ_2 and $\dot{\theta}_2$ tend to zero. The functions f are all periodic because the solutions of Equation (3.1-8) are all periodic. The linearized, constant-coefficient roll-yaw system of Equation (3.1-4) is thus replaced by a system with periodic coefficients.

If any of the solutions of Equation (3.1-9) grow with time it means that uncoupled pitch motion with θ_1, $\theta_3 = 0$ is unstable.

Kane used Floquet theory to evaluate the stability of the θ_1, θ_3 system. The technique is described in detail in Appendix C because it is used later in Chapter 3 to study certain flexible-body problems. Basically, it takes advantage of the fact that the solution of a system of linear, homogeneous, periodic coefficient equations can ordinarily be written as the sum of linearly independent normal solutions, $n_i(t)$. The normal solutions have the property for all time t that

$$n_i(t + T) = \lambda_i n_i(t)$$

where T is the period of the parametric excitation and λ_i is a complex number called the characteristic multiplier of the solution. If $|\lambda_i| \geq 1$ the solution grows indefinitely with time and is therefore unstable. The characteristic multipliers must ordinarily be determined by numerically integrating the differential equations over one cycle. Any convenient complete set of solutions may be used.

Kane's application of Floquet theory to the rigid-body gravity-gradient problem produced the surprising result that planar pitching motion with small θ_1, θ_3 is unstable for certain values of K_i, within the stable regions of Figure 3.3, for amplitudes of θ_2 as low as one degree. That is, the characteristic multipliers of the periodic coefficient roll-yaw system are greater than one in magnitude showing that an initial pitch motion would cause roll-yaw to build up from arbitrarily small but nonzero initial values of θ_1 and θ_3.

The unstable inertia configurations found by Kane within the region of infinitesimal stability are shown in Figure 3.5, for a pitch amplitude of one degree. The immediate neighborhood of each cross contains a region of unstable points. The points shown were found by systematically examining a uniform grid of points in the K_1-K_2 plane, but it will be shown in the next section that regions of potential instability can be located a priori.

Kane's results, which applying only to an idealized rigid body, are very important because of the implication that linearized roll-yaw equations cannot be used for design purposes. Actual gravity gradient satellites (Reference 1.2, for example) invariably execute steady-state pitch oscillations of one degree or more because of magnetic disturbance torques, orbit eccentricity, and so forth. The presence of appreciable pitch oscillation might invalidate a design based on linearized equations similar to Equation (3.1-4).

3.1.4 Interpretation of Roll-Yaw Instability in Terms of Perturbation Solution

The Floquet theory technique is rigorous and accurate but does not easily yield information about the locations of unstable regions. A systematic search of the parameter space of interest is practical when only the inertia parameters K_1 and K_2 are involved, but is much more difficult when other parameters, such as those characterizing the body flexibility, must also be varied.

J.V. Breakwell (private communication) and the present author have independently pointed out that a perturbation solution can be used to locate the general regions of unstable roll-yaw motion. The general

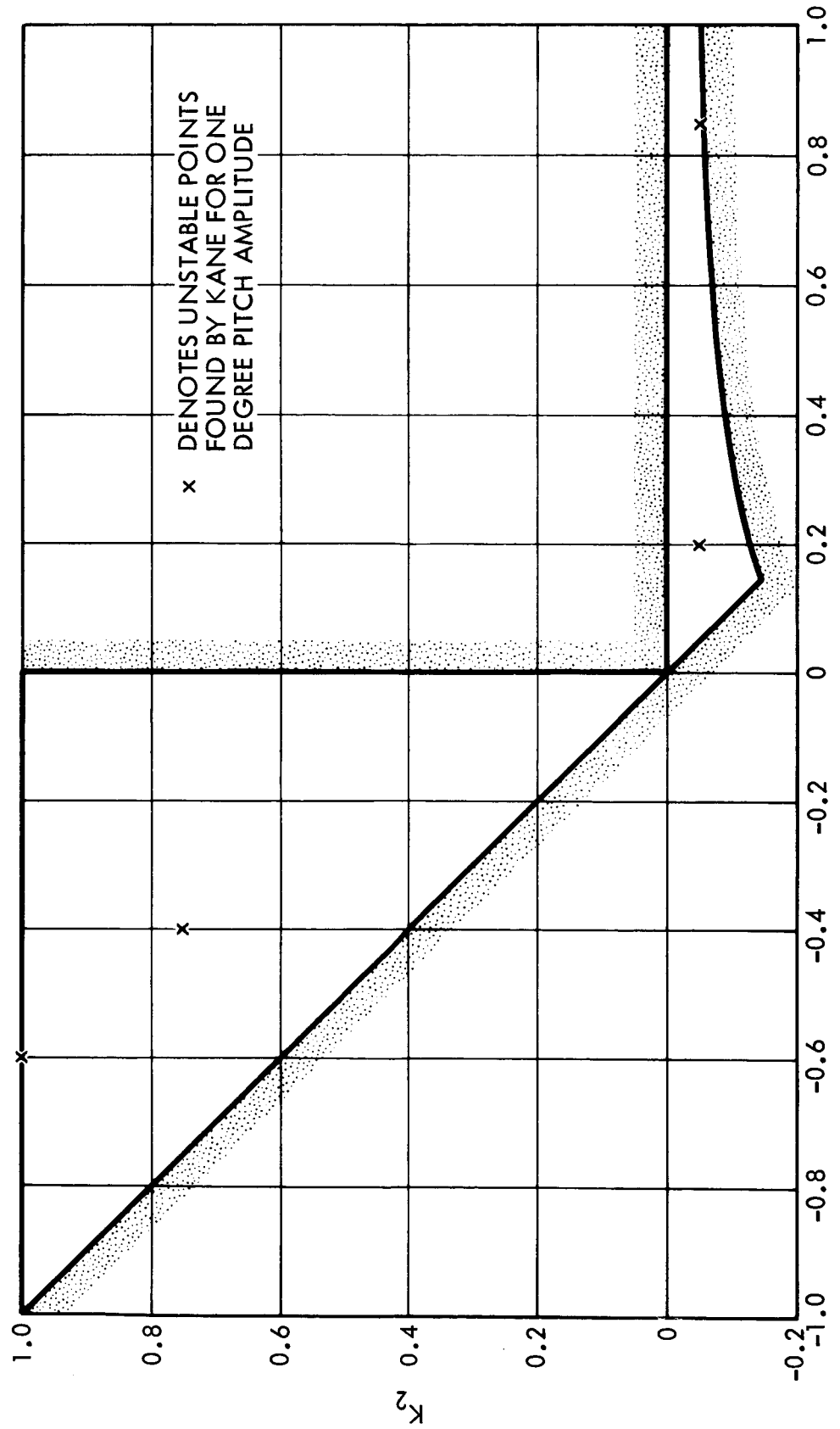

Figure 3.5. Locations of Points for Which Pure Pitch Motion is Unstable

technique is outlined in References 3.5 and 3.6, among other sources. Given a general system of second-order linear equations with periodic coefficients, we can write it in matrix form as

$$[M](\ddot{\underset{\sim}{x}}) + [C](\dot{\underset{\sim}{x}}) + [K](\underset{\sim}{x}) = \epsilon\left[[M_1](\ddot{\underset{\sim}{x}}) + [C_1](\dot{\underset{\sim}{x}}) + [K_1](\underset{\sim}{x})\right] \tag{3.1-10}$$

where $(\underset{\sim}{x})$ is the solution vector, $[M]$, $[C]$ and $[K]$ are constant matrices and $[M_1]$, $[C_1]$ and $[K_1]$ are periodic with zero mean and frequency ω_p. ϵ is proportional to the amplitude of periodic excitation.

For small ϵ we may seek a solution in the form

$$(\underset{\sim}{x}) = (\underset{\sim}{x}_o) + \epsilon(\underset{\sim}{x}_1)$$

where $(\underset{\sim}{x}_o)$ is the solution for $\epsilon = 0$. $(\underset{\sim}{x}_o)$ will have the form

$$(\underset{\sim}{x}_o) = \sum_i e^{s_i t}(\underset{\sim}{C})_i \tag{3.1-11}$$

where the s_i are the roots of the characteristic equation

$$\Delta(s) = \left|[M]s^2 + [C]s + [K]\right| = 0$$

and the $(\underset{\sim}{C})_i$ are vector constants. Each element of the coefficient matrices $[M_1]$, $[C_1]$ and $[K_1]$ can be expanded in Fourier series

$$\sum_n\left[D_n \exp(in\omega_p t) + E_n \exp(-in\omega_p t)\right] \tag{3.1-12}$$

for appropriate constants D_n, E_n. After substituting Equations (3.1-11) and (3.1-12) into (3.1-10) and retaining only first-order terms in ϵ, the resulting equation has the form

$$[M](\ddot{\underset{\sim}{x}}_1) + [C](\dot{\underset{\sim}{x}}_1) + [K](\underset{\sim}{x}_1) = f(t) \tag{3.1-13}$$

where f(t) is the sum of terms of form

$$C\, e^{(s \pm n\omega_p i)t}$$

The solution of Equation (3.1-13) will contain terms having denominators $\Delta(s_i \pm n\omega_p i)$. The perturbation solution will then be invalid near frequencies ω given by $s_i = s_j \pm n\omega_p i$ for all i, j, n, because Δ vanishes at those frequencies. Such frequency coincidence does not guarantee instability, but does invalidate the perturbation solution and indicates a possible instability.

The heuristic argument above can be extended (Reference 3.6) to give a method for predicting a range of frequencies near

$$i\omega_p = \pm \frac{(s_i - s_j)}{n} \qquad (3.1\text{-}14)$$

for which unstable parametric excitation occurs.

Applying Equation (3.1-14) to the present problem, we put $s = i\omega$ in the quartic part of Equation (3.1-6) and solve for the two frequencies ω_1, ω_2, $\omega_2 > \omega_1$ of roll-yaw motion. The fundamental parametric resonance will occur for n = 1 in Equation (3.1-14), so the possibilities are

$$\omega_p = \omega_1 + \omega_2,\ \omega_2 - \omega_1,\ 2\omega_2,\ 2\omega_1 \qquad (3.1\text{-}15)$$

Of these, only $\omega_p = \omega_2 - \omega_1$ and $\omega_p = 2\omega_1$ are physically possible. The other kinds of frequency coincidence cannot occur for real, physical rigid bodies.

The curves in the K_1-K_2 plane can conveniently be cross-plotted from the curves of constant ω_1, ω_2 and ω_p of Reference 3.2. A more accurate technique is to choose a value of $s = i\omega_1$ and then solve

Equations (3.1-6) and (3.1-15) for K_1 and K_2. The resulting curves for $\omega_p = 2\omega_1$ emerge as the two roots of a quadratic in K_2.

The two parametric resonance curves are given in Figure 3.6.

The unstable points found by Kane (denoted by crosses) are seen to coincide well with the curve $\omega_p = 2\omega_1$ particularly in the main region. No unstable points corresponding to $\omega = \omega_2 - \omega_1$ were found. Breakwell (private communication) has apparently discovered the analytic reason why they do not occur.

Using Kane's Floquet theory technique at points on the parametric resonance line of Figure 3.6, the author has reproduced Kane's points and has also found other unstable points (indicated by circles). No stable points have been found on the line and it seems certain that it represents the center of a continuous narrow strip of unstable points.

3.2 Infinitesimal Amplitude Stability Behavior of a Class of Flexible Satellites in Circular Orbit

With the rigid-body results as background, the central problems of Chapter 3 can be stated:

a) How does the infinitesimal amplitude stability behavior described by Debra and Delp (Section 3.1.2) change when the satellite becomes flexible?

b) Does the instability of noninfinitesimal pitching motion, found by Kane for a rigid body (Section 3.1.3), have a significance for a body with realistic flexibility and damping? The first of these questions will be treated in this section and the second in Section 3.3.

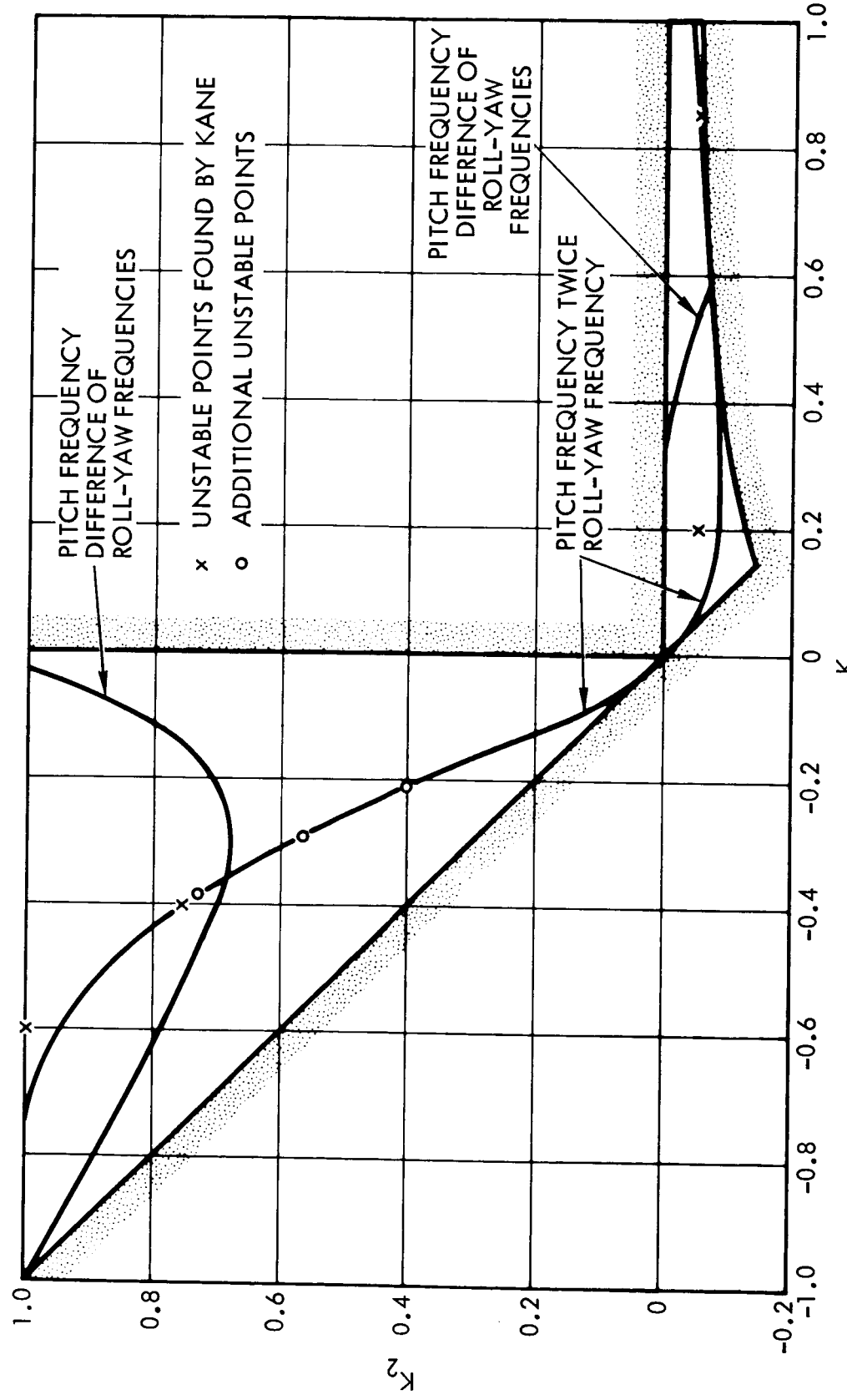

Figure 3.6. Loci of Coincidence Between Pitch and Roll-Yaw Frequencies, Showing Relationship to Numerical Results

The problems posed are meaningful because current and proposed gravity-gradient satellites have significant flexibility and damping. There are three main types:

A. Extremely flexible satellites consisting of two or more rigid bodies connected by very weak spring hinges (Reference 3.7, for example).

B. Continuously flexible satellites with distributed stiffness and damping. This type has been proposed (Reference 5.4) but not yet flight tested.

C. Magnetically anchored satellites (Reference 1.3) which are rigid and obtain damping through use of the earth's magnetic field.

The present problems concern satellites of types A and B, type C satellites being excluded because they have a non-zero magnetic torque acting on the satellite as well as a gravitational torque.

The approach will be to select a class of satellites which can be readily compared with the class of rigid satellites, and to examine the differences in behavior. The selected satellite configurations will somewhat resemble actual satellites, but simplifications will be made to make the analysis more tractable.

3.2.1 Selection of Flexible Body Configuration

3.2.1.1 Inertial Configuration

The inertia parameters K_1 and K_2 completely determine the configuration of a rigid satellite. For any rigid satellite, there are an

infinite number of flexible bodies which have the same inertia distribution. Selection of a particular flexible body configuration for study must be accomplished by carefully examining the problem for solution: to determine how the behavior of a flexible body differs from that of a corresponding rigid body.

One necessary condition is clearly that the inertia properties of the body chosen should be the same as for the corresponding rigid body when the elastic deformation is zero. Hence, we can use the same quantities K_1 and K_2 to describe the behavior.

Real flexible bodies have an infinite number of flexible degrees of freedom. The general equations for such a body are complicated. For clarity, we select a body which has only one flexible degree of freedom. The stiffness and damping can therefore be characterized by only two parameters. A suitable parameter for describing the stiffness is the natural frequency of the elastic mode. The presence of a nonuniform gravitational field alters the effective natural frequency of a flexible body because elastic deformation changes the gravitational potential energy. To specify the stiffness unambiguously, we use the natural frequency of the body when it is at rest in a uniform gravitational field.

As a physically intuitive measure of the damping, we use the fraction of critical damping of the elastic system in a uniform gravitational field.

Another constraint on the selection of a configuration for study is posed by the necessity of studying the system behavior for values of the inertia parameters K_1 and K_2 which cover the entire physically

realizable region. The flexible body selected for study must be flexible over the entire range of inertia parameters. This requirement places severe restrictions on the body to be considered. For example, consider the body of Figure 3.7, which is made up of two rigid bodies, B and B^*, connected by a flexible joint parallel to axis B_1. Body B^* extends out along the axis B_2. The body illustrated cannot be compared meaningfully to an equivalent rigid body when the inertias are such that the parametric point K_1, K_2 for the body lies near the line A_1-A_2 of Figure 3.4, because on that line the body considered must have zero dimension along axis B_2. Therefore Body B^* will have zero length and therefore zero mass and the composite body will behave exactly the same as the corresponding rigid body. A similar situation exists near points A_3 and A_4, where the dimension along axis B_1 must shrink to zero.

Examination of Figure 3.4 shows that the only body dimension which is not zero somewhere in that region of the K_1-K_2 plane which is stable for a rigid body is the dimension along axis B_3. Thus, a main body having a subsidiary body aligned nominally along axis B_3 could retain its flexible nature over the entire rigid-body region. The shape in the limiting regions A_1-A_2, A_3-A_4 is that of two parallel plates, one inside the other, hinged along a principal axis of each.

In the above discussion, it has been tacitly assumed that the two rigid bodies forming the composite body are joined at their centers of gravity. The purpose of this restriction is only to reduce the number of quantities to be varied in a parametric analysis. Effect of center of gravity offset should form a separate study.

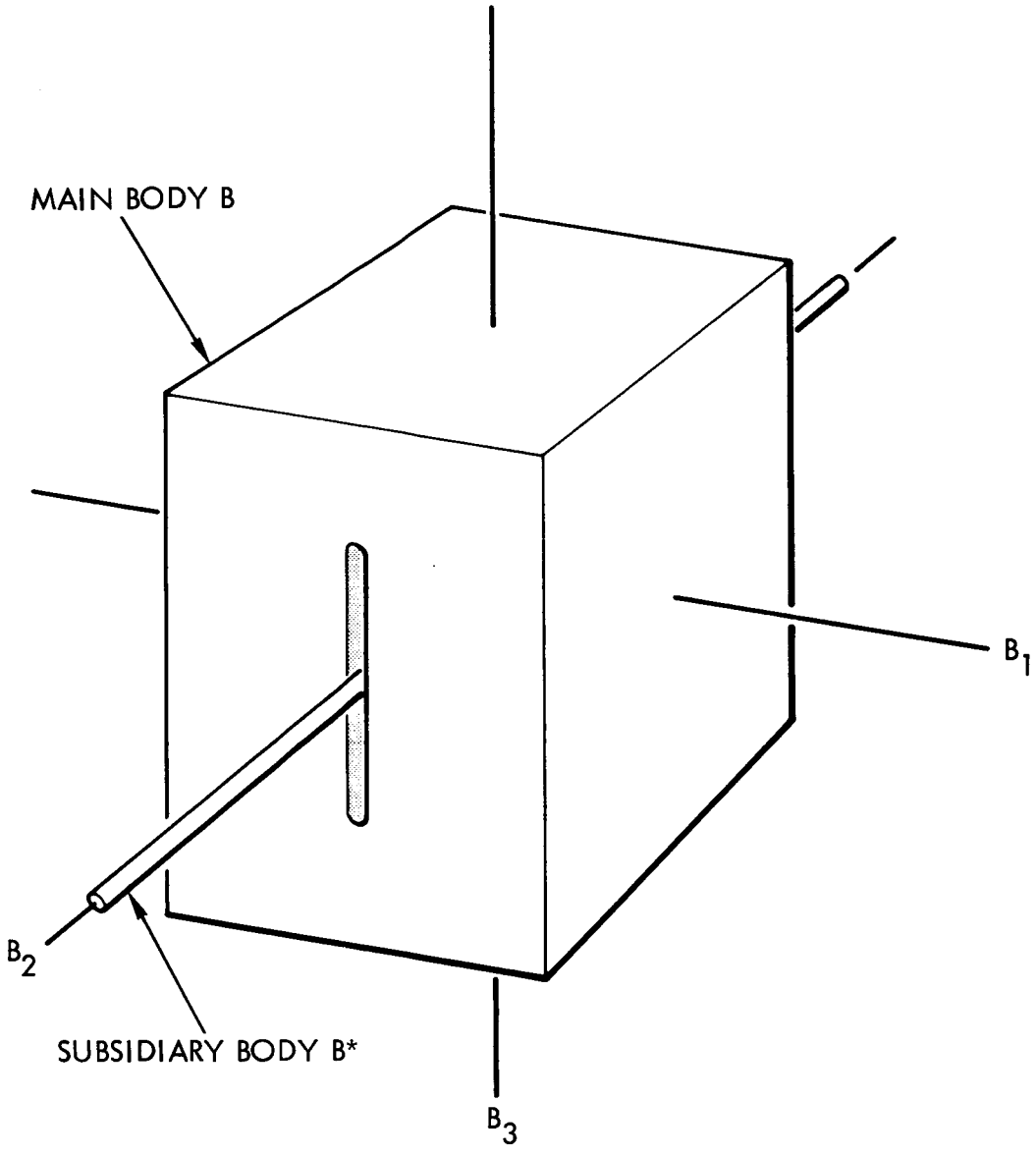

Figure 3.7. Two Rigid Bodies Connected With a Hinge Along Axis B_1

It is not necessary that the subsidiary body be the same shape over the entire stable region. The obvious choice is to have the main body and the subsidiary body inertially similar; i.e., to choose their inertias in constant ratios. This alternative is impractical for studying effects of damping, because such a composite body has a mode of oscillation which is identical to that of an equivalent rigid body and is not damped, even though the joint between bodies is dissipative. That is, a composite body, made up of two inertially similar components has undamped modes of motion.

Since it is not practical to give the same inertia properties to the two bodies, the most physically meaningful choice is to have the second (subsidiary) body in the shape of an ideal rod with no moment of inertia about the B_3 axis. The principal body must then have three distinct variable moments of inertia, in order to cover the entire stable region.

3.2.1.2 Hinge Axis Direction

There remains the selection of the direction of the axis of the hinge between the two composite bodies. First, suppose that there is a hinge axis along axis B_2, nominally perpendicular to the orbit plane. Then, for small amplitudes, there will be two modes of purely planar motion in the pitch plane, each corresponding to a natural frequency. For high stiffness, one mode is nearly the same as the planar pitch libration of a rigid body, while the other is close to the elastic mode of the satellite in a uniform gravitational field. The problem of the stability of planar motion is then complicated by the fact that

parametric excitation of roll-yaw motion occurs at two frequencies, with unusual behavior possible when the two frequencies are harmonically related. Also, incorporation of damping in the hinge along axis B_2 would guarantee ultimate stability of pitch motion for any initial pitch amplitude, because the parametric excitation of roll-yaw by pitch will gradually diminish to zero.

If the hinge along the B_2 axis is the only hinge, there is a further complication. In this case, it is clear physically, and can be confirmed analytically, that linearized roll-yaw equations are not coupled to the elastic motion. That is, the roll-yaw frequencies and modes are the same for the flexible body as for the equivalent rigid body and no damping exists.

For a simplified, realistic problem, a hinge must be oriented along the roll (B_1) axis or along the yaw (B_3) axis. A hinge along the B_3 axis, however, has no meaning if the subsidiary body is a rod aligned with the B_3 axis, as discussed above. The rod has no moment of inertia about axis B_3, and therefore the presence of a hinge is immaterial.

3.2.1.3 Summary of Configuration to be Studied

The considerations above indicate that the appropriate geometry for the present study is a main rigid body having distinct moments of inertia I_1, I_2, I_3 and coupled to a body which is a rod aligned nominally along axis B_3 and hinged along B_1. Such a configuration can be characterized by the dimensionless ratios K_1 and K_2 and one additional parameter specifying the relationship between the rod inertia and one of the main body inertias. (While there are four independent inertia parameters, three for the main body and one for the rod, the equations can be reduced to

non-dimensional form by dividing through by any one of the parameters.) There remains only the selection of the ratio between the rod inertia and the main body inertias. For reasons of simplicity, this ratio has been established somewhat arbitrarily by selecting the moments of inertia of the two bodies about axis 1 to be identical, so that the principal moments of inertia are I_1, I_2, I_3 and I_1, I_1, 0, respectively.

The final configuration, then, is a class of gravity-gradient satellites having a single elastic degree of freedom (rotation about the hinge axis) and three rigid-body degrees of freedom. A member of the class is determined completely by specifying:

a) The inertia parameters K_1 and K_2, measured with zero elastic deflection

b) The elastic stiffness

c) The hinge damping.

The configuration selected is not realistic because it has no pitch damping. Incorporation of a second damped hinge along axis B_2 would greatly complicate the physical picture. The present study should be considered as an approach to the more realistic problem.

As the elastic stiffness of the satellite decreases, it will behave less and less like a flexible body and more like two coupled rigid bodies. Comparison between its behavior and that of a rigid satellite will become less and less meaningful. Attention will be concentrated mainly on flexible satellites having elastic natural frequencies somewhat higher than the rigid-body libration frequencies.

3.2.2 Equations of Motion for Flexible Body

The equations of motion are derived from the angular momentum principle in Appendix B, using the coordinate system of Figure 3.8. The orientation of the main body B, having inertias I_1, I_2, I_3 relative to a local-vertical coordinate system, is described by the same set of angles θ_1, θ_2, θ_3 used for the rigid body (Section 3.1.1). The subsidiary rod body B^* with inertias I_1, I_1, 0 is rotated relative to B through an angle α about axis B_1. Relative rotation is resisted by a linear torsional spring and damper, having constants k and c.

The derivation of Appendix B retains θ_2 as a large angle for use in the noninfinitesimal-amplitude stability studies described in Sections 3.2.5 and 3.2.6. The linearized version of the equations is: (dots indicate derivatives with respect to dimensionless time, $\tau = \omega_o t$)

$$\begin{bmatrix} \ddot{\theta}_1 \\ \ddot{\theta}_3 \\ \ddot{\alpha} \end{bmatrix} + \begin{bmatrix} 0 & 2(K_2 - 1) & -\zeta\omega_n \\ (K_1 + 1) & 0 & 0 \\ 0 & -2(K_2 - 1) & 2\zeta\omega_n \end{bmatrix} \begin{bmatrix} \dot{\theta}_1 \\ \dot{\theta}_3 \\ \dot{\alpha} \end{bmatrix}$$

$$+ \begin{bmatrix} 4(2K_2 - 1) & 0 & \frac{-\omega_n^2}{2} \\ 0 & -K_1 & 0 \\ -8(K_2 - 1) & & \omega_n^2 + 4 \end{bmatrix} \begin{bmatrix} \theta_1 \\ \theta_3 \\ \alpha \end{bmatrix} \qquad (3.2\text{-}1)$$

and

$$\ddot{\theta}_2 + \omega_p^2 \theta = 0 \qquad (3.2\text{-}2)$$

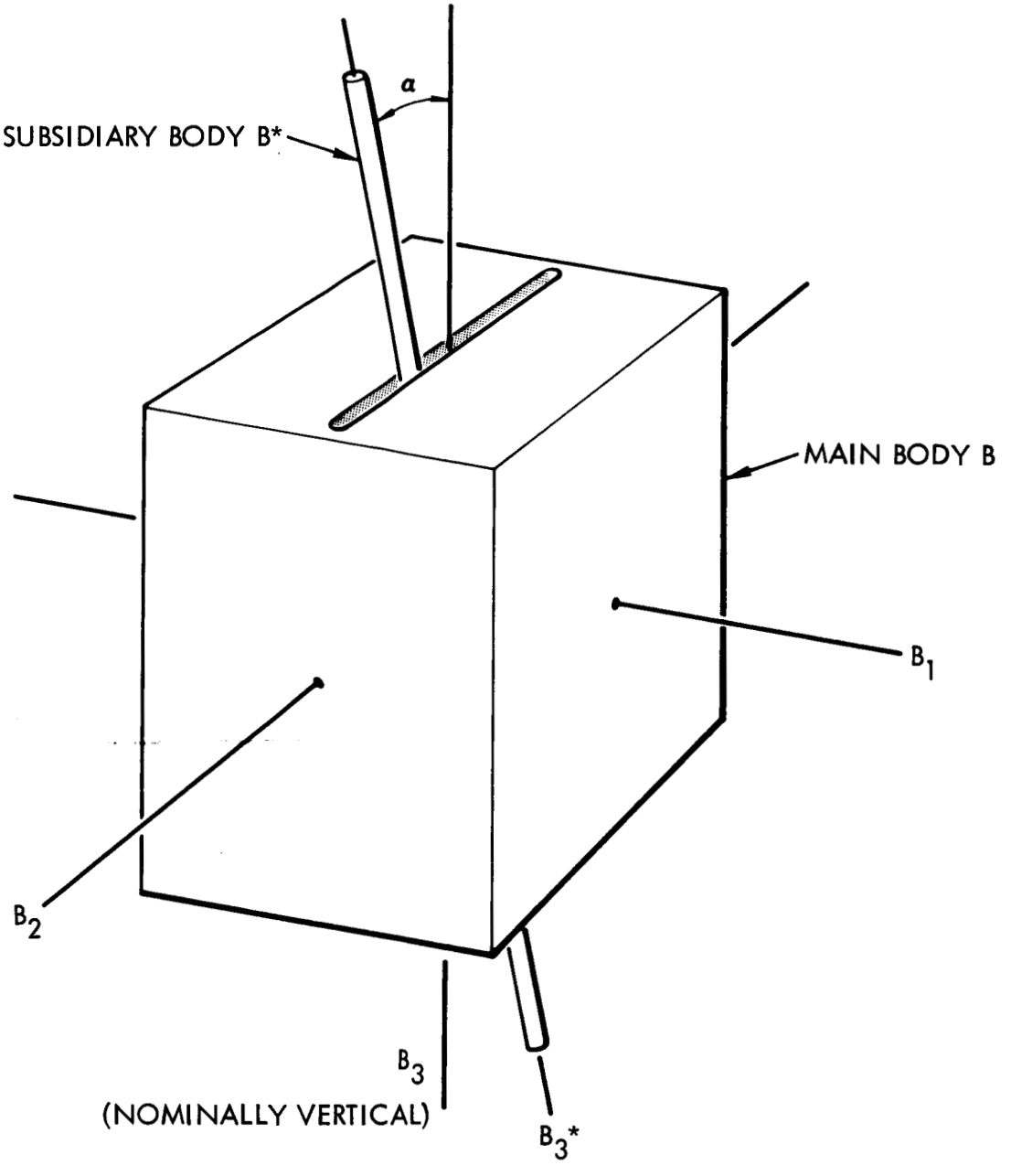

Figure 3.8. Configuration for Study: An Arbitrary Rigid Body B Coupled to a Rod B^* by a Hinge Along Axis B_1

Here

$$K_1 = \frac{I_1 - I_2}{I_3}$$

$$K_2 = \frac{I_1 + I_2 - I_3}{2I_1} \qquad (3.2\text{-}3)$$

are the inertia parameters. They are analogous to the parameters K_1 and K_2 of Equation (3.1-3), used for a rigid body, but include the inertias of both bodies B and B^*. Throughout Section 3.2, the definition of Equation (3.2-3) will be used.

In addition, referring to Equation (3.2-1)

$\omega_n = \frac{1}{\omega_o}\sqrt{\frac{2k}{I_1}}$ the dimensionless natural frequency of the body at rest in uniform gravity

$\zeta = \frac{c}{I_1\omega_o}$ the fraction of critical damping under the same circumstances

$\omega_p = \sqrt{\frac{3(K_1 + K_2)}{1 + K_1K_2}}$ the frequency of pitch oscillation.

3.2.3 Stability of Infinitesimal Motion Without Damping

The stability of the linearized system, Equations (3.2-1), is determined by the roots of the characteristic equation. For $\zeta = 0$ (no damping) the roll-yaw characteristic equation, obtained by taking the Laplace transform of Equation (3.2-1) and evaluating the determinant, is

$$s^6 + \left(6K_2 + 2 + K_1 - 2K_1K_2 + \omega_n^2\right)s^4$$

$$+ \left[\omega_n^2(3K_2 - K_1K_2 + 1) + 8(K_1 + 3K_2 - 1 - 2K_1K_2)\right]s^2$$

$$+ \left[16K_1(1 - 2K_2) - 4K_1K_2\omega_n^2\right] = 0 \qquad (3.2\text{-}4)$$

For $\omega_n^2 \longrightarrow \infty$ we recover

$$s^4 + s^2(3K_2 - K_1K_2 + 1) - 4K_1K_2 = 0$$

agreeing with the rigid-body equation.

The pitch characteristic equation remains, as in the rigid case,

$$s^2 + \omega_p^2 = 0 \qquad (3.2\text{-}5)$$

$$\omega_p^2 = \frac{3(K_1 + K_2)}{1 + K_1K_2} \qquad (3.2\text{-}6)$$

we now proceed to interpret the requirement that Equations (3.2-4) and (3.2-5) have no roots with positive real parts, in terms of requirements on K_1, K_2 and ω_n.

First, from Equation (3.2-6) as in the rigid case

$$K_2 \succ -K_1 \qquad (3.2\text{-}7)$$

Equation (3.2-4) is a cubic in

$$p \stackrel{\text{Def}}{=} s^2$$

We write it in the form

$$F(p) = p^3 + Ap^2 + Bp + C = 0 \qquad (3.2\text{-}8)$$

Descartes' rule of signs gives as necessary conditions

$$A(K_1,\ K_2) > 0$$

$$B(K_1,\ K_2) > 0$$

$$C(K_1,\ K_2) > 0 \qquad (3.2\text{-}9)$$

Substituting from Equation (3.2-4), we find that Equations (3.2-9) require, respectively

$$K_2 > \frac{-\left(\omega_n^{\,2} + 2 + K_1\right)}{6 - 2K_1} \qquad (3.2\text{-}10a)$$

$$K_2 > \frac{8 - \omega_n^{\,2} - 8K_1}{3\left(\omega_n^{\,2} + 8\right) - K_1\left(\omega_n^{\,2} + 16\right)} \qquad (3.2\text{-}10b)$$

$$K_1\left[4 - K_2\left(\omega_n^{\,2} + 8\right)\right] > 0 \qquad (3.2\text{-}10c)$$

For the cases of interest, $\omega_n^{\,2} \geq 1$, and, physically, $|K_i| \leq 1$. Requirements 3.2-7 and 3.2-10c are strongest for all values of K_1, K_2. Equation (3.2-10c) requires:

$$\text{If } K_1 < 0: \qquad K_2 > \frac{4}{\omega_n^{\,2} + 8}$$

$$\text{If } K_1 > 0: \qquad K_2 < \frac{4}{\omega_n^{\,2} + 8} \qquad (3.2\text{-}11)$$

Requirements 3.2-7 and 3.2-10c lead to the stability diagram of Figure 3.9, with the location of the dotted boundaries still uncertain.

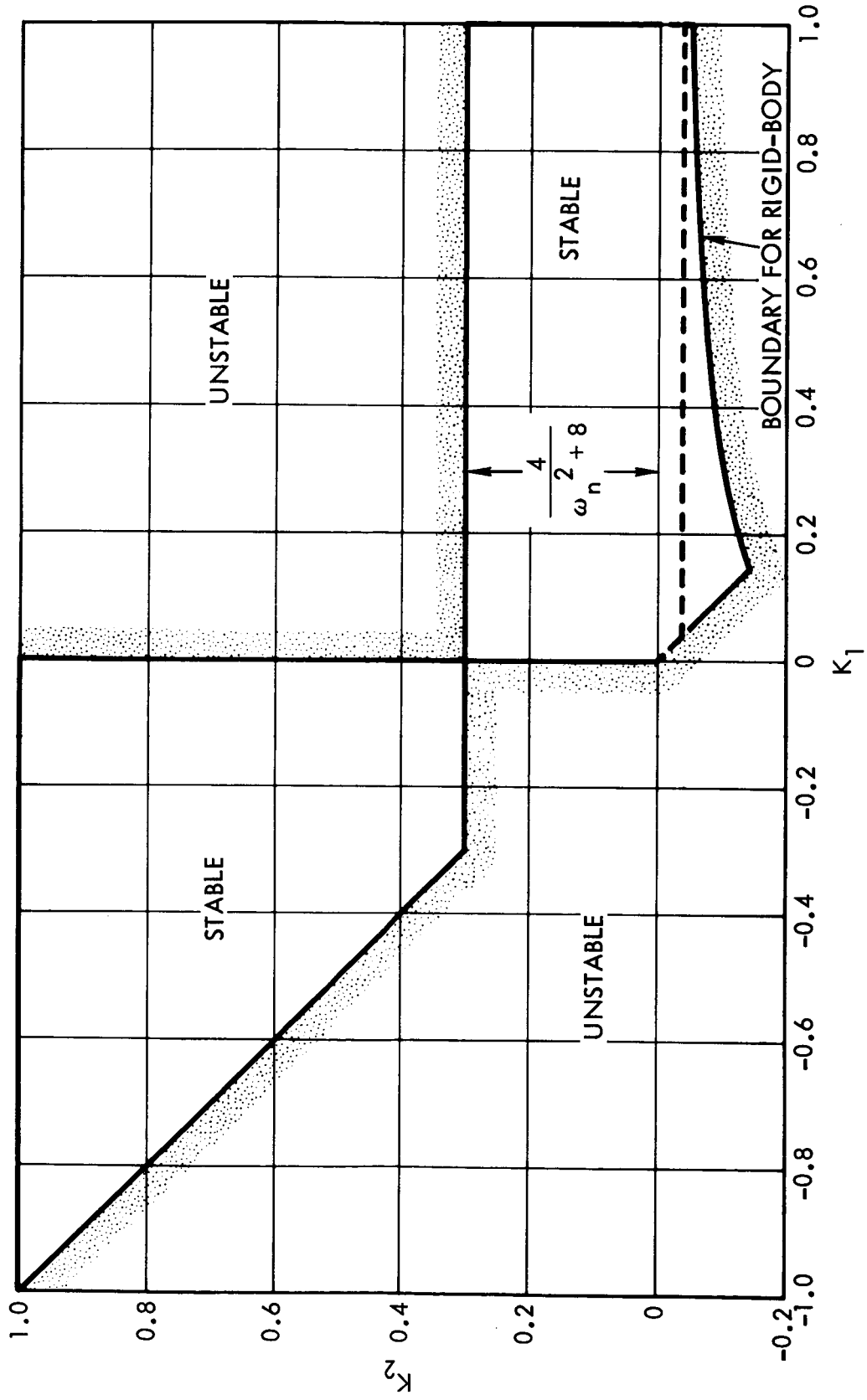

Figure 3.9. Partial Stability Diagram for Flexible Body

The principal change from the rigid-body case (Figure 3.3) is an increase in size of the Delp region and a shrinking of the main region. We now determine the remaining boundaries.

The requirements of Equations (3.2-9) limit the cubic, Equation (3.2-8) to one of the three forms shown in Figure 3.10. Of these, only curve II yields three negative real roots, corresponding to $s = \pm i\omega$. The transition from neutrally stable to unstable behavior occurs when the cubic has a double root. There are several ways of finding the condition. A convenient method, leading to hand solution, is to write Equation (3.2-8) in the factored form

$$(p + r)^2(p + r_3) = 0 \qquad (3.2\text{-}12)$$

with $-r$ the location of the double root, and $-r_3$ the third root.

Comparison of Equations (3.2-12) and (3.2-8) leads to the conditions

$$2r + r_3 = A(K_1, K_2)$$

$$r^2 + 2rr_3 = B(K_1, K_2)$$

$$r^2 r_3 = C(K_1, K_2) \qquad (3.2\text{-}13)$$

For a hand solution we choose r as a parameter. Substituting the expressions for A, B and C from Equation (3.2-4) and into Equation (3.2-13) and eliminating K_1, we find

$$(\alpha_1\alpha_2 - \alpha_3\alpha_4)K_2^2 + (\beta_1\alpha_2 + \beta_2\alpha_1 - \beta_3\alpha_4 - \beta_4\alpha_3)K_2 + (\beta_1\beta_2 - \beta_3\beta_4) = 0$$

(3.2-14)

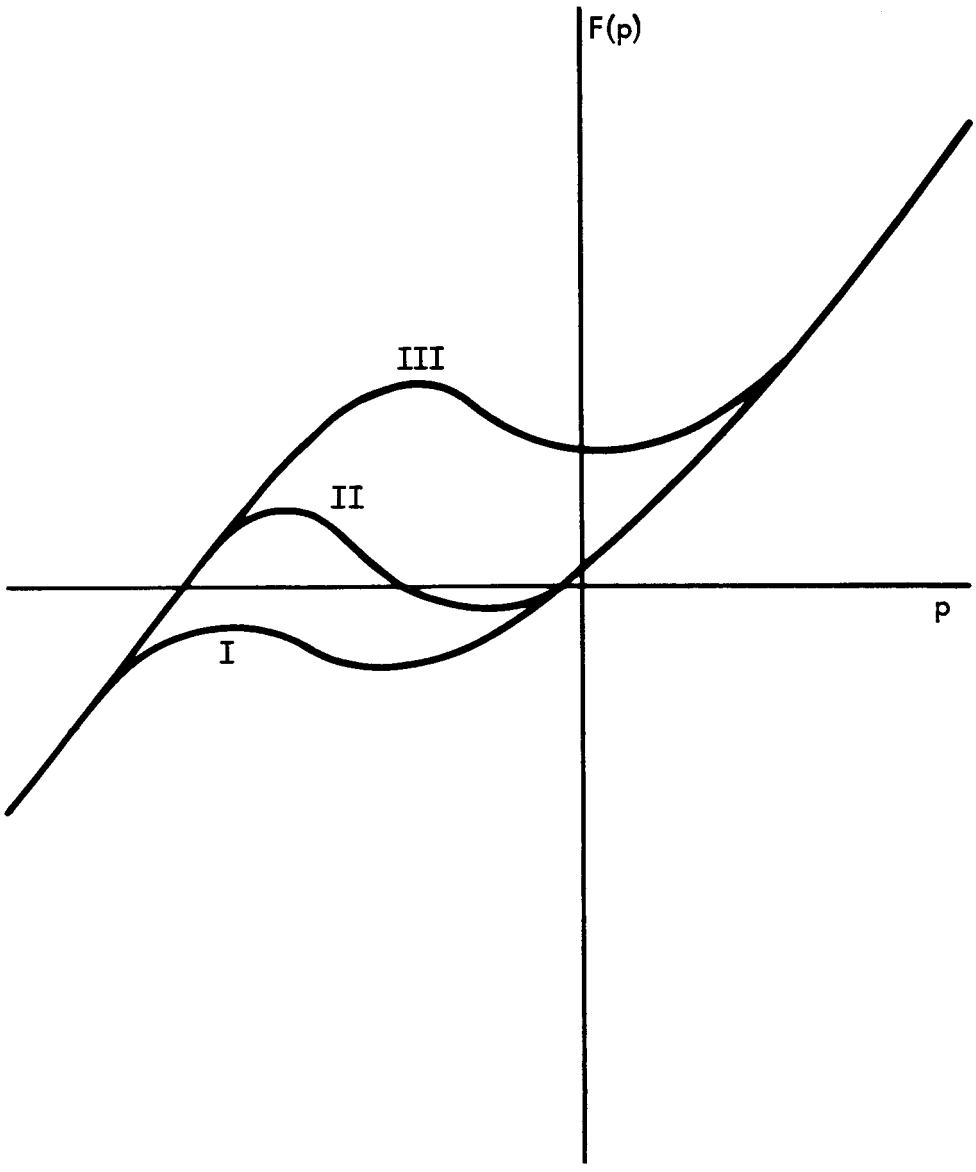

Figure 3.10. Possible Shapes for the Cubic of Equation (3.2-8)

with

$$a_1 = 3\left(4r - \omega_n^2 - 8\right)$$

$$\beta_1 = 4r + 2r\omega_n^2 - 3r^2 - \omega_n^2 + 8$$

$$a_2 = 2\left(-2\omega_n^2 - 16 + r^2\right)$$

$$\beta_2 = 16 - r^2$$

$$a_3 = 6r^2$$

$$\beta_3 = r^2\left(2 + \omega_n^2 - 2r\right)$$

$$a_4 = 4r - \omega_n^2 - 16$$

$$\beta_4 = 8 - 2r$$

and

$$K_1 = \frac{r^2\left(6K_2 + 2 + \omega_n^2 - 2r\right)}{-4K_2\omega_n^2 + (16 - r^2)(1 - 2K_2)} \qquad (3.2\text{-}15)$$

For given r and ω_n^2 the quadratic Equation (3.2-14) yields two values of K_2 for which double roots exist. The corresponding values of K_1 are found from Equation (3.2-15). $K_1(r)$ and $K_2(r)$ are then the parametric equations of the stability boundary curve. The stable and unstable sides of the curve are found by varying K_1 or K_2 slightly and observing the sign of the cubic, Equation (3.2-8). The physically realizable portion of the stability boundary is a curve in the lower right quadrant, which, for $\omega_n^2 \longrightarrow \infty$, approaches the curved rigid-body stability boundary of Equation (3.1-7d).

The entire infinitesimal-amplitude stability picture is presented in Figures 3.11 to 3.13 for several values of ω_n^2. The effect of the double-root condition is to decrease the size of the Delp region.

The rather complex behavior in the region $K_1 > 0$ has been checked numerically by the Floquet procedure of Appendix C. Stable points are shown as circles and unstable points as x's.

3.2.4 Infinitesimal-Amplitude Stability Boundaries With Damping

The discussion of stability in the previous section referred to stability in the sense of boundedness, with roots on the imaginary axis. We now investigate the asymptotic stability of the roll-yaw system, Equations (3.2-1), for $\zeta \neq 0$.

We first note that the pitch equation is unchanged by the introduction of damping, so that $K_1 + K_2 > 0$ is still the condition for pitch stability. The examination of roll-yaw stability in the presence of damping is facilitated by application of Zajac's recent extension of the Kelvin-Tait-Chetaev theorem (Reference 3.8).

The equations for a large class of satellite attitude problems can be cast in the form

$$[A](\ddot{\underset{\sim}{x}}) + [G](\dot{\underset{\sim}{x}}) + [C](\dot{\underset{\sim}{x}}) + [K](\underset{\sim}{x}) = 0 \qquad (3.2\text{-}16)$$

where

- $[A]$ is a positive-definite inertia matrix
- $(\underset{\sim}{x})$ is the coordinate vector
- $[C]$ is a symmetric damping matrix which is either positive definite or positive semidefinite
- $[G]$ is a skew-symmetric matrix resulting from gyroscopic terms in the equations of motion
- $[K]$ is a symmetric stiffness matrix.

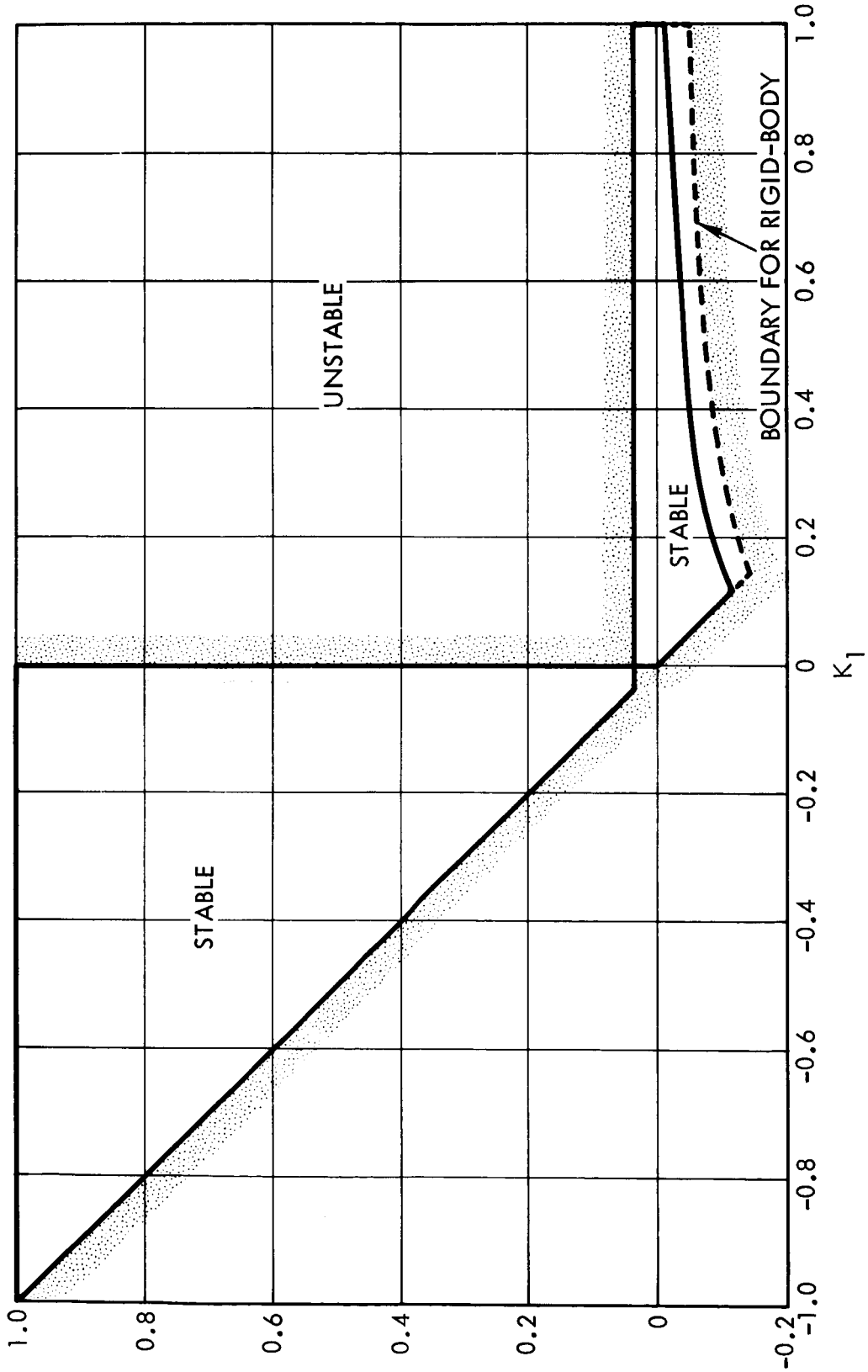

Figure 3.11. Regions of Infinitesimal Stability for $\omega_n = 10$

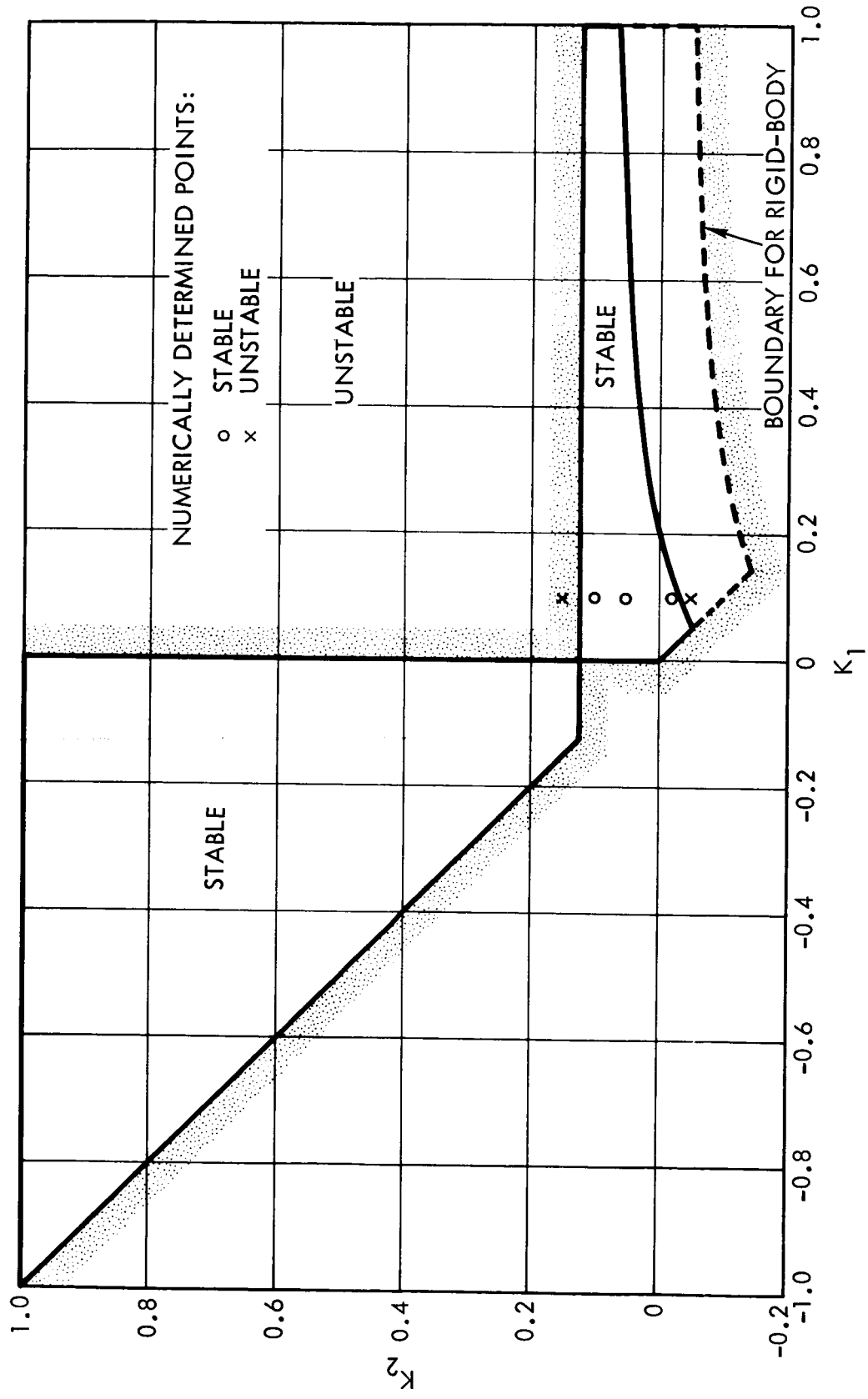

Figure 3.12. Regions of Infinitesimal Stability for $\omega_n = 5$

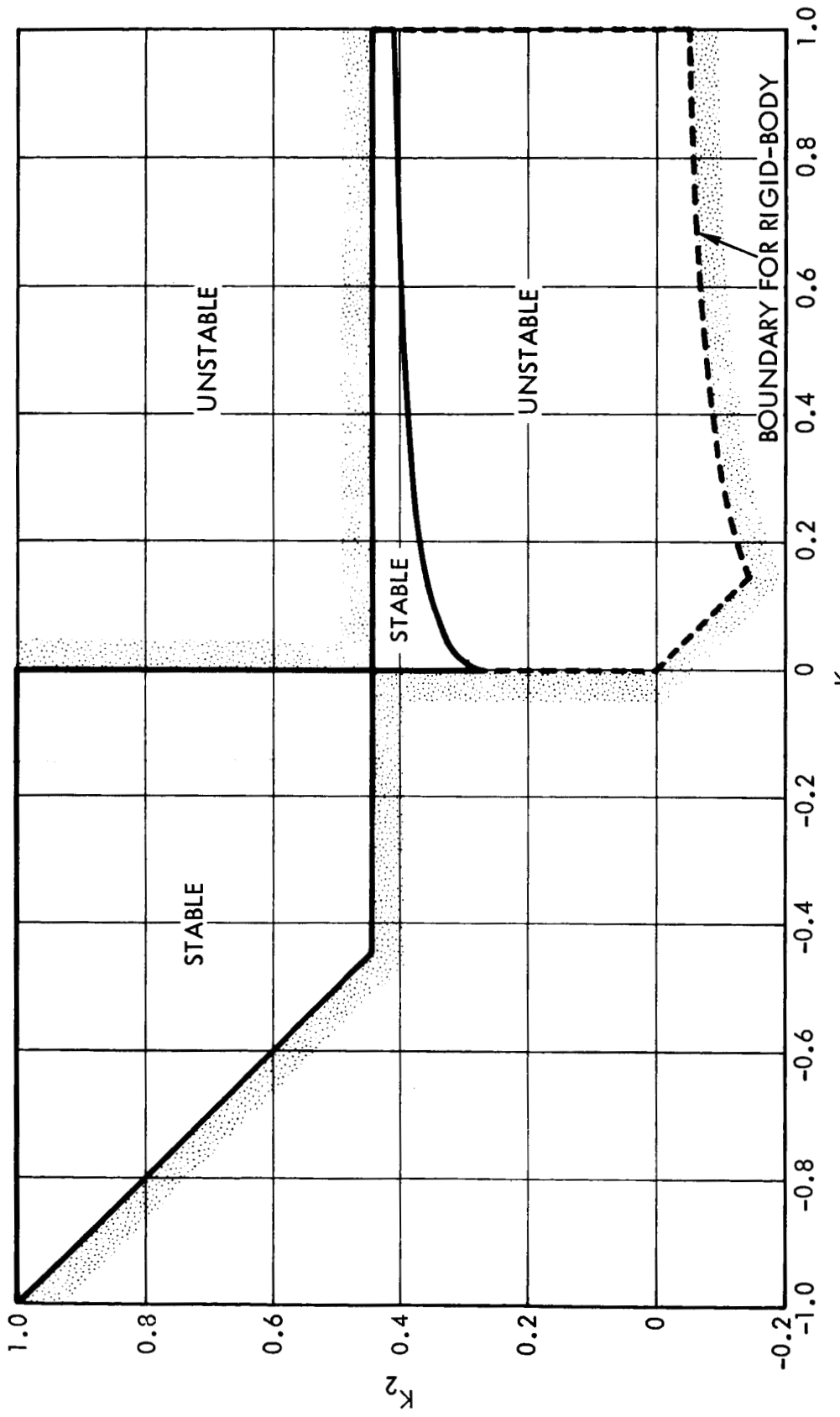

Figure 3.13. Regions of Infinitesimal Stability for $\omega_n = 1$

In the conventional passive linear systems encountered in structural dynamics, the coefficients of the coordinate velocities form a symmetric, positive-definite damping matrix. For systems such as the one considered here, the velocity matrix may have a skew-symmetric component, as seen in Equations (3.1-4). Thomson, in Reference 3.9, showed that it is possible to achieve neutral stability with such a system, even though the system would be unstable without the matrix of velocity coefficients.

Loosely, the Kelvin-Tait-Chetaev theorem states that such gyroscopic stabilization of an unstable system is not usually feasible when damping is introduced.

In the present situation the damping matrix will be shown to be positive semidefinite rather than positive definite. Zajac has extended the Kelvin-Tait-Chetaev theorem to cover this case. His result is (Reference 3.8) the following:

In the equation

$$[I](\ddot{\underset{\sim}{x}}) + [C](\dot{\underset{\sim}{x}}) + [G](\dot{\underset{\sim}{x}}) + [K](\underset{\sim}{x}) \qquad (3.2\text{-}17)$$

let

$[I]$ be the unit matrix

$[C]$ be a symmetric, positive semidefinite matrix

$[G]$ be a skew-symmetric matrix

$[K]$ be a diagonal matrix

Then the system described by Equation (3.2-17) is stable if the diagonal elements of $[K]$ are <u>all positive</u> and unstable if they are <u>all negative</u>. For the proof, we refer to Reference 3.8.

3.2.4.1 Application of Kelvin-Tait-Chetaev Theorem

We rewrite the linearized equations of the present problem, Equations (3.2-1), in the more symmetric form described in Appendix B, Section B.8.

$$\begin{bmatrix} I_1 & 0 & 0 \\ 0 & I_3 & 0 \\ 0 & 0 & I_1 \end{bmatrix} \begin{bmatrix} \ddot{\theta}_1 \\ \ddot{\theta}_3 \\ \ddot{\beta} \end{bmatrix} + \begin{bmatrix} 0 & (I_2 - I_3 - I_1)\omega_o & 0 \\ -(I_2 - I_3 - I_1)\omega_o & 0 & 0 \\ 0 & 0 & 0 \end{bmatrix} \begin{bmatrix} \dot{\theta}_1 \\ \dot{\theta}_3 \\ \dot{\beta} \end{bmatrix} + \begin{bmatrix} c & 0 & -c \\ 0 & 0 & 0 \\ -c & 0 & c \end{bmatrix} \begin{bmatrix} \dot{\theta}_1 \\ \dot{\theta}_3 \\ \dot{\beta} \end{bmatrix} + \begin{bmatrix} 4(I_2 - I_3)\omega_o^2 + k & 0 & -k \\ 0 & (I_2 - I_1)\omega_o^2 & 0 \\ -k & 0 & 4I_1\omega_o^2 + k \end{bmatrix} \begin{bmatrix} \theta_1 \\ \theta_3 \\ \beta \end{bmatrix} = \begin{bmatrix} 0 \\ 0 \\ 0 \end{bmatrix} \quad (3.2\text{-}18)$$

or, abbreviating

$$[A](\ddot{\underset{\sim}{x}}) + [G_1](\dot{\underset{\sim}{x}}) + [C_1](\dot{\underset{\sim}{x}}) + [K_1](\underset{\sim}{x}) = (\underset{\sim}{0}) \quad (3.2\text{-}19)$$

Here

$$\beta = \theta_1 + \alpha$$

c is the dashpot constant

k is the spring constant

The positive definiteness of $[C_1]$ is determined by its eigenvalues, which are 0, 0, 2c, so that $[C_1]$ is positive semidefinite.

Equations (3.2-18) are not in the form needed for application of the theorem. They can be reduced to that form by premultiplying by $[A]^{-1}$ and making the transformation

$$(x) = [M](y)$$

where $[M]$ is the modal matrix of the eigenvalue problem

$$\left[[A]^{-1}[K] - \lambda[I]\right](\underset{\sim}{x}) = 0$$

The norms of the modal columns can be adjusted so that the new matrices of velocity coefficients

$$[G'] = [M]^{-1}[A]^{-1}[G_1][M]$$

$$[C'] = [M]^{-1}[A]^{-1}[C_1][M]$$

are still skew-symmetric and symmetric positive semidefinite, respectively. Then stability is determined by the elements of the diagonal matrix

$$[M]^{-1}[A]^{-1}[K_1][M]$$

which are the roots λ of

$$\left|[K] - \lambda[A]\right| = 0 \qquad (3.2\text{-}20)$$

There is no need to carry out the transformations explicitly; the diagonal elements are simply the eigenvalues λ_i defined by Equation (3.2-20), and are given by

$$\left[(I_2 - I_1)\omega_o^2 - \lambda I_3\right]\left\{\left[4(I_2 - I_3)\omega_o^2 + k - \lambda I_1\right]\left[4I_1\omega_o^2 + k - \lambda I_1\right] - k^2\right\}$$

with roots

$$\lambda_1 = \frac{(I_2 - I_1)}{I_3}\omega_o^2$$

$$\lambda_{2,3} = \frac{2(I_1 + I_2 - I_3)\omega_o^2 + k}{I_1} \pm \frac{\left[4(I_2 - I_3 - I_1)^2\omega_o^4 + k^2\right]^{1/2}}{I_1}$$

or, introducing the K-notation [Equations (3.2-3)],

$$\frac{\lambda_1}{\omega_o^2} = -K_1$$

$$\frac{\lambda_{2,3}}{\omega_o^2} = 4K_2 + \frac{\omega_n^2}{2} \pm \left[16(K_2 - 1)^2 + \frac{\omega_n^4}{4}\right]^{1/2}$$

For all the λ's to be greater than zero we require

$$K_1 < 0 \qquad (3.2\text{-}21a)$$

$$K_2 > -\frac{\omega_n^2}{8} \qquad (3.2\text{-}21b)$$

a positive discriminant, leading to

$$16(K_2 - 1)^2 + \frac{\omega_n^4}{4} > 0 \qquad (3.2\text{-}21c)$$

which is always satisfied, and two negative roots of the quadratic, leading to

$$\left(4K_2 + \frac{\omega_n^2}{2}\right)^2 > 16(K_2 - 1)^2 + \frac{\omega_n^4}{4}$$

$$K_2 > \frac{4}{\omega_n^2 + 8} \qquad (3.2\text{-}21d)$$

Conditions (3.2-21) are sufficient for stability of the damped system. Condition (3.2-21d) is the same as for stability of the main region in the undamped case, Equation (3.2-11). Condition (3.2-21a) does not hold for $K_1 > 0$, so that the stability of the Delp region in the presence of damping is not guaranteed.

To prove instability from Zajac's extension to the Kelvin-Tait-Chetaev theorem, we require that all of the inequalities, Equations (3.2-21) be reversed. Since (3.2.21b) never occurs for a system stable in the absence of damping, the theorem says nothing definite about the stability of the modified Delp region.

3.2.4.2 Stability of Damped System from Characteristic Equation

The characteristic equation for the damped system is obtained by Laplace transforming Equations (3.2-1) and evaluating the determinant. The result was given in Equation (3.2-4) for the case $\zeta = 0$. In general it has the form

$$s^6 + A_5 s^5 + A_4 s^4 + A_3 s^3 + A_2 s^2 + A_1 s + A_o$$

$$A_i = A_i(K_1, K_2) \qquad (3.2\text{-}22)$$

A_4, A_2 and A_o are given in Equation (3.2-4) for the undamped case and are not changed by the introduction of damping. The other coefficients are

$$A_5 = 2\zeta\omega_n$$

$$A_3 = 2\zeta\omega_n(3K_2 + 1 - K_1K_2)$$

$$A_1 = 8\zeta\omega_n(-K_1K_2) \qquad (3.2\text{-}23)$$

A necessary condition is $A_i > 0$. We see immediately that

$$A_1 > 0 \qquad (3.2\text{-}24)$$

requires $K_1K_2 < 0$ and means that the portion of the Delp region for which $K_2 > 0$ is unstable. A_5 and A_3 are always positive in the regions of interest.

3.2.4.3 Results: Infinitesimal Stability for Damped Case

Figures 3.14 and 3.15 show the stability picture in the case of damping for $\omega_n = 5$ and 1. Condition (3.2-24) shows that the quadrant $K_1 > 0$, $K_2 > 0$ is unstable but gives no information about the quadrant $K_1 > 0$, $K_2 < 0$, which contains a small triangular portion of the modified Delp region. Bodies in this region are nearly spherical and not of particular interest.

Stability could be evaluated through the Routh-Hurwitz criterion, but the first three Routh-Hurwitz determinants give no new information and the results may not merit the algebra required to proceed further.

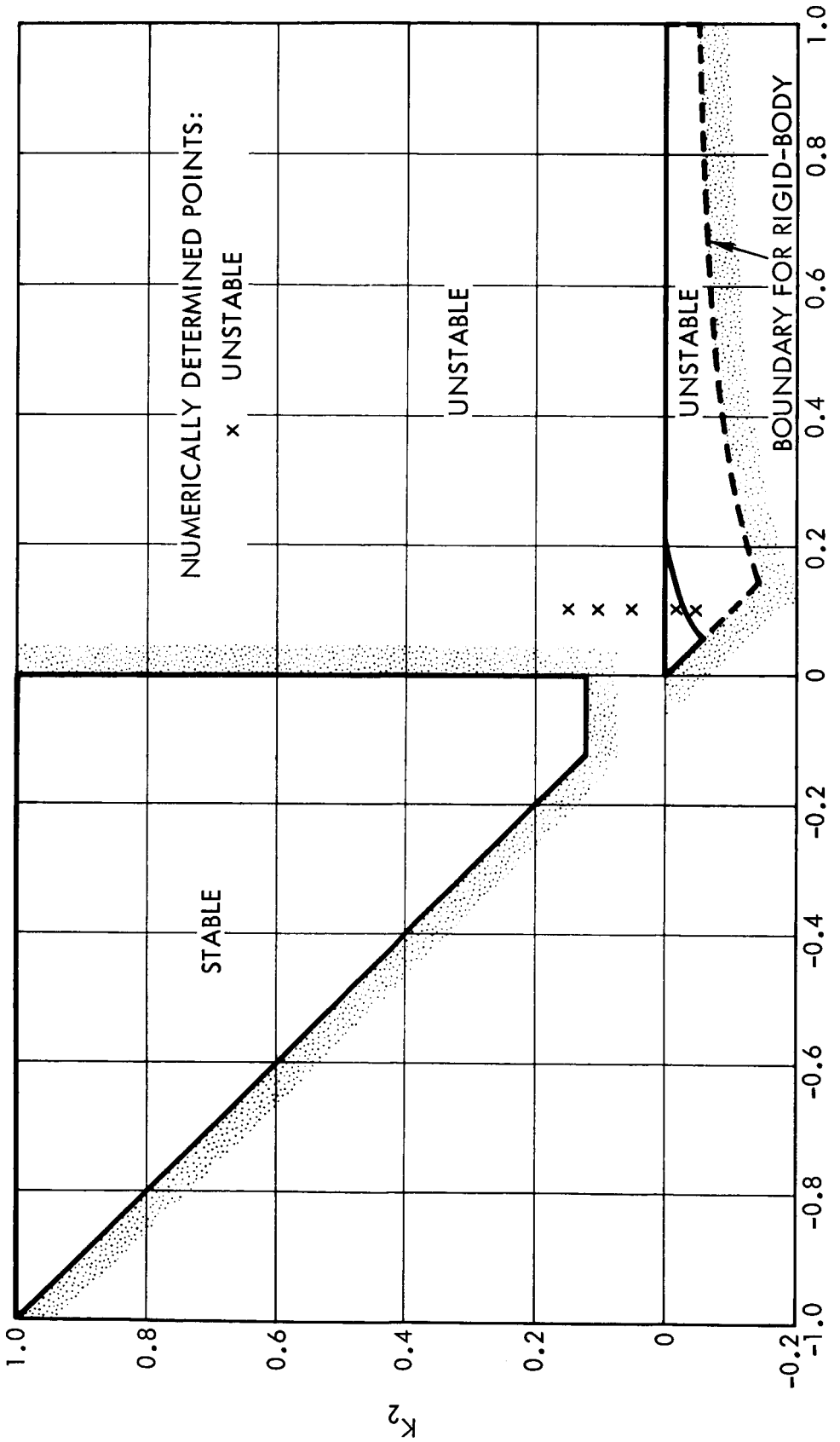

Figure 3.14. Regions of Infinitesimal Stability for Damped System, With $\omega_n = 5$

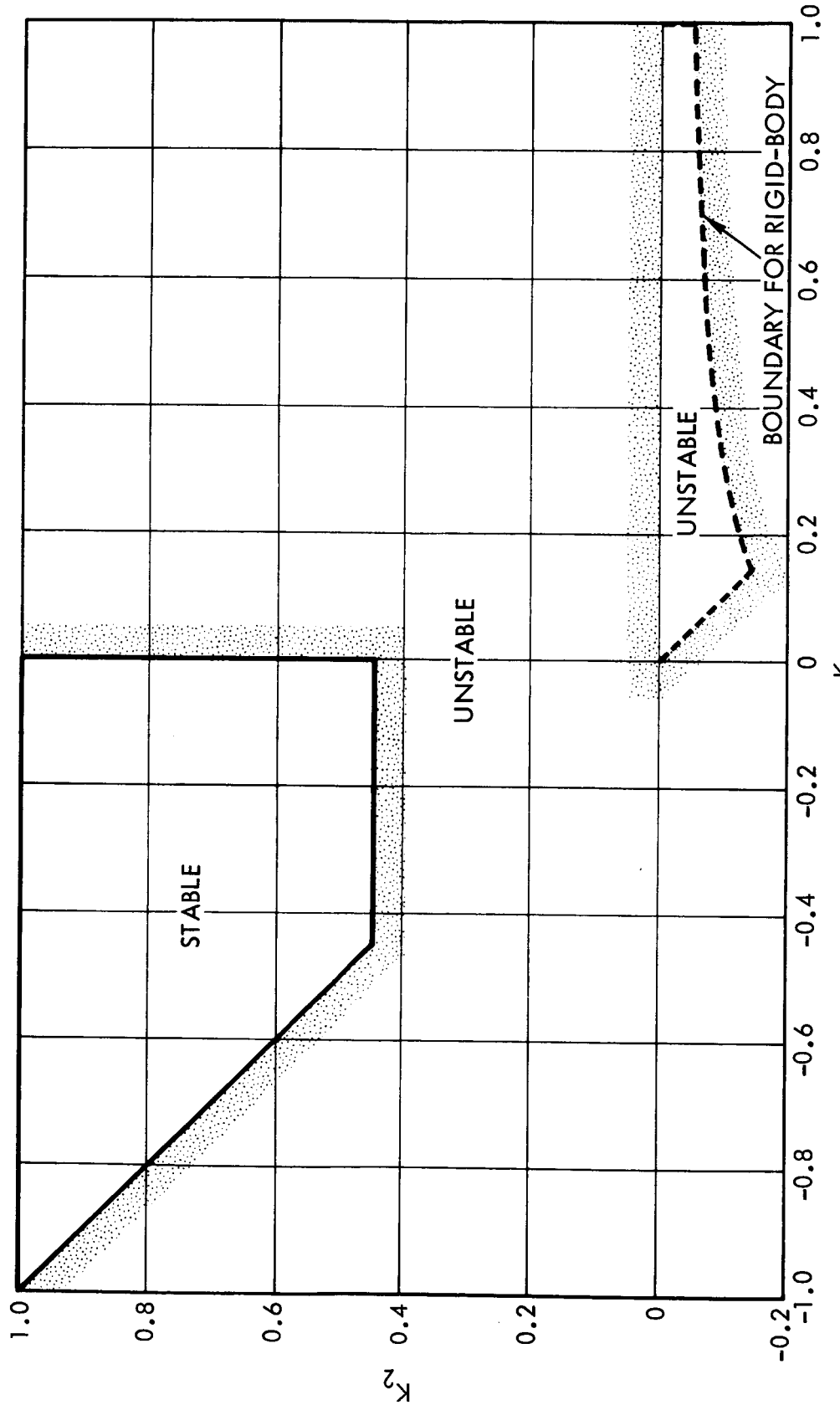

Figure 3.15. Region of Infinitesimal Stability for Damped System, With $\omega_n = 1$

Numerical evaluation at discrete points through the Floquet procedure has confirmed the results for the case $\omega_n = 5$. Unstable points are marked by crosses in Figure 3.14. The point taken in the small triangular region showed instability.

3.2.5 A Physical Interpretation

One result of the investigation of infinitesimal stability has been the reduction in size of the main stable region in the K_1-K_2 plane, which would seem to lead to the conclusion that the flexible body considered is "less stable" than a rigid body. The actual situation is somewhat different: The reduction in the size of the region is a statement of the unsurprising fact that an unstable main body can be stabilized by coupling it to a gravitationally stabilized rod (the subsidiary body) through a sufficiently strong spring. The misleading reduction in area is a consequence of the introduction of the parameters K_1 and K_2, which are very convenient computationally but not very meaningful physically.

To examine the situation, consider the symmetric linearized Equations (3.2-18), for the case $I_1 + I_2 > 2I_1 > I_3$ (the main region for the composite body), and for no damping.

We will determine the conditions for stability in the absence of the velocity-dependent gyroscopic terms. That is, the conditions under which a small angular displacement is resisted by a restoring moment, irrespective of the angular rate. Such a discussion would have no meaning for the Delp region, $K_1 > 0$, because as Zajac has shown, the velocity-dependent gyroscopic terms are necessary to provide stability.

In the absence of the coefficients of $\dot{\theta}_1$, $\dot{\theta}_3$ and $\dot{\beta}$, the system of Equation (3.2-18) can be represented by the linear mechanical analog of Figure 3.16, which has the same equations of motion. k_b and k_c are positive, while k_a can be either positive or negative. For convenience we take $I_1 = m_1 = 1$.

The characteristic equation for the system of Figure 3.16 is

$$\left(s^2 + k_a + k_b\right)\left(s^2 + k_c + k_b\right) - k_b^2 = 0$$

following the procedure of Section 3.2.4.1, we derive the condition for no positive real root. It is

$$k_a > -\frac{k_b k_c}{k_b + k_c} \qquad (3.2\text{-}26)$$

That is, k_a need not be positive, it only needs to be greater than a particular negative number. Then

$$\frac{I_1 k_a}{4} = (I_2 - I_3)\omega_o^2$$

can be negative, corresponding to a main body which is gravitationally unstable by itself.

Converting to the K_1-K_2 notation, we have

$$k_a = \frac{4(I_2 - I_3)\omega_o^2}{I_1} = 4(2K_2 - 1)\omega_o^2$$

$$k_b = \frac{k}{I_1} = \frac{\omega_n^2 \omega_o^2}{2}$$

$$k_c = 4$$

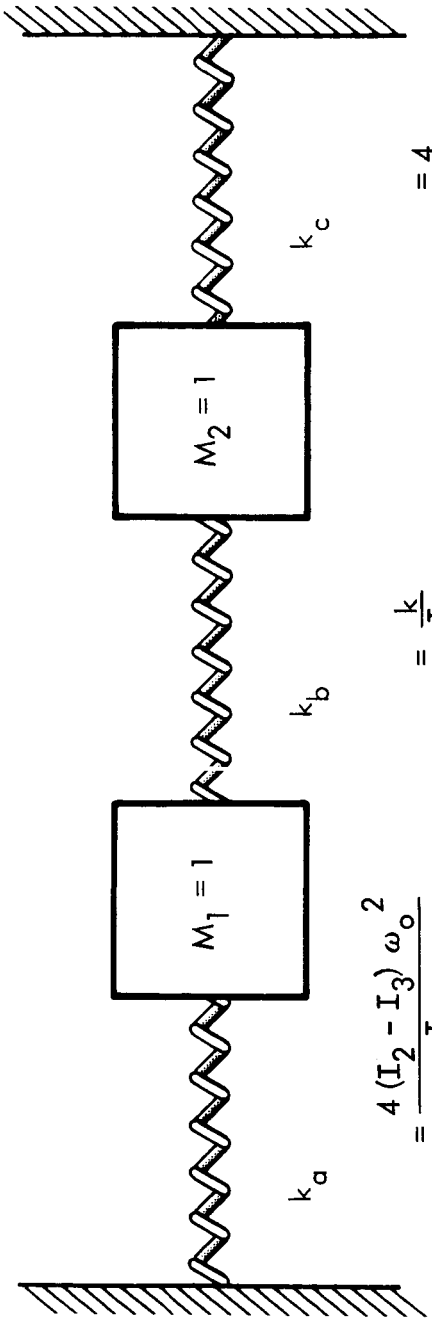

Figure 3.16. Mechanical Analog for Equations (3.2-18), Ignoring Gyroscopic Terms

so the inequality (3.2-26) converts to

$$K_2 > \frac{4}{\omega_n^2 + 8}$$

which is Condition (3.2-11) of Section 3.2.3, showing that the horizontal stability boundary in the main region of the K_1-K_2 plane merely represents a necessary condition for stabilization of an unstable main body by the addition of a (gravitationally stable) subsidiary rod body.

3.3 Stability of Planar Pitching Motion for a Flexible Satellite

The preceding section has established the stability behavior of the particular flexible satellite chosen for study, on the basis of linearized equations. We now proceed to examine the feasibility of purely planar pitching motion at noninfinitesimal amplitude, the problem studied by Kane for the rigid body. We wish to determine whether purely planar motion can exist for noninfinitesimal amplitudes of motion, or whether small initial deviations in the roll and yaw coordinates will build up and cause the motion to become three-dimensional.

The problem will be studied by Kane's Floquet theory technique (Appendix C).

We first derive the equations of motion for the flexible body, retaining the pitch angle θ_2 as a large angle but considering θ_1, θ_3 and α to be small. The derivation and the final equations [Equations (B-11)] are given in Appendix B. The pitch equation, as in the rigid case, is

$$\ddot{\theta}_2 + \frac{\omega_p^2}{2} \sin \theta_2 = 0$$

$$\omega_p^2 = \frac{3(K_1 + K_2)}{1 + K_1 K_2} \qquad (3.3\text{-}1)$$

Where dots denote derivatives with respect to

$$\tau = \omega_o t$$

The roll-yaw equations couple with the equation for elastic deformation to form a sixth-order system whose coefficients are functions of θ_2, $\dot{\theta}_2$ and the parameters K_1, K_2, ζ, ω_n. The coefficients are periodic functions of time because θ_2 is periodic.

As shown in Appendix C, the stability of the sixth-order roll-yaw system can be evaluated by determining its characteristic multipliers λ_i defined by

$$\left[\underset{\sim}{x}_i\left(t + \frac{2\pi}{\Omega}\right)\right] = \lambda_i\left[\underset{\sim}{x}_i(t)\right] \quad i = 1, \cdots 6 \tag{3.3-2}$$

$$(\underset{\sim}{x}_i) = \begin{bmatrix} \theta_1 \\ \theta_3 \\ \alpha \\ \dot{\theta}_1 \\ \dot{\theta}_3 \\ \dot{\alpha} \end{bmatrix}_i \tag{3.3-3}$$

where $(\underset{\sim}{x}_i)$, $i = 1, 2 \cdots 6$ are a fundamental set of solutions of the system, each corresponding to a particular set of initial conditions, called normal solutions, and Ω is the frequency of parametric excitation.

Except in special cases, a sixth-order system will have six distinct λ_i which in general are complex numbers. If any of them are greater than one in magnitude, that part of the solution will grow without bound, until limited by physical nonlinearities not implicit in the original equations.

The characteristic multipliers are a logical extension of constant-coefficient techniques to systems with periodic coefficients. For a system with constant coefficients (zero pitch amplitude), the Floquet procedure leads [Appendix C, Equation (C-13)] to characteristic multipliers

$$\lambda_i = \exp\left(s_i \frac{2\pi}{\Omega}\right) \tag{3.3-4}$$

where s_i are the characteristic roots of the linear system, and Ω is the frequency of variation of the coefficients. Equation (3.3-4) can be used for program checkout and also for numerical stability evaluation of constant coefficient equations.

If, for a particular set of values of K_1, K_2, ζ, ω_n, there exist one or more λ_i such that $|\lambda_i| > 1$ then an initial planar pitching motion, with infinitesimal roll and yaw angles, will not remain planar, because roll and yaw amplitudes will build up.

The procedure for determining the characteristic multipliers, given in Appendix C, involves using a computer to numerically integrate the sixth-order system over one period of the pitch motion. The integration is performed six times, starting with different initial conditions. The multipliers appear as the eigenvalues of a sixth-order matrix formed from the solutions.

The computer program requires between 3 and 10 minutes on the IBM 7094, depending on the values of ω_n and K_1. The large amount of computer time required makes it necessary to use the perturbation-solution technique of Section 3.1.4 to locate regions of possible instability.

3.3.1 Selection of Parameters for Examination

It was shown in Section 3.1.4 that, for small amplitudes of parametric excitation, instabilities may occur where

$$\omega_p \simeq \pm \frac{s_i - s_j}{n} \qquad (3.3\text{-}5)$$

where s_i, s_j are any two of the characteristic roots of the corresponding constant-coefficient system, and n is a positive integer.

In particular, parametric resonance occurs for

$$\omega_p \simeq 2\omega \tag{3.3-6}$$

with ω one of the three frequencies of the undamped sixth-order roll-yaw system.

In the present study, attention is confined to possible unstable points in the K_1-K_2 plane defined by Equation (3.3-6). Equation (3.3-5) predicts other loci of possible instability which should be studied in a more comprehensive investigation. Kane's results for the rigid body lead us to the conclusion that the double-frequency line given by Equation (3.3-6) is the most promising place to begin.

In the selection of the body stiffness parameter ω_n^2, two considerations limit the choice:

A. Since we are considering a "flexible body," as opposed to "two loosely coupled rigid bodies," we will restrict ω_n^2 to be somewhat higher than the rigid-body frequencies. The K_1-K_2 format is not particularly suitable for an investigation of the behavior of an extremely flexible system.

B. The computer time required to integrate over one cycle of ω_p at given accuracy is proportional to ω_n, and cases for which $\omega_n > 10$ are prohibitively expensive.

3.3.2 Location of Lines of Parametric Resonance

The parametric resonance condition, Equation (3.3-6), occurs where a root

$$s = i\omega \tag{3.3-7}$$

of Equation (3.2-4) coincides with the small-amplitude pitch frequency

$$\omega = \frac{\omega_p}{2} = \frac{3(K_1 + K_2)}{2(1 + K_1 K_2)} \tag{3.3-8}$$

To find where resonance occurs, the simplest procedure is to treat ω as a parameter. We substitute Equation (3.3-7) into Equation (3.2-4) and eliminate K_1 by Equation (3.3-8). The result is the following quadratic for K_2

$$\begin{aligned} &6(A + B)(4\omega^4 - \omega^2 + 4)K_2^2 \\ &+ \left[4(A + B)(4\omega^4 - 11\omega^2) + C(3 + 4\omega^4)\right]K_2 \\ &+ \left[-2\omega^2(3 + 4\omega^2)(A + B) - 7\omega^2 C\right] = 0 \end{aligned} \tag{3.3-9}$$

where

$$A = \omega_n^2 + 4 - \omega^2$$

$$B = -\frac{\omega_n^2}{2}$$

$$C = \left(-\omega^2 + \omega_n^2 + 4\right)\left(-\omega^2 - 4\right) + 4\omega_n^2$$

Equation (3.3-9) can be solved for K_2 for given ω and ω_n. Then K_1 is obtained, inverting Equation (3.3-8) as

$$K_1 = \frac{4\omega^2 - 3K_2}{3 - 4\omega^2 K_2} \tag{3.3-10}$$

The locus of parametric resonance is a line in the K_1-K_2 plane, shown for ω_n = 1, 5 and 10 in Figures 3.17 to 3.19. The curve begins at the intersection of the infinitesimal stability boundaries and terminates on the line $K_2 = 1$. ω varies from zero to $\sqrt{3}/2$ along the curve. A second branch of the curve, in the modified Delp region, is not shown. It was shown in Section 3.2.4 that most, if not all, of the modified Delp region is unstable if any damping exists, so that it is not important to study it.

As ω_n^2 tends to infinity the parametric resonance curve approaches the shape given in Figure 3.6 for the rigid-body resonance line.

3.3.3 Stability of Planar Pitching Motion of the Undamped System

Having located the resonance line, we can evaluate stability by the Floquet procedure for various values of K_1 and K_2 on and near the line. Figures 3.17 to 3.19 show the results for ω_n = 1, 5 and 10 for a one degree half-amplitude of pitch motion. Points on the line (to six decimal accuracy) are all unstable and points some distance away are stable.

It is clear that, as in the rigid-body case, a narrow strip exists in which planar pitch motion is impossible for even a one-degree amplitude of motion.

The characteristic multipliers λ_i for the stable cases were found to consist of three complex-conjugate pairs on the unit circle. Characteristic multipliers for the unstable cases consist of two conjugate pairs and two real roots, one of which is slightly less than -1, indicating instability. The fact that the instability arises from the

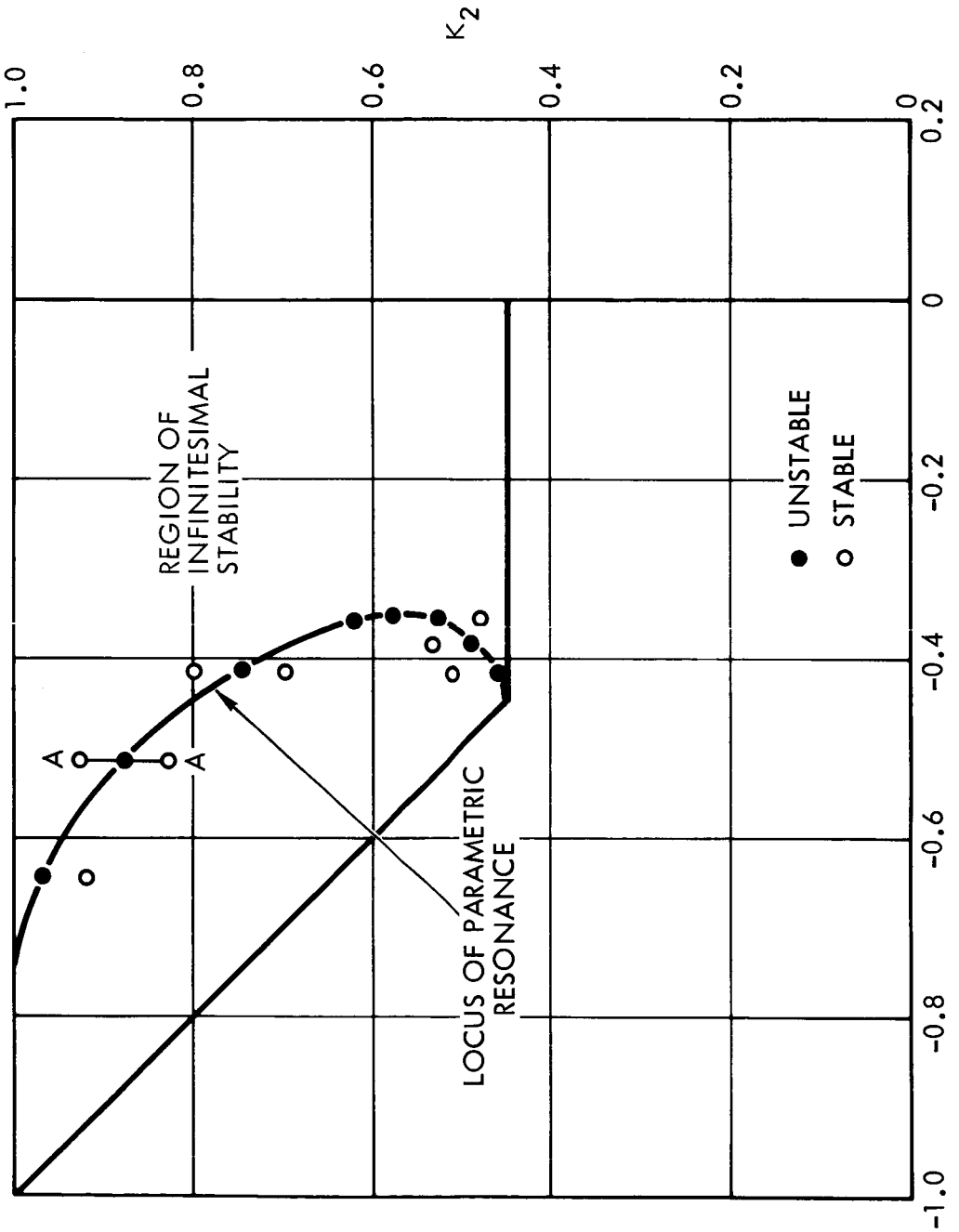

Figure 3.17. Locus of Parametric Resonance for $\omega_n = 1$, Showing Numerical Stability Results for One Degree Pitch Amplitude

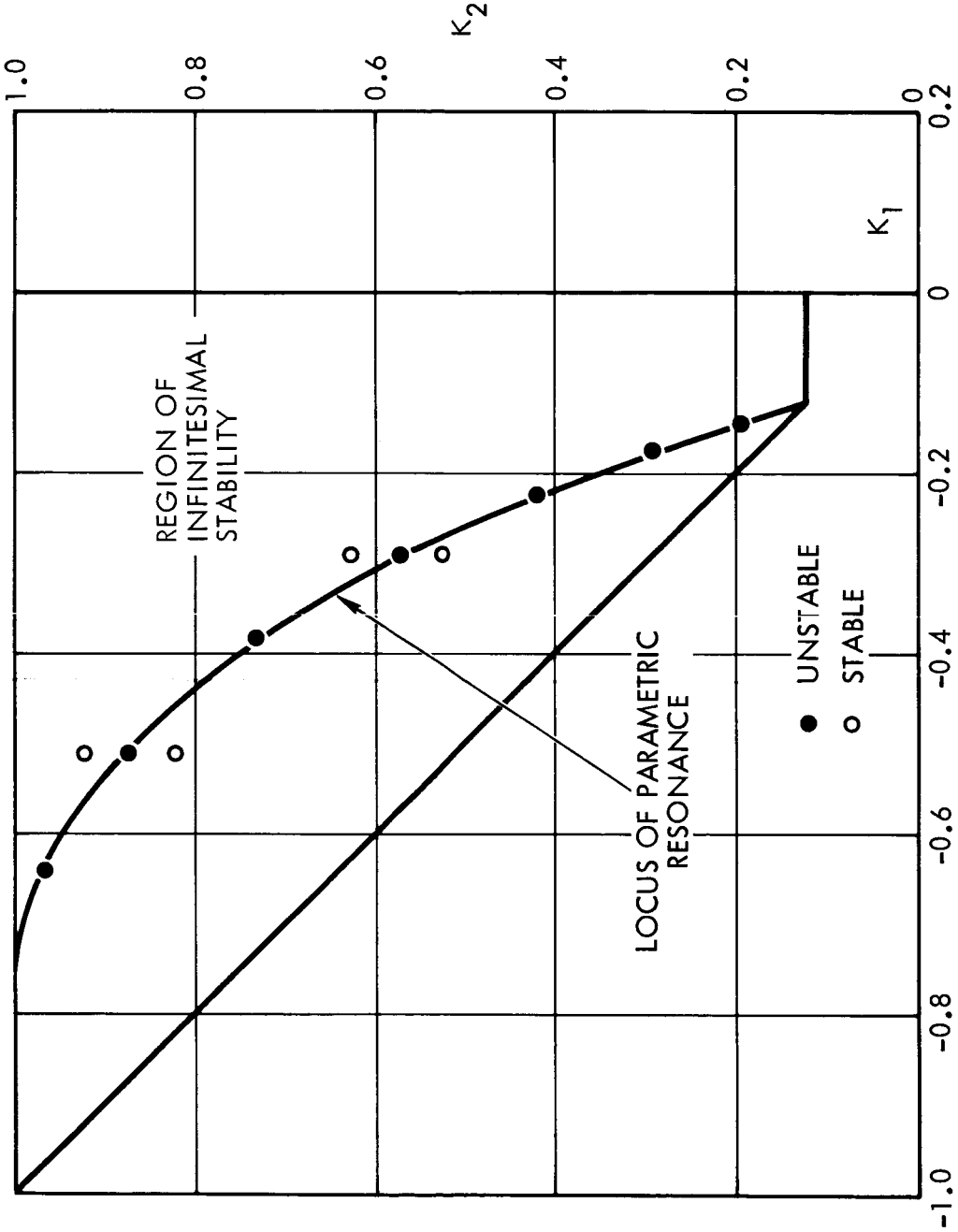

Figure 3.18. Locus of Parametric Resonance for $\omega_n = 5$, Showing Numerical Stability Results for One Degree Pitch Amplitude

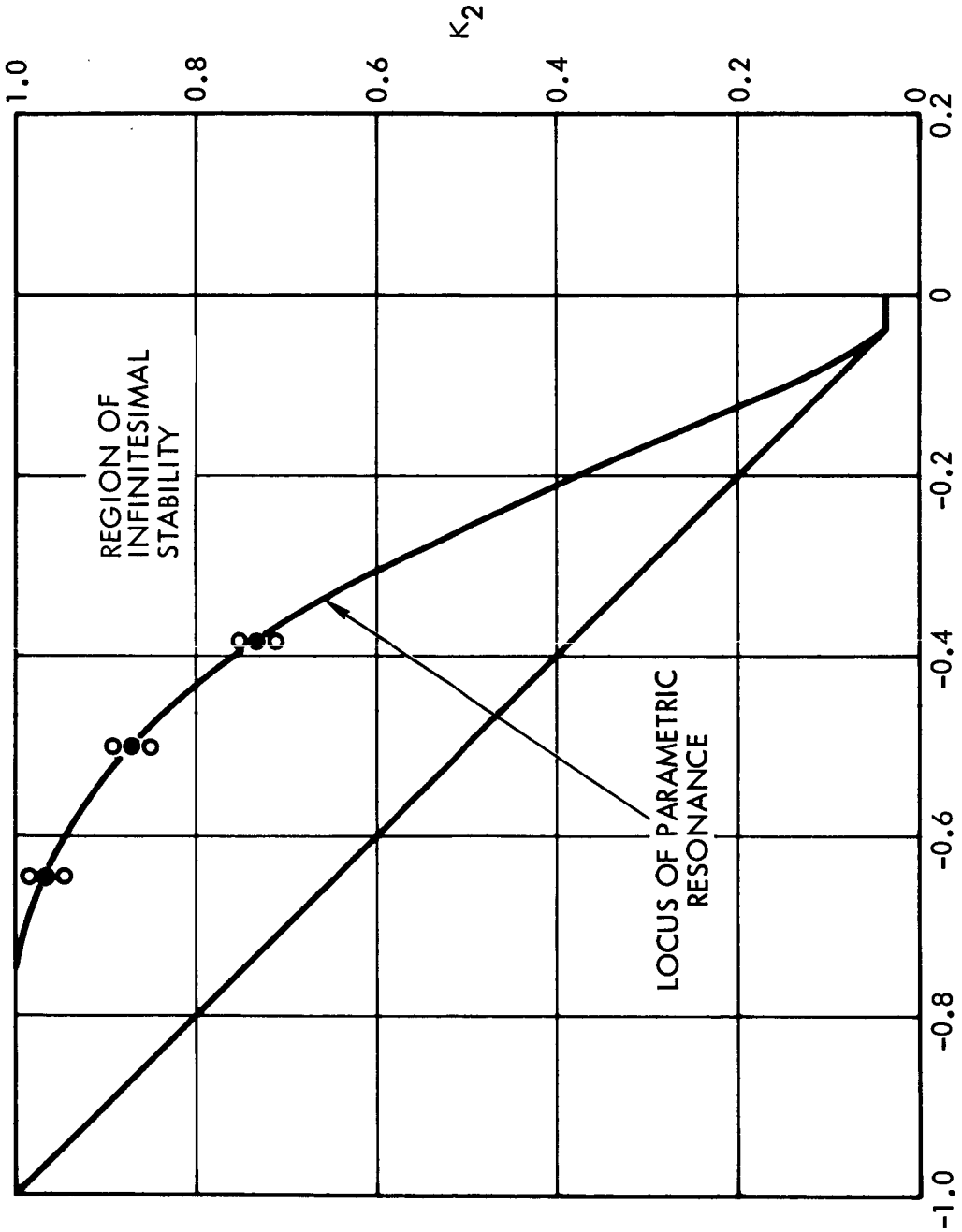

Figure 3.19. Locus of Parametric Resonance for $\omega_n = 10$, Showing Numerical Stability Results for One Degree Pitch Amplitude

parametric resonance condition $\omega_p = \omega$ is indicated by the fact that in the constant-coefficient case (zero pitch amplitude), one of the characteristic roots is

$$s = i\omega = i\frac{\omega_p}{2}$$

and, from Equation (3.3-4), the corresponding multiplier is

$$\lambda = \exp(i\pi) = -1$$

The characteristic multipliers for one degree pitch amplitude are not very large. For one degree pitch amplitude, they typically lie in the range $1 < |\lambda| < 1.05$ corresponding to a growth of 5 percent or less per cycle. In a medium-altitude satellite with a pitch period of 4 hours, the roll-yaw amplitude would take about 57 hours to double, at the rate of 5 percent per cycle.

Figure 3.20 shows how the characteristic multiplier varies as the inertia parameters are varied along the line A-A of Figure 3.17. The unstable region for this case has a width of about 0.02 in K_2, or 2 percent of the stable range, corresponding to a small but perhaps quite significant range of inertia ratios.

3.3.4 Effect of Damping on Stability of Planar Pitch Motion

Damping is one of the chief differences between the idealized rigid body considered by Kane and the somewhat less idealized flexible body considered here.

It is known that a system of linear equations with periodic coefficients may be stabilized by adding damping. Usually not much damping is required. For example, if a damping term is added to the Mathieu equation, so that it has the appearance

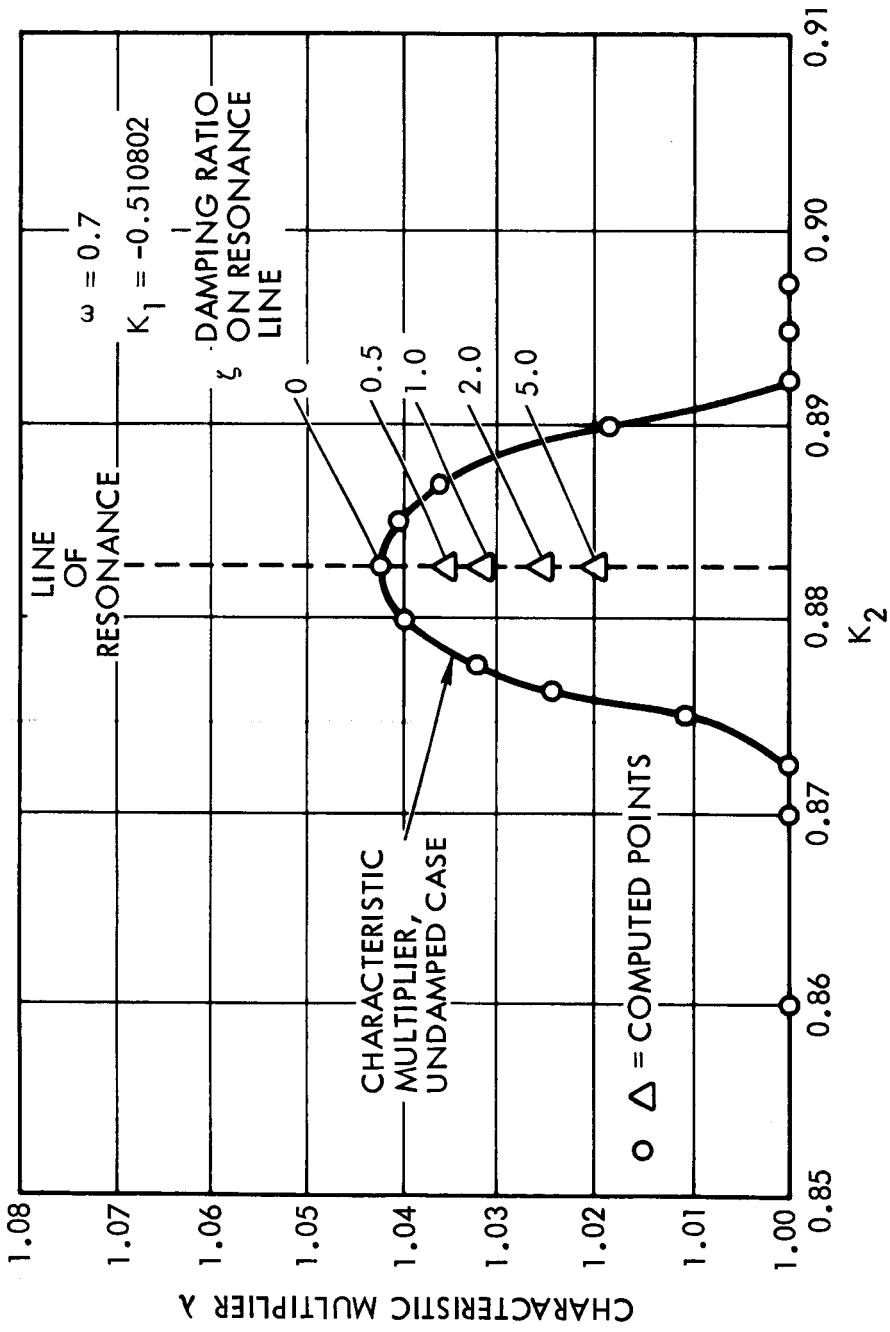

Figure 3.20. Variation of Characteristic Multiplier Across Band of Parametric Resonance, Showing Effect of Damping on Stability. Half Amplitude One Degree

$$\ddot{x} + 2\zeta\omega_n\dot{x} + \left(\omega_n^2 - a\cos 2t\right)x = 0$$

The transformation

$$x = \bar{x}\exp(-\zeta\omega_n t) \qquad (3.3\text{-}11)$$

leads to

$$\ddot{\bar{x}} + \left[\omega_n^2(1 - \zeta^2) - a\cos 2t\right]\bar{x} = 0$$

which is in the exact Mathieu form. If the coefficients ω_n, a, ζ are such that $\bar{x}$ grows 5 percent in time π, then Equation (3.3-11) indicates that x(t) will still be stable unless

$$1.05\exp(-\zeta\omega_n\pi) > 1$$

If $\omega_n = O(1)$ (natural frequency comparable to parametric frequency) then x is stable even for ζ as low as about

$$\frac{\ln(1.05)}{\pi} \simeq 0.015$$

When damping is present, most of the characteristic multipliers are inside the unit circle. In unstable cases, there are two real roots, one slightly less than -1.

Some of the results of applying the Floquet procedure to damped systems are shown in Figures 3.21 and 3.22. Only cases on the line of parametric resonance were considered. The bar graphs show the portions of the resonance line which are stabilized by the addition of various amounts of damping.

A thorough investigation for $\zeta = 0.1$, 0.5 and 1.0 was carried out for $\omega_n = 1$, but only $\zeta = 0.5$ was considered in detail for $\omega_n = 5$. Additional data for $\omega_n = 5$, not shown on the graph, indicates that the trend is similar to the case of $\omega_n = 1$; at higher values of damping there are fewer unstable points.

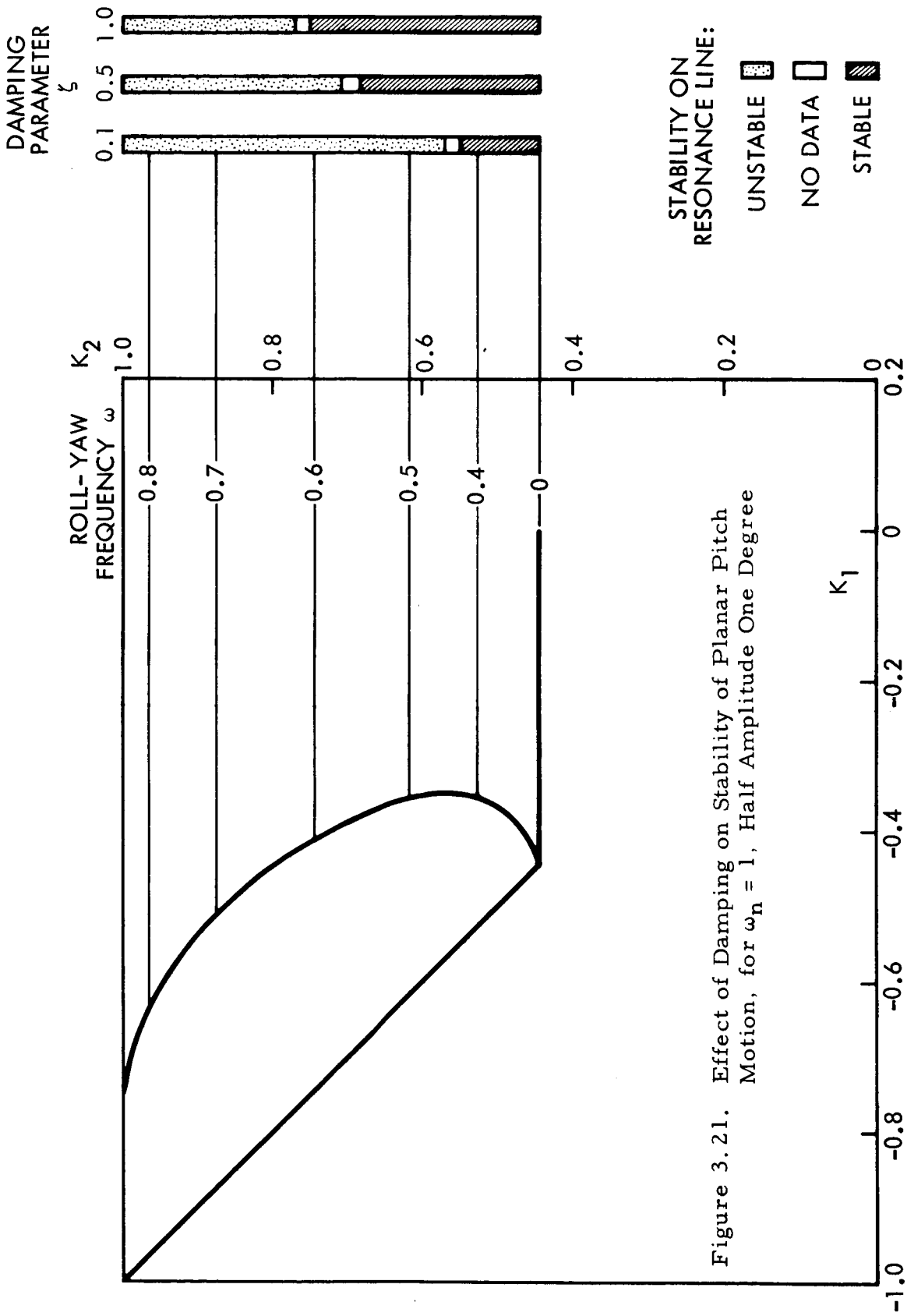

Figure 3.21. Effect of Damping on Stability of Planar Pitch Motion, for $\omega_n = 1$, Half Amplitude One Degree

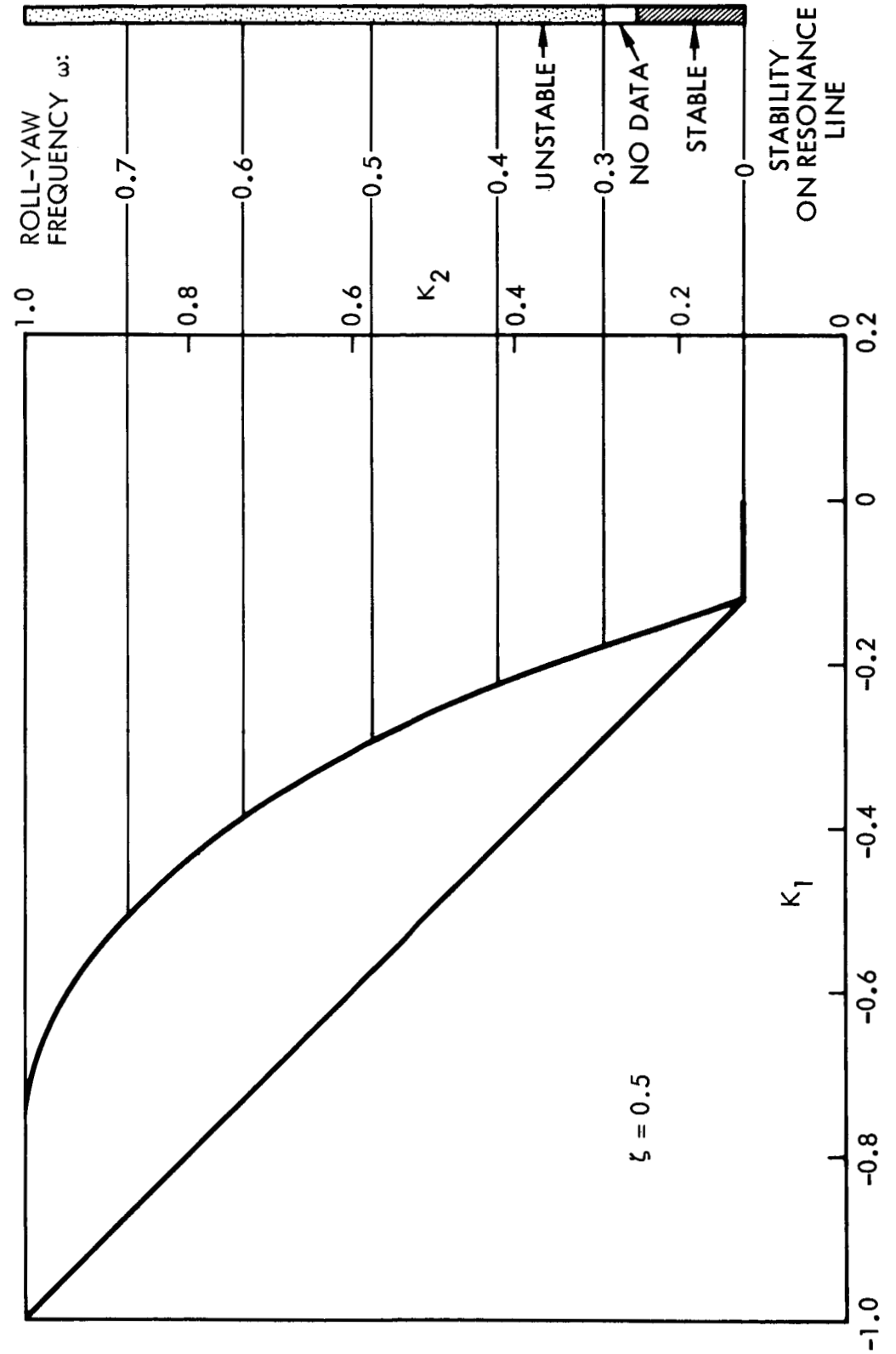

Figure 3.22. Effect of Damping on Stability of Planar Pitch Motion, for $\omega_n = 5$, Half Amplitude One Degree

The curves of parametric resonance were derived for the undamped case. They presumably shift slightly when damping is introduced. It is possible, though unlikely, that some of the points in the K_1-K_2 plane which were stabilized by the addition of damping are only stable because they are not on the resonance line in the damped case, and that unstable points exist nearby.

Conclusions which can be drawn from Figures 3.21 and 3.22 are

A. For fixed roll-yaw frequency ω, systems having higher ω_n require more damping to stabilize them. For $\omega_n = 10$, no data is shown because no realistic damping will change the characteristic multiplier even 1 percent.

   This result is not surprising and can be predicted from constant-coefficient theory. When two modes of oscillation of a system are far apart in frequency, introducing damping in the high-frequency mode adds practically no damping to the other.

B. For a fixed value of ω_n, systems with higher ω need more damping to stabilize them. This result is the opposite of what would be expected on the basis of the linearized equations. The low-frequency mode should be easier to damp when it is closer to the high frequency mode. The reason for this phenomenon appears to be that the parametric-excitation terms in the equations become more significant when ω is increased. Examination of Equations (B-11) in Appendix B shows that the parametric

excitation terms do not change when ω_n changes, but are strong functions of K_1 and K_2, and therefore of ω.

C. The unstable regions for high ω are surprisingly persistent. Even for a relatively low ω_n of one, and a relatively high damping, $\zeta = 1$, a substantial band of unstable points still exists along the resonance line. Bodies in this region have a distinctly non-spherical shape and relatively strong gravity-gradient restoring torques. They might otherwise be suitable candidates for satellite configurations.

Figure 3.20 shows the effect of adding various amounts of damping for the case $\omega = 0.7$, $\omega_n = 1$. It seems evident that the resonance band, though it may become narrower, persists even for very high values of damping, and fairly low natural frequency.

It must be pointed out that even the case $\omega_n = 1$ represents a relatively stiff system because, as seen in the third of Equations (3.2-18), gravitational-centrifugal effects add stiffness so that the uncoupled frequency is $\sqrt{\omega_n^2 + 4}$, while the natural frequency considering only elastic effects would be ω_n.

The "rigid-body" frequencies are thus in the neighborhood of one orbit rate, while for $\omega_n = 1$ the "elastic" frequency is of the order of $\sqrt{5} \simeq 2.2$ orbit rates.

Similar studies should be carried out on bodies of lower stiffness, but the present format and the use of the K_1-K_2 parameters are not really appropriate.

3.3.5 Summary and Conclusions

In summary, it has been shown that the impossibility of pure pitching motion, found by Kane for a class of rigid bodies, occurs also for a class of flexible bodies and that it is not readily removed by damping. Linear analysis techniques, which do not predict the instability, are not adequate in this case.

The entire discussion has presupposed a system free of disturbance torques, so that pitch motion took place at the frequency of free pitch oscillations. A case of at least equal importance is the case of forced pitch oscillations due to orbit eccentricity or other disturbances. It is possible that analogous instability phenomena could occur in such a case.

The class of satellites studied is unrealistic principally because they have no flexibility or damping about the pitch axis. It is possible that the addition of a pitch spring would cause pure planar motion to become stable for all inertia ratios. It seems much more likely, however, that two bands of unstable inertia ratios would emerge, corresponding to the two pitch frequencies.

Chapter 4. Static Behavior of Long Wires and Rods Attached to Vertically Stabilized Satellites

This chapter examines the effect of small centrifugal and gravitational forces on the flexible appendages of a vertically-oriented satellite. The forces involved are very small, but can be significant in very flexible space structures.

4.1 Internal Forces in Vertically-Stabilized Satellite

Consider the vertically-oriented satellite of Figure 4.1. Coordinate axes B_i pass through the center of mass. Unit vectors $\hat{B}_i$ are directed along B_i. The satellite is assumed to move in such a manner that $\hat{B}_3$ always points toward the earth's center, and $\hat{B}_2$ is normal to the orbit plane. $\hat{B}_1$ is then tangent to the assumed circular orbit. It may be shown (Chapter 3) that such motion is possible only when B_i are principal axes.

It is shown in Appendix A, Section A.4, that a mass point m in such a satellite has acting on it a constraint force given by

$$\overline{F}_c = m\omega_o^2\left(x_2\hat{B}_2 - 3x_3\hat{B}_3\right) \qquad (4\text{-}1)$$

where

ω_o is the orbital angular frequency

x_i are the coordinates of m along the axes B_i

$\overline{F}_c$ is the resultant force needed to hold m fixed relative to the orbiting, rotating satellite.

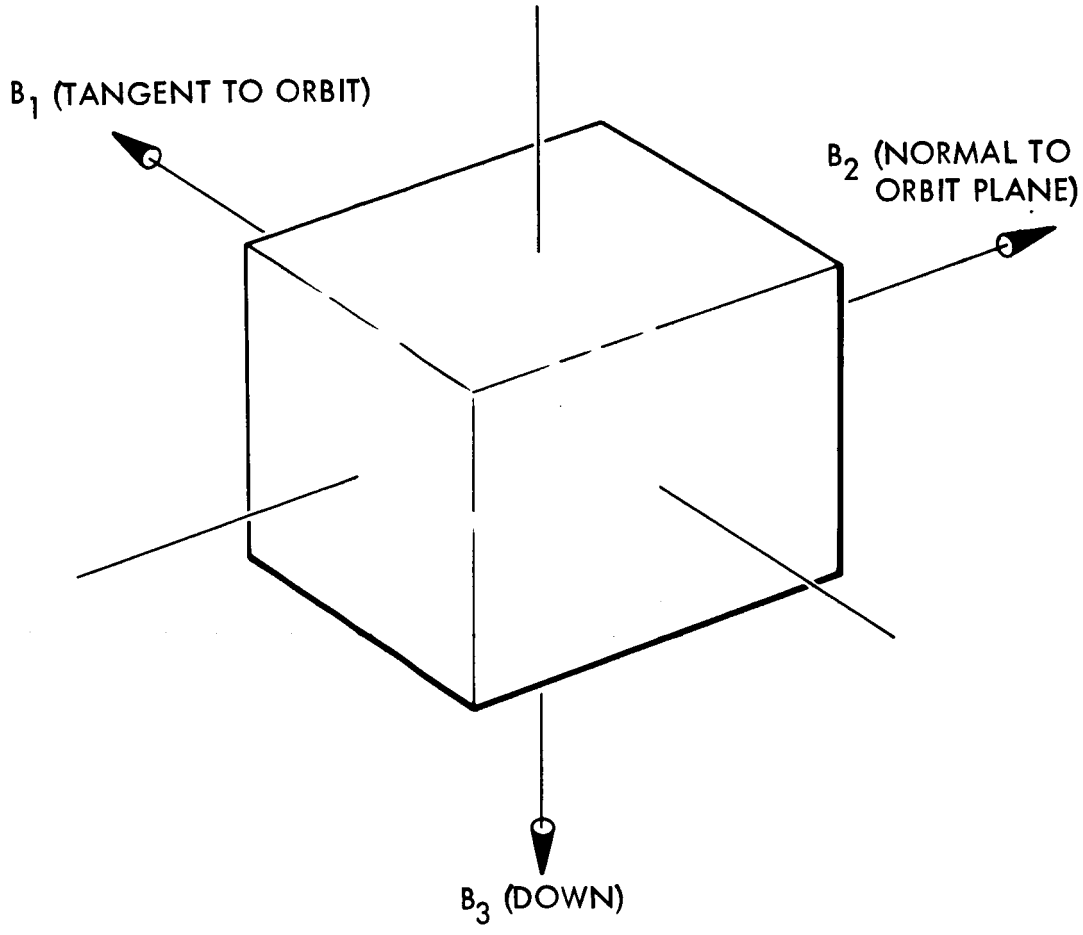

Figure 4.1. Coordinate System

4.2 Elastically Deflecting Mass Point

Let us suppose that m is suspended elastically so that it can deflect relative to the satellite, and denote its location by

$$x_i = \ell_i + y_i - \frac{m'y_i}{M} \tag{4-2}$$

where

ℓ_i represent the location of the mass point for zero elastic deflection

y_i represent the elastic deflection components

M is the total satellite mass

The third term in Equation (4-2) results from the fact that x_i are measured relative to the center of mass, which shifts when m moves. It is necessary to assume:

A. That the deflections of m do not rotate the principal axes of the satellite, so that the axes B_i are still principal axes.

B. That only one mass moves, or that, if two or more move, they move symmetrically so that they can be replaced by a single equivalent mass, m'.

For simplicity we assume that the elastic restoring force is given by

$$\overline{F}_c \cdot \hat{B}_i = -k_i(y_i) y_i \hat{B}_i \tag{4-3}$$

i.e., that the restoring force in a particular direction is a nonlinear function of the elastic deflection in that direction.

Combination of Equation (4-1) with (4-3) yields three scalar equations for the elastic deflections y_i

$$k_1(y_1)y_1 = 0 \tag{4-4}$$

$$\left[k_2 + \left(1 - \frac{m'}{M}\right)m\omega_o^2\right]y_2 = -m\omega_o^2\ell_2 \tag{4-5}$$

$$\left[k_3 - 3\left(1 - \frac{m'}{M}\right)m\omega_o^2\right]y_3 = 3m\omega_o^2\ell_3 \tag{4-6}$$

Equation (4-4) says simply that there is no constraint force in the $\hat{B}_1$ direction.

Equation (4-5) says that the constraint force in the $\hat{B}_2$ direction is proportional to the distance of the neutral point from the orbit plane, ℓ_2. In addition to the spring force, k_2, an additional spring stiffness term appears due to gravitational-centrifugal effects, increasing the elastic stiffness and reducing the deflection y_2 for given ℓ_2.

Equation (4-6) is more interesting. Consider first that k_3 is a constant. Then Equation (4-6) states that the spring restoring force can be reduced by gravitational effects which produce a negative spring force, so that the system is like that of Figure 2.2.

The deflection

$$y_3 = \frac{\ell_3}{\frac{k_3}{3m\omega_o^2} - \left(1 - \frac{m'}{M}\right)} \tag{4-7}$$

becomes larger for given k_3, as $m\omega_o^2$ is increased, and is unbounded for

$$\frac{k_3}{3m\omega_o^2} = \left(1 - \frac{m'}{M}\right)$$

For

$$\frac{k_3}{3m\omega_o^2} < 1 - \frac{m'}{M}$$

Equation (4-7) predicts a negative deflection position

$$y_3 = \frac{-\ell_3}{\left(1 - \frac{m'}{M}\right) - \frac{k_3}{3m\omega_o^2}} \tag{4-8}$$

This position is one of unstable equilibrium because Equation (4-6) shows that the overall spring constant is a negative number.

The behavior described by Equations (4-7) and (4-8) is analogous, to some extent, to the behavior of an unbalanced rotating shaft. The reader is referred to Reference 4.1 for details.

4.3 Nonlinear Deflection of a Cantilever Under Gravitational Loading

We have shown that Equation (4-6) has no stable solutions for

$$3\left(1 - \frac{m'}{M}\right)m\omega_o^2 > k_3 > 0 \quad , \quad k_3 \text{ constant}$$

which can occur for sufficiently small k_3.

For the case $k_3 = k_3(y_3)$, stable solutions will exist if the nonlinear spring has a "hardening" characteristic.

The negative gravitational spring force will remain linear with y_3 for

$$y_3 << \text{orbit radius}$$

which is always satisfied, but the elastic spring can stiffen until it balances the negative gravitational spring.

The most practical case is that of appendages with tip masses, in the shape of cantilever beams (Figure 4.2), such as might be used to form an inertia array.

The nonlinear deflection of a cantilever beam under load applied at the tip, normal to the undeformed position, is solved in Reference 4.2 in terms of elliptic integrals. The graphical results of the investigation are shown in Figure 4.3 with the modified notation:

P = applied force

L = beam length

Δ = reduction in length

y_3 = beam deflection

EI = flexural rigidity of beam

The results of the calculation can be used to find the equilibrium points at which the force applied to the beam is balanced by the elastic restoring force. The condition is, from Equation (4-6),

$$P\left(\frac{y_3}{L}\right) = k_3(y_3)y_3 = 3m\omega_o^2\left[\left(1 - \frac{m'}{M}\right)y_3 + \ell_3\right]$$

The simplest case is $\ell_3 = 0$, corresponding to a cantilever at the radial location of the center of gravity. Define

$$a = 3m\omega_o^2\left(1 - \frac{m}{M}\right)\frac{L^3}{EI} \tag{4-9}$$

$$L_{cr} = \left[\frac{EI}{m\omega_o^2\left(1 - \frac{m'}{M}\right)}\right]^{1/3}$$

L_{cr} is the length above which a beam with given EI, m, ω_o is unstable in the straight configuration. Then the equilibrium points are defined

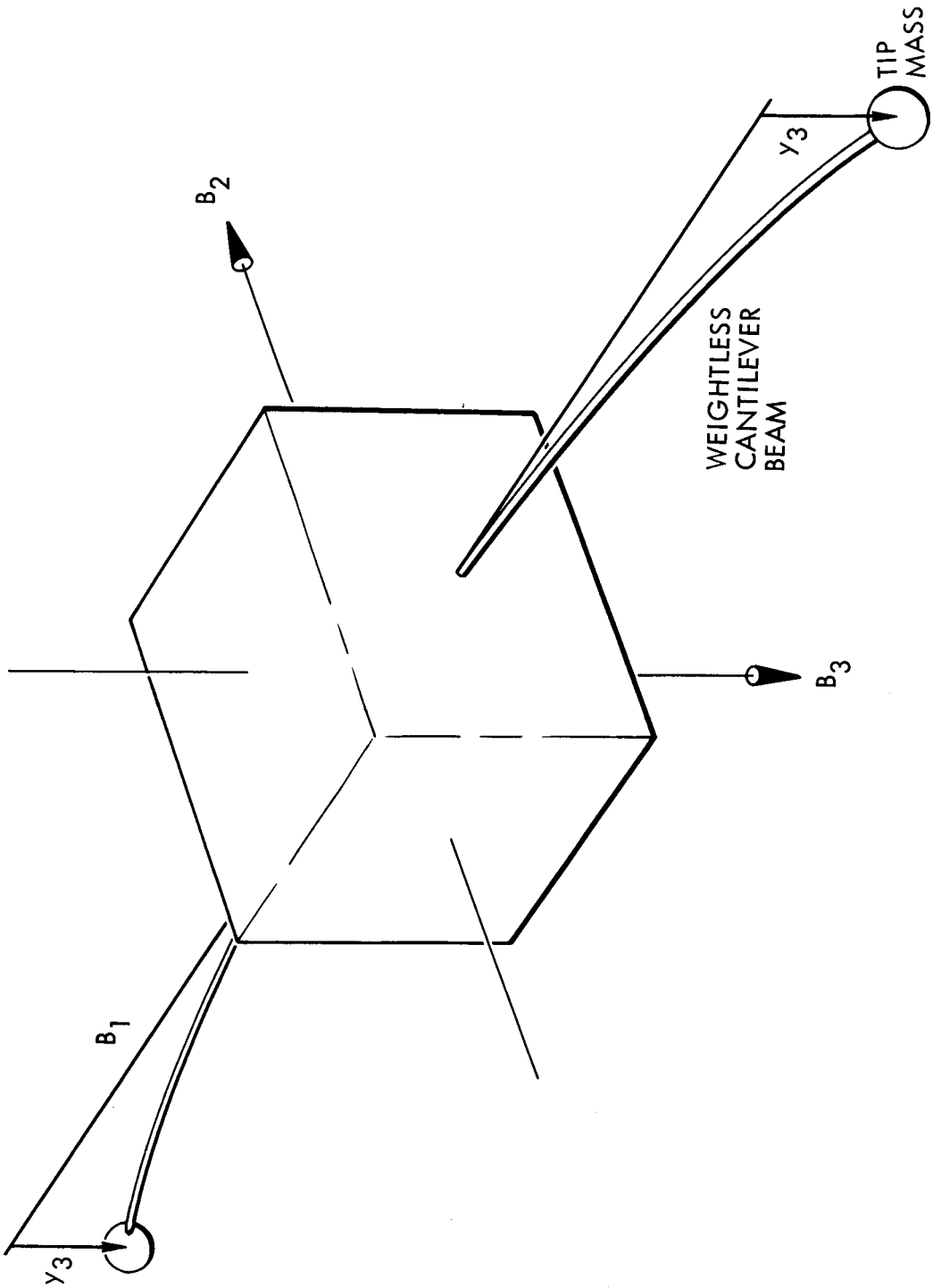

Figure 4.2. Satellite With Appendages

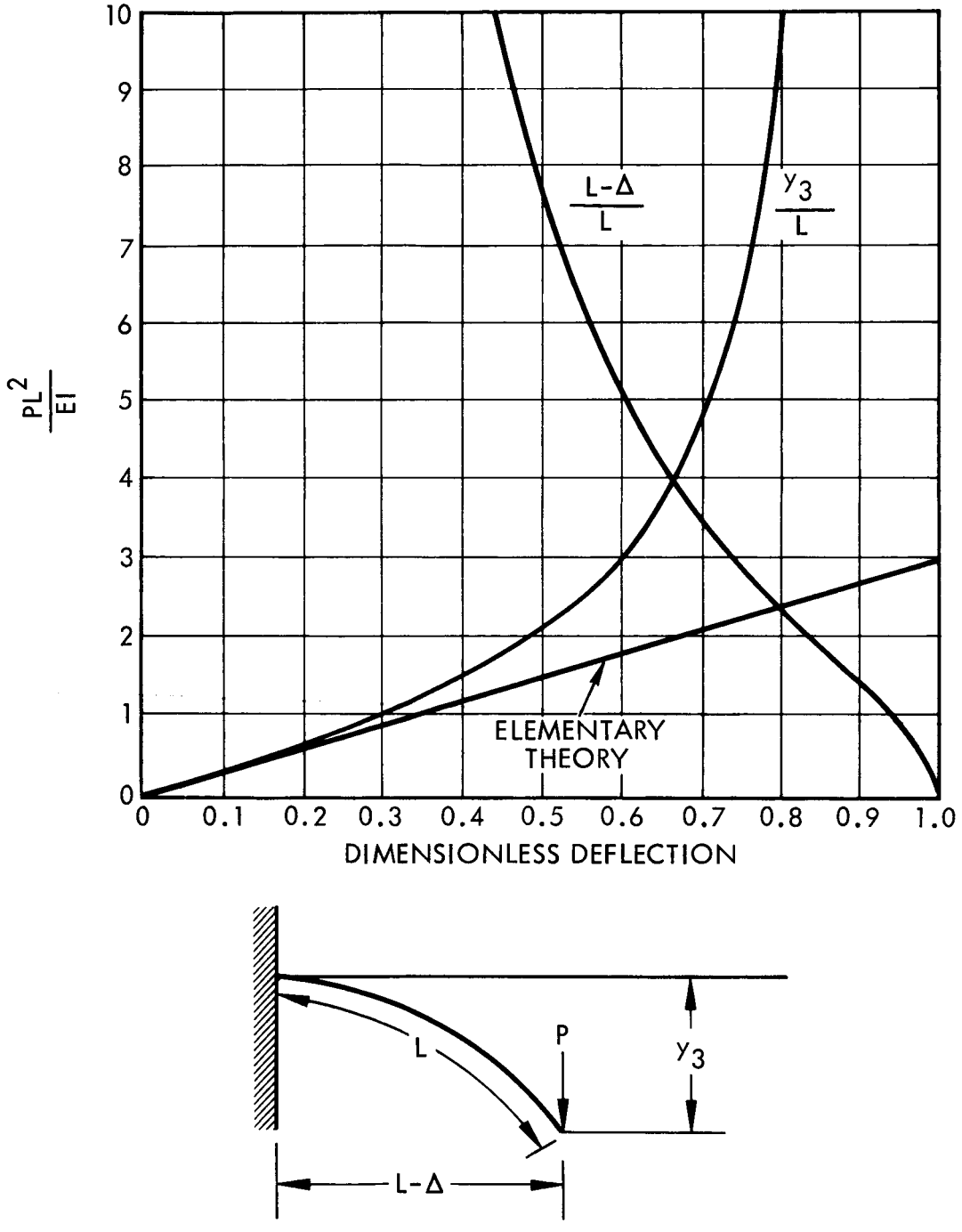

Figure 4.3. Results from Reference 4.2 for Large Deflections of a Cantilever Beam

by the intersection of the curve of Figure 4.3 with the straight line (not shown)

$$P = a\left(\frac{y_3}{L}\right)$$

The results are plotted in Figure 4.4 The elastic curves are somewhat approximate but the tip locations are accurate. Note the drastic deflection for lengths only slightly greater than the critical length.

The stable equilibrium deflection for $\ell_3 = 0$ is of course zero for a less than 3, ($L < L_{cr}$) the critical value for which the elastic spring and the gravitational spring cancel for small deflections.

For the rod material used on the NASA Radio Astronomy Explorer (Reference 4.3), attached to a heavy satellite in a 450 mile orbit, the critical length corresponding to $a = 3$ for a 5 pound tip weight is 360 feet.

It should be noted that equilibrium deflections exist for both positive and negative y_3 because both gravitational and elastic forces are odd functions of y_3.

For cantilevers which are not horizontal in the undeformed state the applied force has a component parallel to the undeformed beam as well as along it. Reference 4.4 gives the closed form solution for large deflection of a cantilever under general planar tip loading. The results of Reference 4.4 could be used to plot deflection curves for more general cases.

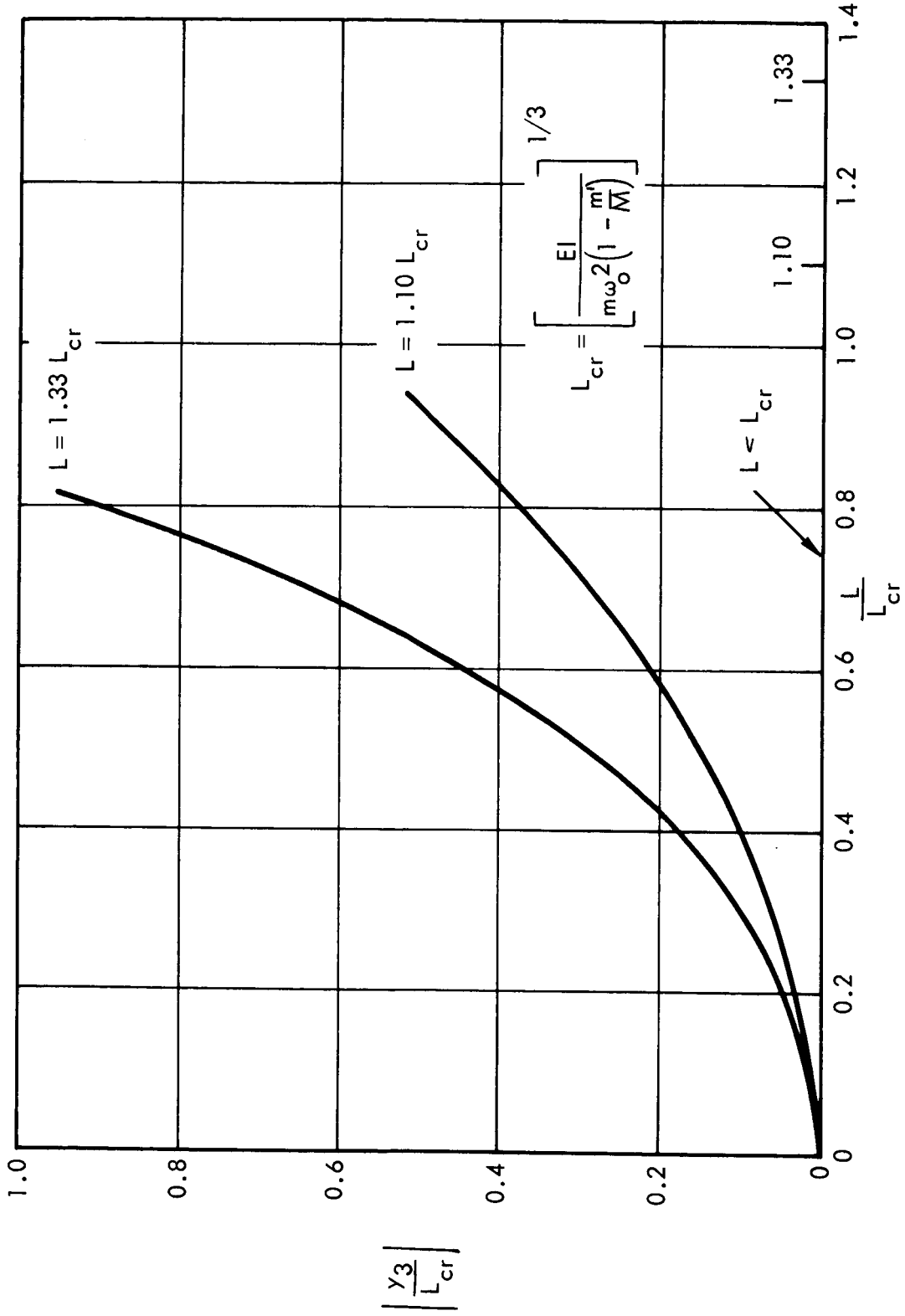

Figure 4.4. Equilibrium Shapes of Weightless Cantilever With Tip Mass, as a Function of Beam Length

4.4 Discussion of the Deflection of a Beam With Distributed Mass

We close this chapter with a brief examination of the more difficult problem of the deflection of a cantilever with distributed mass. It is well known that the deflection curve is given for small deflections by

$$EI \frac{d^4u}{dx^4} = w \tag{4-10}$$

where w is the distributed loading on the beam per unit length, EI is the flexural rigidity, u is the deflection, and x is length along the beam.

We restrict our attention to the case where beam mass is negligible compared to satellite mass, and where the beam is in the orbital plane, making an angle θ with the horizontal (Figure 4.5). Then Equation (4-1) yields

$$\overline{F}_c(x) \cdot \hat{B}_3 = -w(x)$$

$$= -3\rho\omega_o^2(x \sin\theta + u \cos\theta)$$

and, from Equation (4-10),

$$EI \frac{d^4u}{dx^4} - 3\rho\omega_o^2 \cos\theta u = 3\rho\omega_o^2 x \sin\theta \tag{4-11}$$

where $\rho(x)$ is beam mass per unit length.

The solution to this problem can be visualized readily because it is an exact analog of the problem of the forced vibrations of an elastic beam, for which beam deflection v is given by

$$EI \frac{\partial^4 v}{\partial x^4} + \rho \frac{\partial^2 v}{\partial t^2} = f(x)e^{i\omega t} \tag{4-12}$$

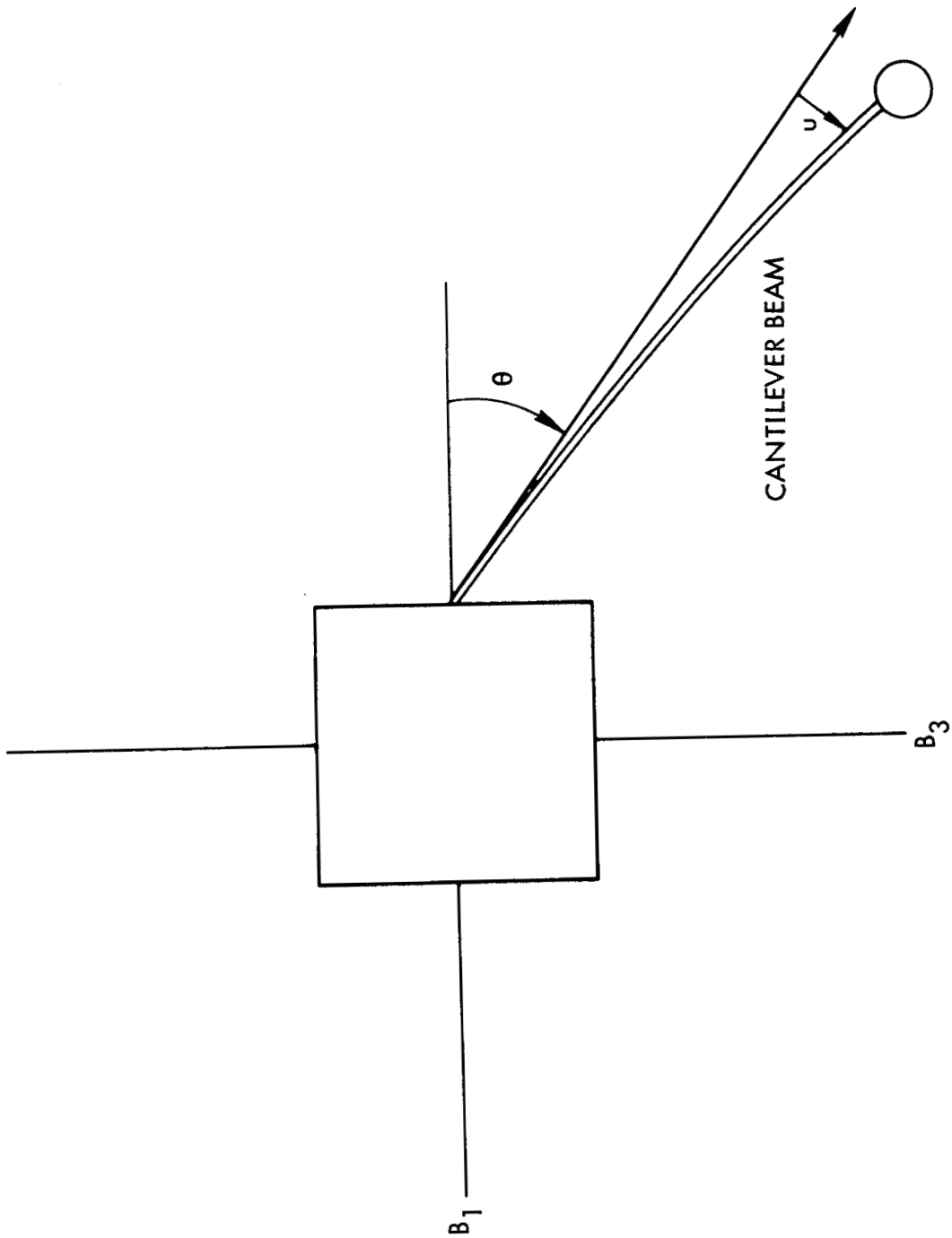

Figure 4.5. Deflection of Beam With Distributed Mass

Separating variables in Equation (4-12) we put

$$v(x, t) = \bar{v}(x)e^{i\omega t}$$

and obtain

$$EI \frac{d^4\bar{v}}{dx^4} - \rho\omega^2\bar{v} = f(x) \qquad (4\text{-}13)$$

which is identical in form to Equation (4-11). Thus the problem of Figure 4.5 is an analog of the forced vibrations of an elastic beam and a solution can be obtained as the sum of a series of normal modes of the beam.

The case $\theta = 0$ corresponds to the problem of free vibrations of a beam. Equation (4-11) for $\theta = 0$ is known to have nontrivial solutions only for discrete values of the quantity $3\omega_o^2$, corresponding in the analog to the natural frequencies of the beam. For other values of $3\omega_o^2$, the only solution is

$$u(x) = 0 \qquad (4\text{-}14)$$

It is natural to conjecture that, as in the lumped-parameter case of Section 4.3, the solution, Equation (4-14), to the distributed-parameter problem is unstable above a critical value of ω_o^2, and large-deflection theory must be used.

Chapter 5. Pitch Libration of a Wire Satellite

Let us suppose it is feasible to construct and place in orbit a satellite consisting of a long flexible beam or wire. Such a device has been seriously suggested as a passive communication reflector (Reference 5.1). We pose the question: what will be the equilibrium attitude of the wire and what will be the elastic motion if the wire is long enough to be affected by the gravitational gradient?

As a preliminary to a possible future examination of the general three-dimensional problem, let us consider the plane motion of the wire in the plane of its assumed circular orbit.

5.1 Coordinate System

Consider the coordinate system of Figure 5.1. Orbital position is denoted by the rotating vector $\overline{R}_o$ rotating at the orbital angular velocity $\omega_o \hat{k}$, where $\hat{k}$ is a unit vector out of the paper. The xy coordinate system with unit vectors $\hat{i}$, $\hat{j}$ is rotated through angle θ from the local vertical.

Length along the wire is measured by the coordinate x. Small in-plane elastic deformation is denoted by y(x). Mass distribution is $\rho(x)$.

The location of the origin and the orientation of the x-axis (the angle θ) are defined by:

$$\int x\rho \, dx = 0$$

$$\int y\rho \, dx = 0$$

$$\int xy\rho \, dx = 0 \qquad (5\text{-}1)$$

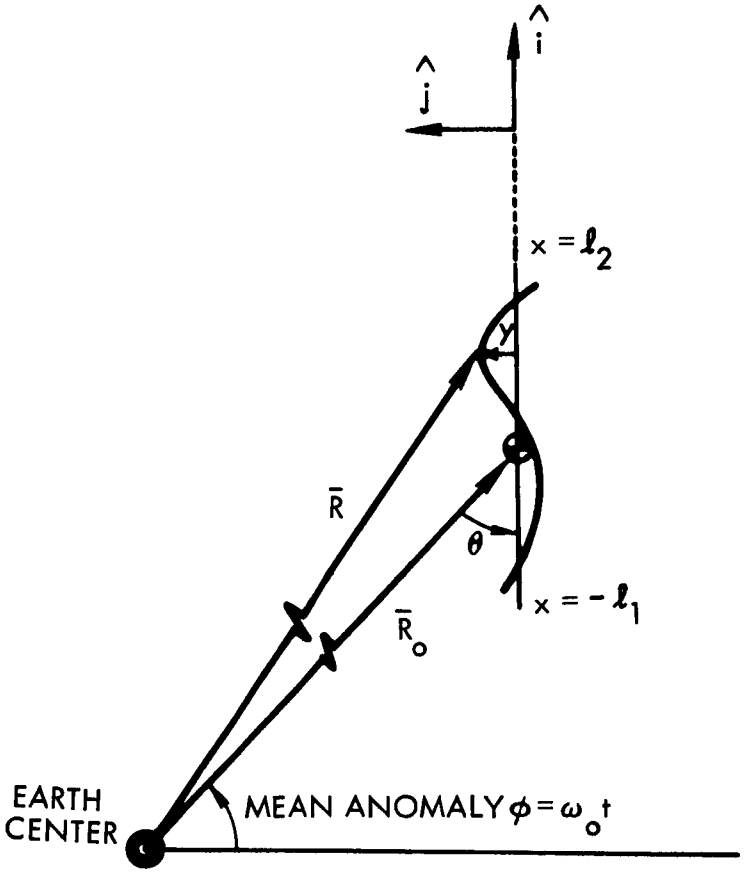

Figure 5-1. Coordinate System

That is, the origin is the center of gravity and the angle θ defines the axis about which the elastic motion has zero angular momentum. For $y = 0$, the wire is a straight line inclined at angle θ to the vertical.

5.2 Bending Equation

The wire is considered to be an ideal Bernoulli-Euler beam with mass distributed along its elastic axis. From the usual beam-element free-body diagram (Figure 5.2), we derive the relationships

$$\frac{\partial M}{\partial x} = V \tag{5-2}$$

$$-\frac{\partial V}{\partial x} + \rho(\overline{F} \cdot \hat{j}) = \rho(\ddot{\overline{R}} \cdot \hat{j}) \tag{5-3}$$

where

M is bending moment

V is the shear

$\overline{F}$ is the gravitational force vector per unit mass.

$$\overline{R} = \overline{R}_o + x\hat{i} + y\hat{j} \tag{5-4}$$

is the position of a mass element.

The linearized moment-curvature relation is

$$M = EI \frac{\partial^2 y}{\partial x^2} \tag{5-5}$$

where EI denotes beam flexural rigidity. Combination of Equations (5-2), (5-3) and (5-5) yields the beam elastic equation

$$-\frac{\partial^2}{\partial x^2}\left(EI \frac{\partial^2 y}{\partial x^2}\right) + \rho\overline{F} \cdot \hat{j} = \rho\ddot{\overline{R}} \cdot \hat{j} \tag{5-6}$$

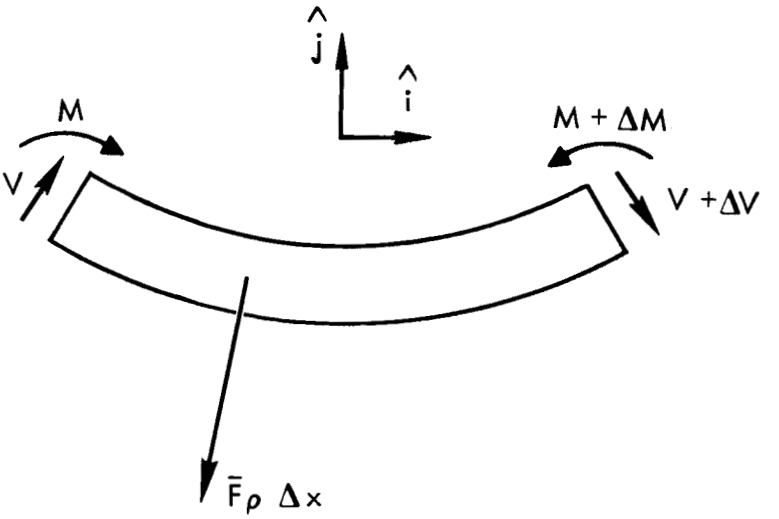

Figure 5-2. Free-Body Diagram of Beam Element

5.3 Rigid Body Equations

Rigid-body rotational and translational equilibrium yield

$$\int_{-\ell_1}^{\ell_2} \rho \, dx \, \ddot{\overline{R}}_o = \int_{-\ell_1}^{\ell_2} \overline{F} \rho \, dx \tag{5-7}$$

$$\frac{d}{dt}\left[\int_{-\ell_1}^{\ell_2} (\overline{R} - \overline{R}_o) \times \dot{\overline{R}} \rho \, dx\right] = \int_{-\ell_1}^{\ell_2} (\overline{R} - \overline{R}_o) \times \overline{F} \rho \, dx \tag{5-8}$$

5.4 Scalar Equations of Motion

The gravitational force $\overline{F}$ is obtained from the general expression [Appendix A, Equation (A-5)] by putting

$$\theta_2 = -\theta$$

$$x_1 = y \ , \ x_2 = 0 \ , \ x_3 = -x$$

$$\hat{B}_1 = \hat{j} \ , \ \hat{B}_2 = -\hat{k}$$

The result, correct to the first power of

$$\left(\frac{\text{satellite length}}{\text{orbit radius}}\right)$$

is

$$\overline{F} = -\omega_o^2 \left[1 - \frac{3(x \cos\theta - y \sin\theta)}{R_o}\right]\left[(R_o \cos\theta + x)\hat{i} + (-R_o \sin\theta + y)\hat{j}\right] \tag{5-9}$$

The derivatives of $\overline{R}$ and $\overline{R}_o$ are obtained from Equation (5-4), using the general formula for differentiating a vector rotating with angular velocity $\overline{\omega}$

$$\frac{d}{dt}(\ ) = \frac{d}{dt}(\ )\Big|_{rel} + \bar{\omega} \times (\ )$$

Results are:

$$\dot{\bar{R}}_o = \omega_o R_o(\sin\theta\hat{i} + \cos\theta\hat{j})$$

$$\ddot{\bar{R}}_o = -\omega_o^2 R_o(\cos\theta\hat{i} - \sin\theta\hat{j})$$

$$\dot{\bar{R}} = -(\omega_o + \dot{\theta})y\hat{i} + \left[\dot{y} + (\omega_o + \dot{\theta})x\right]\hat{j} + \dot{\bar{R}}_o$$

$$\ddot{\bar{R}} = \left[-(\omega_o+\dot{\theta})^2 x - 2(\omega_o+\dot{\theta})\dot{y} - \ddot{\theta}y\right]\hat{i} + \left[\ddot{y} - (\omega_o+\dot{\theta})^2 y + \ddot{\theta}x\right]\hat{j} + \ddot{\bar{R}}_o$$

(5-10)

Substitution of Equations (5-9) and (5-10) into (5-6), (5-7) and (5-8) and use of the conditions of (5-1) yields scalar elastic and rigid body equations:

$$\frac{\partial^2}{\partial x^2}\left(EI\frac{\partial^2 y}{\partial x^2}\right)$$

$$= -\rho(x)\left[\ddot{y} - (\omega_o+\dot{\theta})^2 y + \ddot{\theta}x + \omega_o^2 y + 3\omega_o^2 \sin\theta(x\cos\theta - y\sin\theta)\right]$$

(5-11)

and

$$\left(I + \int_{-\ell_1}^{\ell_2} y^2\rho\,dx\right)\ddot{\theta} + 2(\dot{\theta}+\omega_o)\int_{-\ell_1}^{\ell_2} y\dot{y}\rho\,dx$$

$$= -3\omega_o^2 \sin\theta\cos\theta\left(I - \int_{-\ell_1}^{\ell_2} y^2\rho\,dx\right)$$

(5-12)

where

$$I \overset{\text{Def}}{=} \int_{-\ell_1}^{\ell_2} x^2 \rho \, dx$$

Boundary conditions on Equation (5-11) are that the ends of the beam are free.

$$\frac{\partial^2 y}{\partial x^2} = \frac{\partial^3 y}{\partial x^3} = 0 \text{ at } x = -\ell_1, \ \ell_2. \tag{5-13}$$

The translational equation (5-7) reduces to an identity because a circular orbit has already been assumed.

5.5 Separation of Variables in Beam Equation

Assume a solution of Equation (5-11) in the form

$$y(x, t) = \sum_n q_n(t)\phi_n(x) \tag{5-14}$$

where the $\phi_n(x)$ are the normal modes of a free-free beam having mass distribution $\rho(x)$. $\phi_n(x)$ are known to satisfy (Reference 5.2)

$$(EI\phi_n'')'' - \rho\omega_n^2\phi_n(x) = 0 \tag{5-15}$$

$$\phi_n'' = \phi_n''' = 0 \text{ at } x = -\ell_1, \ \ell_2 \tag{5-16}$$

(Primes denote derivatives with respect to x.)

The ϕ_n also satisfy the orthogonality conditions

$$\int_{-\ell_1}^{\ell_2} \phi_m\phi_n\rho \, dx = M_n\delta_{mn}$$

$$\int_{-\ell_1}^{\ell_2} EI\phi_m''\phi_n'' \, dx = \omega_n^2 M_n \delta_{mn} \tag{5-17}$$

where

$$M_n = \int_{-\ell_1}^{\ell_2} \phi_n^2 \, dx$$

δ_{mn} is the Kronecker delta, and ω_n is the natural frequency of the wire in a uniform gravitational field.

The elastic mode shapes of a free-free beam also satisfy (Reference 5.3)

$$\int_{-\ell_1}^{\ell_2} \phi_n(x)\rho \, dx = 0$$

$$\int_{-\ell_1}^{\ell_2} x\phi_n(x)\rho \, dx \tag{5-18}$$

We substitute Equation (5-14) into Equation (5-11), multiply by $\phi_n(x)$ and integrate with respect to x from $-\ell_1$ to ℓ_2. Using Equation (5-17) we obtain

$$M_n\omega_n^2 q_n = -M_n\ddot{q}_n + M_n\left[(\omega_o + \dot{\theta})^2 - \omega_o^2 + 3\omega_o^2 \sin^2\theta\right]q_n$$

$$-\left(\ddot{\theta} + 3\omega_o^2 \sin\theta\cos\theta\right)\int_{-\ell_1}^{\ell_2} x\rho(x)\phi_n(x) \, dx$$

Or, noting that the integral vanishes by Equation (5-18)

$$\ddot{q}_n + \left(\omega_n^2 - 2\omega_o\dot{\theta} - \dot{\theta}^2 - 3\omega_o^2 \sin^2\theta\right)q_n = 0 \qquad (5\text{-}19)$$

which is a set of equations for the elastic coordinates q_n.

5.6 Discussion of Equations of Motion

The problem posed is described by Equations (5-19) and (5-12). Equation (5-12) can be rewritten using (5-17) as

$$I\ddot{\theta} + 3\omega_o^2 I \sin\theta\cos\theta$$

$$= -2(\dot{\theta} + \omega_o)\sum_n M_n q_n \dot{q}_n - \left(\ddot{\theta} - 3\omega_o^2 \sin\theta\cos\theta\right)\sum_n M_n q_n^2 \qquad (5\text{-}20)$$

The terms on the left-hand side make up the pitch equation for a rigid body. The terms on the right, second order in the small elastic amplitude q_n, show that elastic motion excites rigid-body motion both directly (ω_o term) and parametrically.

Equation (5-19) shows that, for the wire satellite, elastic motion is excited only parametrically. This somewhat surprising conclusion probably applies only to the present case, in which there are no tip weights and the wire has a cross-sectional moment of inertia per unit length (rotary inertia) which is small. Reference 5.4 shows that a satellite consisting of a weightless rod with a tip weight, attached to a rigid body, has linearly coupled elastic and rigid-body motion.

5.7 Applications

In practical applications, it may be desirable to use the flexibility of the wire to damp out an initial rigid-body motion. A necessary

condition is that rigid-body pitching motion $\left[\theta(t) \text{ oscillatory}\right]$ must excite elastic motion. We will therefore consider small rigid-body oscillations and determine the elastic response. Equation (5-20) reduces approximately to

$$\ddot{\theta} + 3\omega_o^2\theta = 0$$

A suitable solution is

$$\theta = -\theta_o \sin \sqrt{3}\,\omega_o t \tag{5-21}$$

Change the time variable to

$$z = \frac{\sqrt{3}\,\omega_o t}{2}$$

Then Equation (5-19) becomes, for small θ

$$\frac{d^2 q_n}{dz^2} + \frac{4\zeta\omega_n}{\sqrt{3}\,\omega_o}\frac{dq_n}{dz} + \left(\frac{4\omega_n^2}{3\omega_o^2} + \frac{8\theta_o}{\sqrt{3}}\cos 2z\right)q_n = 0 \tag{5-22}$$

where an assumed viscous damping factor has been introduced. This is a Mathieu-type equation with damping. Introducing

$$\bar{q}_n = q_n \exp\left(\frac{2\zeta\omega_n t}{\sqrt{3}\,\omega_o}\right)$$

we obtain

$$\frac{d^2\bar{q}_n}{dz^2} + (a - 2q\cos 2z)\bar{q}_n = 0 \tag{5-23}$$

$$a = \frac{4\omega_n^2}{3\omega_o^2}(1 - \zeta^2)$$

$$-2q = \frac{8\theta_o}{\sqrt{3}} \tag{5-24}$$

This is the standard form of Mathieu's equation, predicting that $\bar{q}_n$ will grow without bound if the coefficients lie in an unstable region of the Mathieu stability chart (Figure 5.3).

Unstable growth of $\bar{q}_n$ will not insure that substantial elastic motion will occur, because, from Equation (5-23), q_n is related to $\bar{q}_n$ by a factor which decreases exponentially with time. For q_n to grow without bound [on the basis of the linearized equation, (5-22)] we require (Reference 5.5)

$$\lambda > \exp \frac{2\zeta\omega_n \pi}{\sqrt{3}\,\omega_o} \tag{5-25}$$

where λ is the characteristic multiplier (defined in Appendix C), corresponding to the particular values of the coefficients.

In referring to "unbounded growth" of q_n, we mean only that Equation (5-22) will predict such growth so long as θ varies periodically as indicated by Equation (5-21). When q_n becomes sufficiently large, the q_n terms in Equation (5-20) can no longer be ignored and Equation (5-21) does not hold. Unstable parametric excitation of the elastic modes is not sufficient to guarantee good damping of rigid-body motion, but it is a necessary condition.

There are an infinite number of unstable regions in the a-q plane. For small q, they lie near the lines $a = 1, 4, 9 \cdots$. To obtain a physically realistic wire length, we desire a fairly high value of the natural frequency parameter a. Figure 5.4 (Reference 5.6) shows a detailed plot of the unstable region beginning at $q = 0$, $a = 9$.

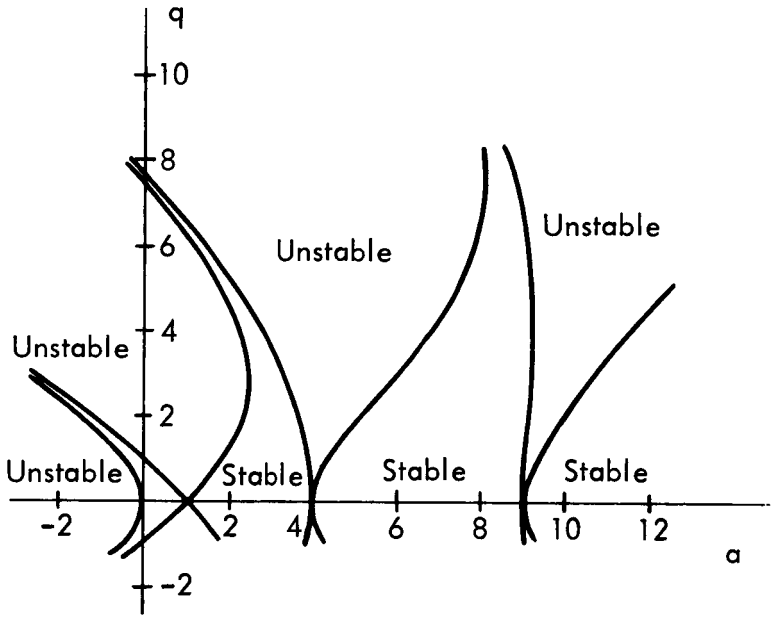

Figure 5.3. Stable and Unstable Regions for Mathieu Equation

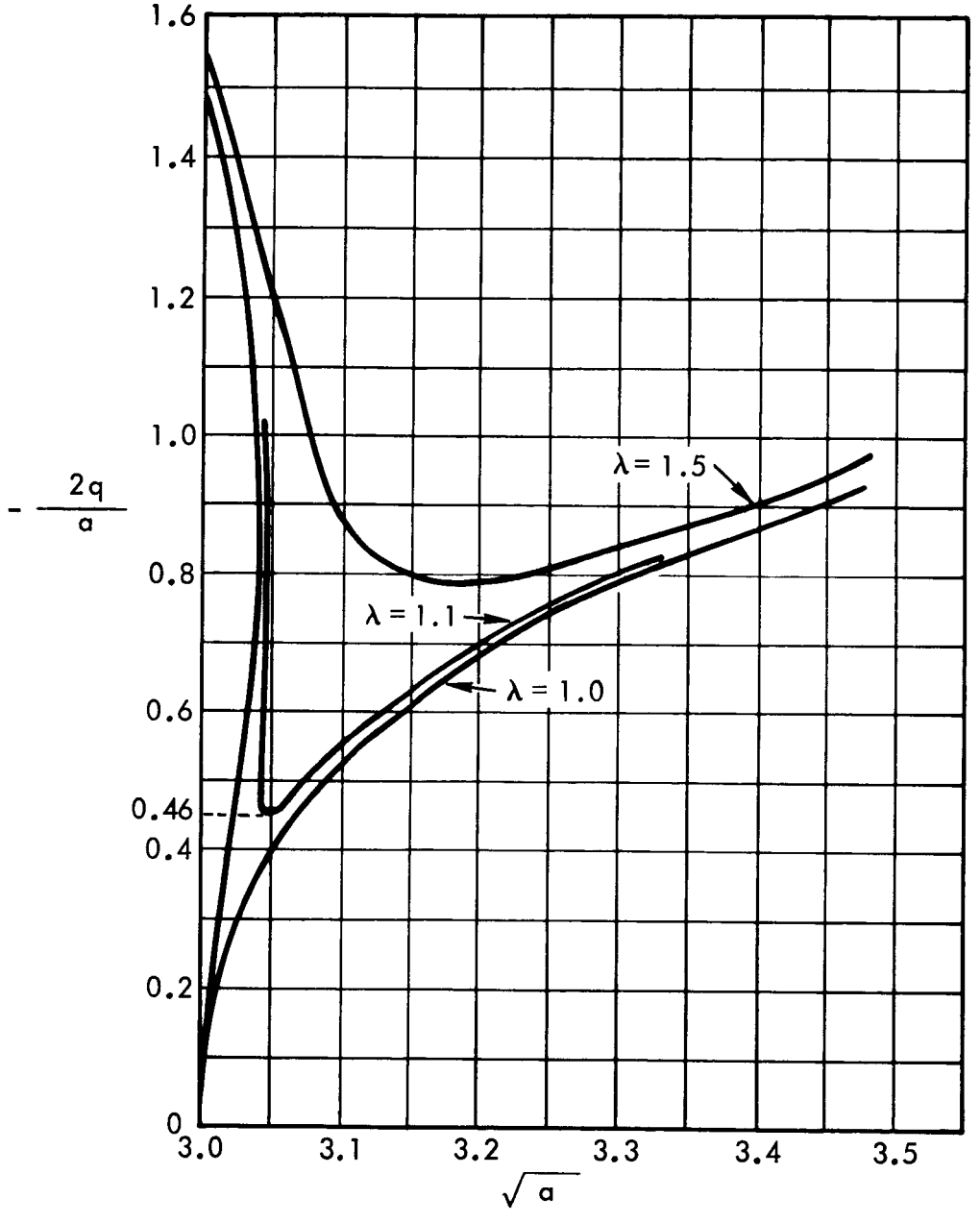

Figure 5.4. Detail of Mathieu Stability Chart Showing Curves of Constant Characteristic Multiplier

For small damping, with a = 9, Equation (5-24) gives

$$\frac{\omega_n}{\omega_o} \simeq \sqrt{\frac{27}{4}} = 2.60$$

Select a realistic $\zeta = 0.01$. Then we require, from Equation (5-25)

$$\lambda > \exp(0.09) = 1.0942$$

Figure 5.4 shows curves of constant λ. It is evident that $\lambda \geq 1.1$ requires

$$-\frac{2q}{a} > 0.46$$

or, approximately

$$\theta_o > \frac{(0.46)9\sqrt{3}}{8} = 0.9 \text{ rad}$$

so that excessive amplitude of rigid-body motion is required to achieve energy transfer to the elastic mode. The same is true for lower values of ζ. The conclusion also holds for the unstable region beginning at a = 2 and for all higher a.

For a wire with a frequency parameter, a near unity, unstable parametric excitation can be realized for reasonable amplitudes. Calculations similar to those above show the solution of Equation (5-22) is unstable for a = 1, for $\theta_o \geq 1.5$ degrees, and for $\zeta \leq 0.03$. The physical configurations corresponding to a = 1, $\left[\omega_n \simeq (\sqrt{3}/2)\omega_o\right]$ are somewhat unrealistic. For the case of a 100 minute orbit (altitude about 450 miles), the required length of a 0.002 inch diameter steel wire is about 120 feet. The gravitational and centrifugal tension is such a wire is only about 10^{-8} lb, so the configuration could be realized if it proved possible to deploy it.

The rod or wire configuration is unusual in that its natural frequency is not changed by placing it in a non-uniform gravitational field. Lowering the frequency to the neighborhood of the orbital angular velocity calls for considerable flimsiness. A configuration combining the wire with gravitationally unstable rigid bodies such as rigid cross-members at the ends of the wire would allow reduction in configuration size.

5.8 Conclusions

A preliminary examination of the gravity-stabilized rod satellite has shown that pitch mode damping can be achieved if the system elastic and inertia parameters are selected correctly. The required configurations are thin wires hundreds of feet long and would be difficult to deploy. Three-dimensional motion has not been examined.

BIBLIOGRAPHY

1.1. Wilhelm, P.G., P.H. Cudmore, R.H. Kronke and R.T. Beal. "In flight attitude determination systems and orbital performance of four gravity gradient NRL satellites." Symposium on Passive Gravity-Gradient Stabilization, May, 1965. National Aeronautics and Space Administration, Ames Research Center, Moffett Field, California.

1.2. Fischell, Robert E. and Frederick F. Mobley. "A system for passive gravity-gradient stabilization of earth satellites." Applied Physics Laboratory Report, TG514, August, 1963.

1.3. Moyer, R.G., R.J. Katucki and L.K. Davis. "A system for passive control of satellites through the viscous coupling of gravity gradient and magnetic fields." Amer. Inst. of Aero. and Astro./ION Astrodynamics Guidance and Control Conference, Paper 64-659, August, 1964, Los Angeles, California.

1.4. Roberson, R.E. and J.V. Breakwell. "Satellite vehicle structure." United States Patent 3,031,154, April 24, 1962 (filed September 20, 1956).

1.5. Yu, E.Y. "Optimum design of a gravitationally oriented two-body satellite." Bell System Technical Journal, 43:49-76, January, 1965.

1.6. Tinling, B.E. and V.K. Merrick. "Exploitation of inertial coupling in passive gravity-gradient-stabilized satellites." Journal of Spacecraft and Rockets, 1:381-387, July-August, 1964.

3.1. Abzug, Malcolm J. Attitude control of multi-part satellites. Ph.D. Dissertation. Department of Engineering, University of California, Los Angeles, California, January, 1962.

3.2. DeBra, D.B. and R.H. Delp. "Rigid body attitude stability and natural frequencies in a circular orbit." Journal of the Astronautical Sciences, 8:14-17, 1961.

3.3. DeBra, D.B. The large angle motions and stability, due to gravity, of a satellite with passive damping in an orbit of arbitrary eccentricity about an oblate body. Ph.D. Dissertation. Department of Engineering Mechanics, Stanford University, Palo Alto, California, May, 1962.

3.4. Kane, T.R. "Attitude stability of earth-pointing satellites." Amer. Inst. of Aero. and Astro. Guidance and Control Conference, August 24-26, 1964, Los Angeles, California.

3.5. Struble, Raimond A. Nonlinear differential equations. New York, McGraw-Hill, 1962. p. 221-235.

3.6. Hsu, C.S. "On the parametric excitation of a dynamic system having multiple degrees of freedom." J. Appl. Mech., 30:367-372, September, 1963.

3.7. Paul, B., J.W. West and E.Y. Yu. "A passive gravitational attitude control system for satellites." Bell System Technical Journal, 42:2195-2237, September, 1963.

3.8. Zajac, E.E. "The Kelvin-Tait-Chetaev theorem and extensions." J. Astro. Sci., 11:46-49, Summer, 1964.

3.9. Thomson, William T. "Spin stabilization of attitude against gravity torque." J. Astro. Sci., 9:31-33, 1956.

4.1. Den Hartog, J.P. Mechanical vibrations. 4th ed. New York, McGraw-Hill, 1956, p. 227-228.

4.2. Bisshopp, K.E. and D.C. Drucker. "Large deflection of cantilever beams." Quarterly of Applied Mathematics, 3-272, 1954.

4.3. Stone, Robert G. "RAE - 1500-ft. antenna satellite." Astronautics and Aeronautics, 3:46-49, March, 1965.

4.4. Mitchell, T.P. "The nonlinear bending of thin rods." J. Appl. Mech., 26:40-43, March, 1959.

5.1. Garber, T.B. "A preliminary investigation of the motion of a long, flexible wire in orbit." Rand Corporation Report, RM-2705-ARPA, March 23, 1961.

5.2. Thomson, William T. Vibration theory and applications. Englewood Cliffs, New Jersey, Prentice-Hall, 1965. p. 307.

5.3. Felgar, R.P. "Formulas for integrals containing characteristic functions of a vibration beam." University of Texas Bureau of Engineering Research, Circular No. 14, 1950.

5.4. Pringle, R., Jr. "On the capture, stability and passive damping of artificial satellites." Stanford University Department of Aeronautics and Astronautics Report, SUDAER 81, April, 1964.

5.5. McLachlan, N.W. Theory and application of Mathieu functions. London, England, Oxford University Press, 1947. p. 97.

5.6. Handbook of mathematical functions, AMS55. Washington, D.C., National Bureau of Standards, 1964.

A. 1. Roberson, R. E. "Gravitational torque on a satellite vehicle." J. Franklin Inst., 265:13-22, January, 1958.

C. 1. Coddington, Earl A. and Norman Levinson. Theory of ordinary differential equations. New York, McGraw-Hill, 1955. p. 78-80.

C. 2. Cesari, Lamberto. Asymptotic behavior and stability problems in ordinary differential equations. New York, Academic Press, 1963. p. 55-59.

Appendix A. Forces and Torques Produced by the Gravitational Gradient

In this appendix, the forces and torques exerted by the earth's gravitational field on a satellite are derived for use in the body of the dissertation. The derivation is straightforward, and appears in the literature (Reference A. 1 for example). It is included for completeness and to maintain some consistency in notation.

A. 1 Coordinate System

The coordinate system is that of Figures 3. 1 and 3. 2 of the text, repeated here as figures A. 1 and A. 2.

The axes B_i are referred to a rotating frame O_i through angles θ_i shown in Figure B. 2. O_i are defined as follows:

O_1 is tangent to the circular orbit, pointing in the direction of motion

O_2 is normal to the orbit with the opposite sense to the orbit angular velocity

O_3 is directed downward, completing the right-hand triad.

The noninfinitesimal rotations θ_i are taken in the sequence θ_3, θ_2, θ_1.

B_i can be considered loosely as fixed in the satellite body; their precise definition is given separately in each chapter of the body of the dissertation.

A. 2 Gravitational Force on a Mass Point

Consider the system of Figure A. 3. The mass center of a general system of mass particles moves in circular orbit about a spherical earth. The position of a general mass point is denoted by the vector

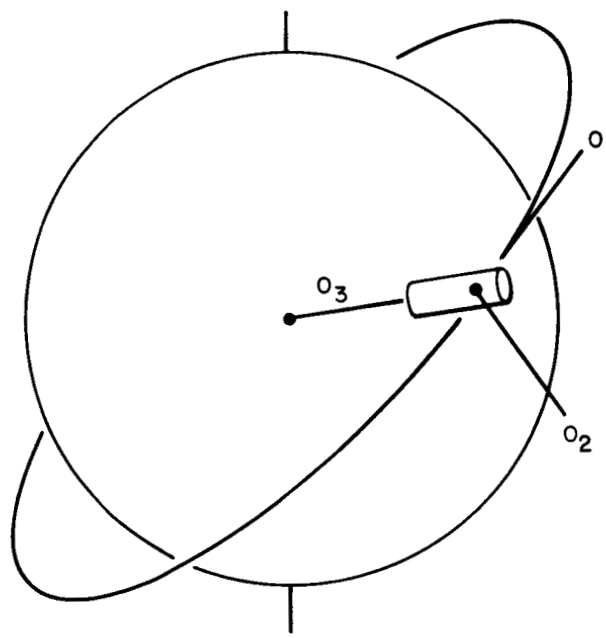

Figure A.1. Orbit Reference Coordinate System

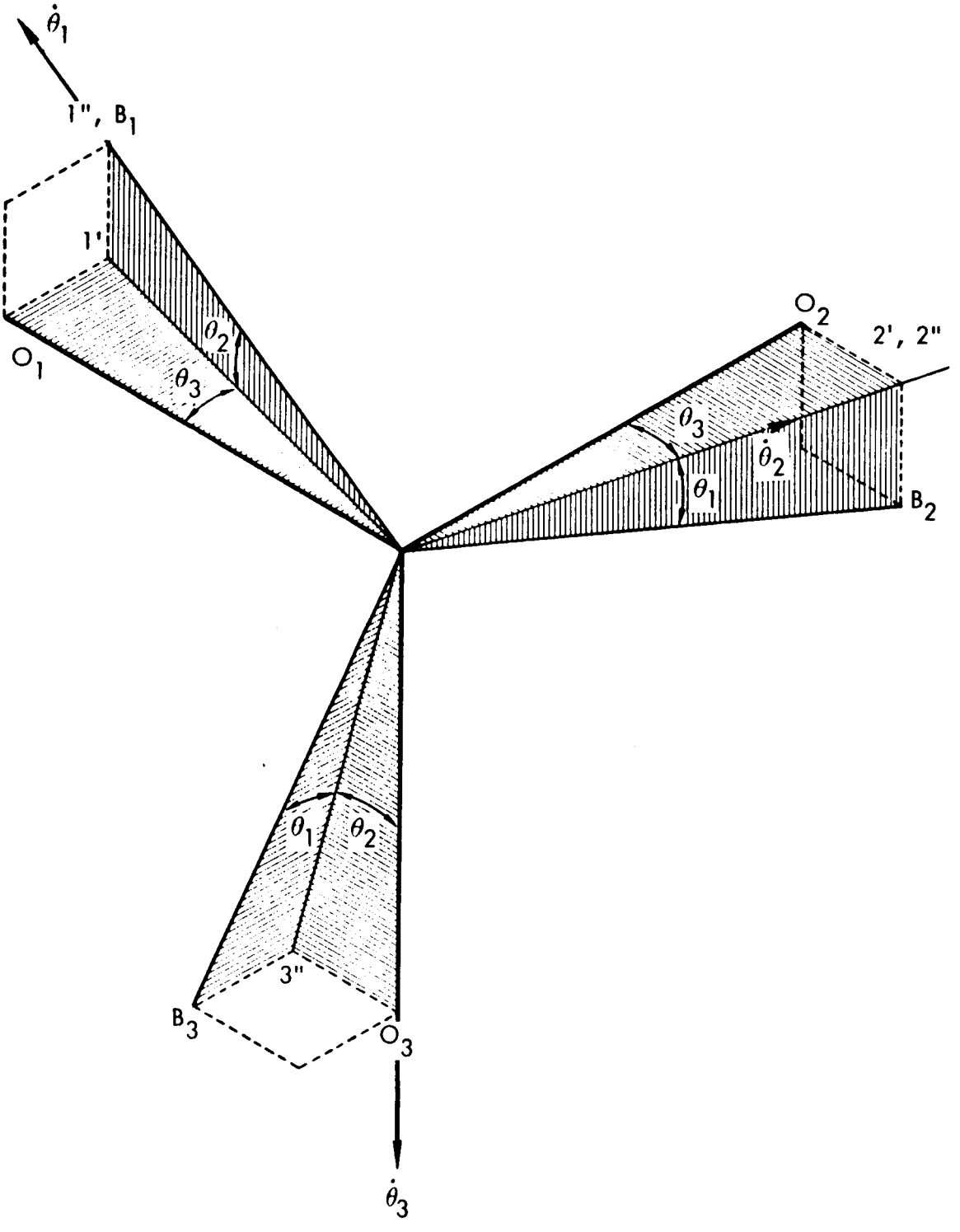

Figure A.2. Rotations Defining Body Coordinates

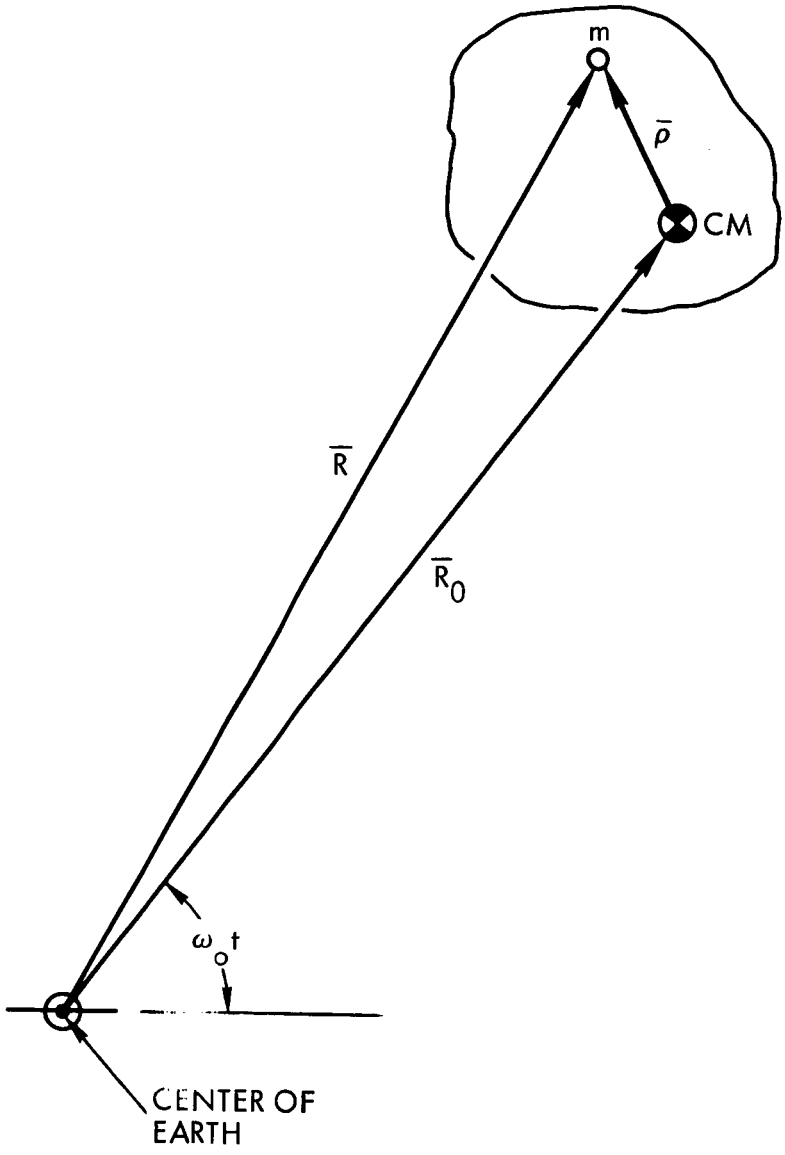

Figure A.3. Definition of Coordinate Vectors

$\overline{R}$ measured from the center of the earth. $\overline{R}_o$ denotes the position of the mass center, and $\overline{\rho}$ is the vector location of the mass point relative to the center of mass.

Newton's law of gravitation gives the gravitational force on a mass m as

$$\overline{F}_g = \frac{-mK\overline{R}}{R^3} = \frac{-mK(\overline{R}_o + \overline{\rho})}{|\overline{R}_o + \overline{\rho}|^3} \tag{A-1}$$

where

R is the scalar magnitude of $\overline{R}$

K is the gravitational constant for the earth

$|\ |$ denotes the scalar magnitude of a vector

For $\overline{R} \gg \overline{\rho}$, expanding by the binomial theorem, we find

$$\overline{F}_g = \frac{-mK}{R_o^3}\left\{1 - \frac{3\rho^2}{2R_o^2} - \frac{3(\overline{R}_o \cdot \overline{\rho})}{R_o^2} + \frac{15}{2}\frac{(\overline{R}_o \cdot \overline{\rho})^2}{R_o^4} + O\left[(\rho/R_o)^3\right]\right\}(\overline{R}_o + \overline{\rho}) \tag{A-2}$$

Parametrizing in the coordinate system of Figure A.2, we put

$$\overline{\rho} = x_1\hat{B}_1 + x_2\hat{B}_2 + x_3\hat{B}_3 \tag{A-3}$$

where the $\hat{B}_i$ are unit vectors along the respective axes B_i. From Figure A.2

$$\overline{R}_o = R_o\left(\hat{B}_1 \sin\theta_2 - \hat{B}_2 \cos\theta_2 \sin\theta_1 - \hat{B}_3 \cos\theta_2 \cos\theta_1\right) \tag{A-4}$$

Substitution of Equations (A-3) and (A-4) into (A-2) gives the components of $\overline{F}_g$ along $\hat{B}_i$. The expression for $\overline{F}_g$ is only needed in the body of the dissertation for the special case

$$\theta_1 = \theta_3 = 0$$

in which case

$$\overline{F}_g = \frac{-mK}{R_o^3}\left[1 - \frac{3(x_1 \sin\theta_2 - x_3 \cos\theta_2)}{R_o}\right]$$

$$\cdot\left[(x_1 + R_o \sin\theta_2)\hat{B}_1 + x_2\hat{B}_2 + (x_3 - R_o \cos\theta_2)\hat{B}_3\right]$$

to first order in the small quantity

$$\left(\frac{\text{body length}}{\text{orbit radius}}\right)$$

For the assumed circular orbit

$$\frac{K}{R_o^3} = \omega_o^2$$

so

$$F_g = -\omega_o^2\left[1 - \frac{3(x_1 \sin\theta_2 - x_3 \cos\theta_2)}{R_o}\right]$$

$$\cdot\left[(R_o \sin\theta_2 + x_1)\hat{B}_1 + x_2\hat{B}_2 + (x_3 - R_o \cos\theta_2)\hat{B}_3\right] \qquad \text{(A-5)}$$

This expression is used in Section 5.4, Chapter 5.

A.3 Inertial Acceleration of a Point Fixed in an Orbiting Satellite

In the notation of the preceding section, let B_i be the principal axes of an orbiting body, and assume that there is no relative motion between parts of the body, and that

$$\theta_1 = \theta_2 = \theta_3 = 0$$

The body then rotates with angular velocity

$$\bar{\omega} = -\omega_o \hat{B}_2$$

The inertial acceleration of a point located by

$$\bar{R} = \bar{R}_o + \bar{\rho}$$

is then

$$\bar{a} = \bar{\omega} \times (\bar{\omega} \times \bar{R})$$

or, in component form

$$\bar{a} = -\omega_o^2 x_1 \hat{B}_1 + \omega_o^2 (R_o - x_3) \hat{B}_3 \qquad \text{(A-6)}$$

A.4 Static Internal Forces in an Orbiting Body

As in Section A.3, consider that the satellite is moving in circular orbit, with no motion relative to axes B_i, and with $\theta_i = 0$. Then the equation of motion of a mass point m is

$$\bar{F}_g + \bar{F}_c = m\bar{a} \qquad \text{(A-7)}$$

where

$\bar{F}_g$ is the gravitational force

$\bar{a}$ is the inertial acceleration of the point

$\bar{F}_c$ is the internal constraint force exerted on the mass point by the rest of the body

Setting $\theta_2 = 0$ and substituting Equations (A-5) and (A-6) into Equation (A-7), we obtain expressions for the components of F_c. Neglecting second-order terms

$$\bar{F}_c = m\omega_o^2 \left(x_2 \hat{B}_2 - 3x_3 \hat{B}_3 \right) \qquad \text{(A-8)}$$

This expression is used in Chapter 4.

A.5 Gravitational Torque on a Rigid Body

In the notation of the previous sections, the torque exerted by the earth's gravity field about the satellite mass center is given by

$$\overline{L} = \sum_{1}^{3} L_i \hat{B}_i = \int \overline{\rho} \times \overline{F}_g \, dm \tag{A-9}$$

where the integral is taken over the mass of the orbiting body. Substituting from Equation (A-1) and noting that

$$\int \overline{\rho} \, dm = 0$$

from the definition of $\overline{\rho}$, we obtain

$$\overline{L} = \frac{3K}{R_o^5} \int (\overline{\rho} \times \overline{R}_o)(\overline{\rho} \cdot \overline{R}_o) \, dm \tag{A-10}$$

correct to the first power of

$$\left(\frac{\text{body length}}{\text{orbit radius}} \right)$$

Expressions for $\overline{\rho}$ and $\overline{R}_o$ are available in Equations (A-3) and (A-4). Let us assume that $\hat{B}_i$ are principal axes, so that

$$\int x_i x_j \, dm = 0 \qquad i \neq j \tag{A-11}$$

The moments of inertia of the rigid body are defined by

$$I_i = \int \left(x_j^2 + x_k^2 \right) dm \quad \begin{cases} i \neq j \neq k, \\ i, j, k = 1, 2, 3 \end{cases} \tag{A-12}$$

Substitution of Equations (A-3) and (A-4) into Equation (A-10) and use of Equations (A-11) and (A-12) yields

$$L_1 = \frac{3K}{2R_o^3}(I_3 - I_2) \sin 2\theta_1 \cos^2 \theta_2$$

$$L_2 = \frac{3K}{2R_o^3}(I_3 - I_1) \sin 2\theta_2 \cos \theta_1$$

$$L_3 = \frac{3K}{2R_o^3}(I_1 - I_2) \sin 2\theta_2 \sin \theta_1 \qquad \text{(A-13)}$$

giving gravitational torques as functions of the attitude angles. These expressions are used in Appendix B to derive equations of motion for Chapter 3.

Appendix B. Derivation of Equations of Motion for Rigid and Flexible Gravity-Gradient Satellites

In this appendix, the equations of motion used in Chapter 3 of the text are derived. The angular momentum principle is used in the derivation given, but all equations have been checked independently by the method of Lagrange's equations. The derivation is straightforward; the only complication is that the pitch angle θ_2 must be retained as a large angle for use in the stability studies of Section 3.3.

It is convenient to proceed by deriving the equations for the two-part flexible satellite of Sections 3.2 and 3.3, digressing at a suitable point to provide the equations needed for the rigid satellite of Section 3.1.

The coordinate system for the two-part satellite is shown in Figure 3.8, reproduced here as Figure B.1. The composite body is made up of two rigid bodies, a main body B and a subsidiary body B^*. The rigid bodies have moments of inertia I_i, I_i^* about principal axes B_i, B_i^*, defined so that B_i coincide with B_i^* when the elastic coordinate α is zero.

The axes B_i are referred to the local-vertical O_1, O_2, O_3 coordinate system through the angles θ_1, θ_2, θ_3 defined in Appendix A.

We adopt the convention that components of vector quantities pertaining to body B^*, carrying the asterisk superscript, are always referred to axes B_i^*. Components of vector quantities pertaining to body B carry no superscript and are referred to axes B_i.

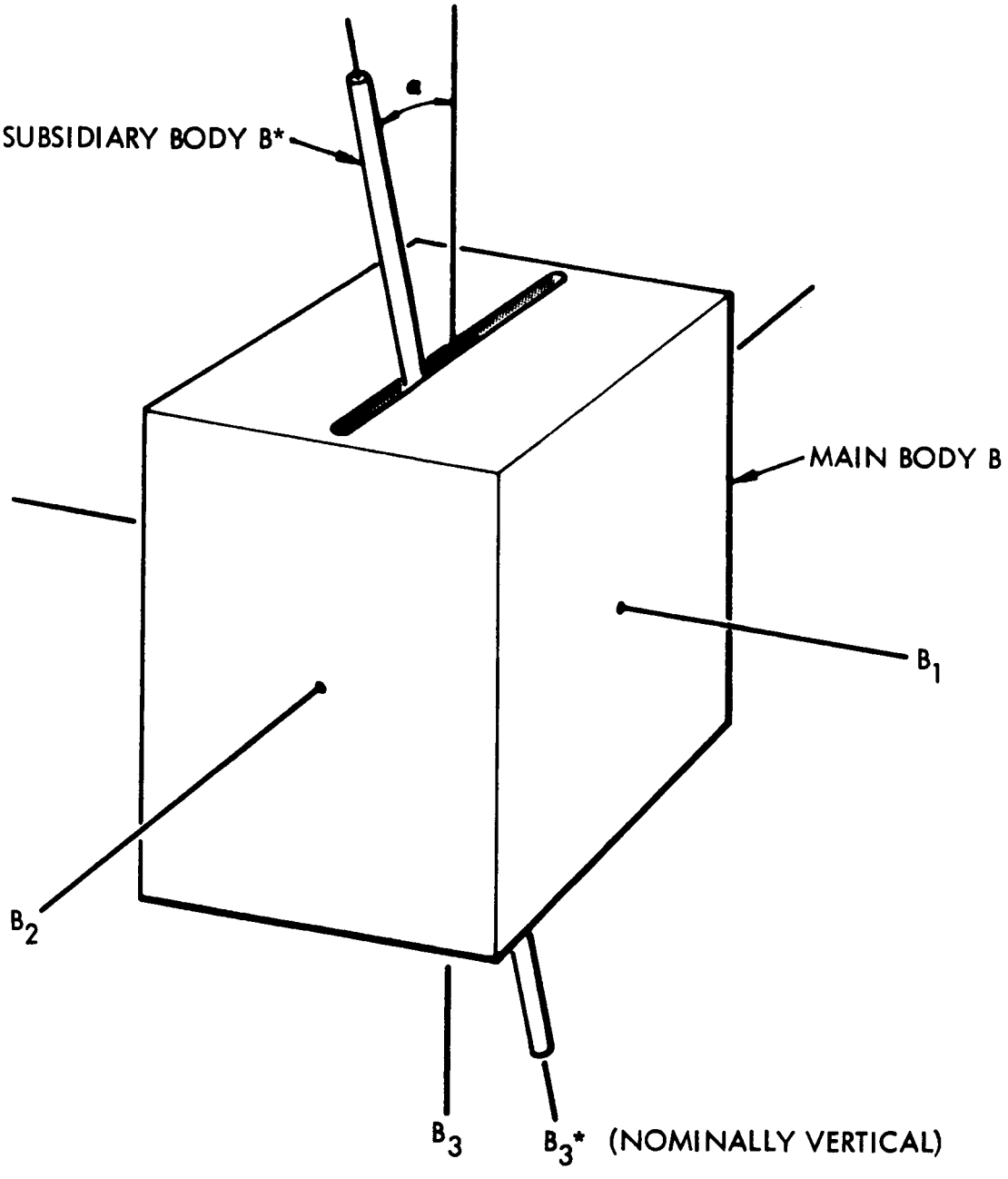

Figure B.1. Configuration for Study, Rigid Body B Coupled to Rigid Body B^* Through Hinge Along Axis B_1

B.1 Terminology

We define the following terminology:

L_i	Components of gravitational moment on B, along B_i
L_i^*	Components of gravitational moment on B^*, along B_i^*
M_i	Components of torque exerted by B^* on B
M_i^*	Components of torque exerted by B on B^*
ω_i, ω_i^*	Components of body angular velocity
I_i, I_i^*	Principal moments of inertia
I_i'	$I_i + I_i^*$
k	Stiffness of torsional spring between B and B^*
c	Angular damping constant of damper between B and B^* (dimensions are those of torque divided by angular rate)

B.2 Dynamical Equations of Motion

The dynamical equations of motion for the two bodies (Euler's Equations), are

$$I_1\dot{\omega}_1 - (I_2 - I_3)\omega_2\omega_3 = L_1 + M_1 \qquad \text{(B-1a)}$$

$$I_2\dot{\omega}_2 - (I_3 - I_1)\omega_3\omega_1 = L_2 + M_2 \qquad \text{(B-1b)}$$

$$I_3\dot{\omega}_3 - (I_1 - I_2)\omega_1\omega_2 = L_3 + M_3 \qquad \text{(B-1c)}$$

$$I_1^*\dot{\omega}_1^* - \left(I_2^* - I_3^*\right)\omega_2^*\omega_3^* = L_1^* + M_1^* \qquad \text{(B-2a)}$$

$$I_2^*\dot{\omega}_2^* - \left(I_3^* - I_1^*\right)\omega_3^*\omega_1^* = L_2^* + M_2^* \qquad \text{(B-2b)}$$

$$I_3^*\dot{\omega}_3^* - \left(I_1^* - I_2^*\right)\omega_1^*\omega_2^* = L_3^* + M_3^* \qquad \text{(B-2c)}$$

B.3 Kinematical Equations of Motion

The body rates ω_i may be expressed in terms of the angular rates $\dot{\theta}_i$ by reference to Figure A.2, remembering that the O_i system rotates with angular velocity $-\omega_o$ about O_2. To first order in θ_1, θ_3, $\dot{\theta}_1$, $\dot{\theta}_3$, they are

$$\omega_1 = \dot{\theta}_1 - \sin\theta_2\dot{\theta}_3 - \omega_o\cos\theta_2\theta_3$$

$$\omega_2 = \dot{\theta}_2 - \omega_o$$

$$\omega_3 = \cos\theta_2\dot{\theta}_3 - \dot{\theta}_2\theta_1 - \omega_o\sin\theta_2\theta_3 + \omega_o\theta_1 \qquad \text{(B-3)}$$

The angular rates of B^*, for small θ_1, θ_2, α, differ from those of B by the relative rotation α and also because the components are taken along different axis systems. They are

$$\omega_1^* = \omega_1 + \dot{\alpha}$$

$$\omega_2^* = \omega_2$$

$$\omega_3^* = \omega_3 - \dot{\theta}_2\alpha + \omega_o\alpha \qquad \text{(B-4)}$$

B.4 Gravity Torques

The gravity torques L_i on B_i are obtained by taking θ_1 and θ_3 to be small angles in Equations (A-13). They are

$$\begin{bmatrix} L_1 \\ L_2 \\ L_3 \end{bmatrix} = \frac{K}{R_o^3} \begin{bmatrix} (I_3 - I_2) \cos^2 \theta_2 \theta_1 \\ -(I_1 - I_3) \sin \theta_2 \cos \theta_2 \\ -(I_2 - I_1) \sin \theta_2 \cos \theta_2 \theta_1 \end{bmatrix} \qquad \text{(B-5)}$$

where K, R_o are as defined in Appendix A.

$$\frac{K}{R_o^3} = \omega_o^2$$

The gravity torques L_i^* on B_i^* can be obtained directly from Equations (B-5) by putting

$$I_i \longrightarrow I_i^*$$

$$\theta_1 \longrightarrow \theta_1 + \alpha$$

The latter relation is only valid because θ_1 is the third rotation in the sequence, so that, if the θ_i described the rotation of B_i^* instead of B_i, θ_2 and θ_3 would have the same values. We obtain

$$\begin{bmatrix} L_1^* \\ L_2^* \\ L_3^* \end{bmatrix} = 3\omega_o^2 \begin{bmatrix} \left(I_3^* - I_2^*\right) \cos^2 \theta_2 (\theta_1 + \alpha) \\ -\left(I_1^* - I_3^*\right) \sin \theta_2 \cos \theta_2 \\ -\left(I_2^* - I_1^*\right) \sin \theta_2 \cos \theta_2 (\theta_1 + \alpha) \end{bmatrix} \qquad \text{(B-6)}$$

B.5 Constraint Relations

The constraint moments M_i, M_i^* are not independent, but are related by action and reaction. First, we have

$$M_1 = -M_1^* = k\alpha + c\dot{\alpha} \tag{B-7}$$

giving the spring and damper torques about axis B_1.

Equating constraint moments about axes B_2 and B_3 gives, for small α,

$$M_2 = -M_2^* + M_3^*\alpha$$

$$M_3 = -M_3^* - M_2^*\alpha \tag{B-8}$$

B.6 Derivation of Equations

Adding Equations (B-1) and (B-2) two by two, and substituting from Equations (B-3), (B-4), (B-5), and (B-6) we obtain three second-order equations in the four variables, θ_1, θ_2, θ_3, α. We retain θ_2 as a large angle, but keep only first-order terms in θ_1, θ_2 and θ_3.

The resulting equations contain the constraint moments only in the form

$$M_2 + M_2^* = M_3^*\alpha$$

$$M_3 + M_3^* = -M_2^*\alpha$$

Equation (B-2c) shows that $M_3^*\alpha$ is second order, but $M_2^*\alpha$ must be retained and can be evaluated from Equation (B-2b) as

$$M_2^*\alpha = \alpha\left[I_2^*\ddot{\theta}_2 + 3\omega_o^2\left(I_1^* - I_3^*\right)\sin\theta_2\cos\theta_2\right]$$

Speaking loosely, the three equations obtained describe the motion of the non-rigid system as a whole. To complete the description of

the motion, we must consider the moments acting on one of the rigid bodies separately. A suitable choice is Equation (B-1a). Substituting from Equations (B-3), (B-5) and (B-7) into Equation (B-1a) we obtain a fourth independent second-order equation. Summarizing the results of the above operations, the equations of motion are, in order

$$I_1'\left[\ddot{\theta}_1 - \sin\theta_2\ddot{\theta}_3 - \left(\dot{\theta}_2 + \omega_o\right)\cos\theta_2\dot{\theta}_3 + \omega_o \sin\theta_2\dot{\theta}_2\theta_3\right]$$

$$+ \left(I_3' - I_2'\right)\left[\left(\dot{\theta}_2 - \omega_o\right)\left(\cos\theta_2\dot{\theta}_3 - \dot{\theta}_2\theta_1 - \omega_o \sin\theta_2\theta_3 + \omega_o\theta_1\right) - 3\omega_o^2 \cos^2\theta_2\theta_1\right]$$

$$+ I_1^*\ddot{a} - 3\omega_o^2\left(I_3^* - I_2^*\right)\cos^2\theta_2 a + \left(I_2^* - I_3^*\right)\left(\dot{\theta}_2 - \omega_o\right)^2 a = 0 \qquad \text{(B-9a)}$$

$$I_2'\ddot{\theta}_2 + \left(I_1' - I_3'\right)\cdot 3\omega_o^2 \sin\theta_2\cos\theta_2 = 0 \qquad \text{(B-9b)}$$

$$I_3'\left(\cos\theta_2\ddot{\theta}_3 - \dot{\theta}_2 \sin\theta_2\dot{\theta}_3 - \ddot{\theta}_2\theta_1 - \dot{\theta}_2\dot{\theta}_1 - \omega_o \cos\theta_2\dot{\theta}_2\theta_3 - \omega_o \sin\theta_2\dot{\theta}_3 + \omega_o\dot{\theta}_1\right)$$

$$+ \left(I_2' - I_1'\right)\left[\left(\dot{\theta}_2 - \omega_o\right)\left(\dot{\theta}_1 - \sin\theta_2\dot{\theta}_3 - \omega_o \cos\theta_2\theta_3\right) + 3\omega_o^2 \sin\theta_2\cos\theta_2\theta_1\right]$$

$$- \left(I_1^* - I_2^*\right)\left[\left(\dot{\theta}_2 - \omega_o\right)\dot{a} + 3\omega_o^2 \sin\theta_2\cos\theta_2 a\right] - I_3^*\ddot{\theta}_2 a$$

$$- I_3^*\left(\dot{\theta}_2 - \omega_o\right)\dot{a} + aI_2^*\ddot{\theta}_2 + 3\omega_o^2\left(I_1^* - I_3^*\right)\sin\theta_2\cos\theta_2 a = 0 \qquad \text{(B-9c)}$$

$$I_1\left(\ddot{\theta}_1 - \sin\theta_2\ddot{\theta}_3 - \dot{\theta}_2\cos\theta_2\dot{\theta}_3 - \omega_o\cos\theta_2\dot{\theta}_3 + \omega_o\sin\theta_2\dot{\theta}_2\theta_3\right)$$

$$+\left(I_3 - I_2\right)\left\{\left(\dot{\theta}_2 - \omega_o\right)\left[\cos\theta_2\dot{\theta}_3 - \left(\dot{\theta}_2 - \omega_o\right)\theta_1 - \omega_o\sin\theta_2\theta_3\right]\right.$$

$$\left. - 3\omega_o^2\cos^2\theta_2\theta_1\right\} - ka - c\dot{a} = 0 \qquad \text{(B-9d)}$$

B.7 Simplification

Equations (B-9) are the general equations for the two-body satellite, for large θ_2. They are simplified somewhat in the particular case under consideration, for which

$$I_1^* = I_1$$

$$I_2^* = I_1$$

$$I_3^* = 0 \qquad \text{(B-10)}$$

For reasons given in Section 3.2.1.

We further simplify the form by introducing quantities K_i, defined by

$$K_1 = \frac{I_1' - I_2'}{I_3'} = \frac{I_1 - I_2}{I_3}$$

$$K_2 = \frac{I_2' - I_3'}{I_1'} = \frac{I_2 + I_1 - I_3}{2I_1} \qquad \text{(B-11)}$$

and the dimensionless natural frequency and damping rate of the elastic mode, given by

$$\omega_n^2 = \frac{2k}{I_1\omega_o^2}$$

$$\zeta\omega_n = \frac{c}{I_1\omega_o}$$

It is usually convenient to put the equations in the form

$$\ddot{\theta}_j = G_j(\theta_i,\ \dot{\theta}_i,\ a,\ \dot{a}) \quad ,\quad j = 1 \cdots 3$$

$$\ddot{a} = G_4(\theta_i,\ \dot{\theta}_i,\ a,\ \dot{a})$$

which can be achieved by algebraic recombination of Equations (B-9). The transformation is valid only for

$$\theta_2 \neq \frac{\pi n}{2} \quad ,\quad n \text{ odd}$$

The result is

$$\begin{aligned}
\ddot{\theta}_1 = &\left\{2K_2 \cos\theta_2(\dot{\theta}_2 - \omega_o) + 2\omega_o \cos\theta_2 - \frac{\sin^2\theta_2}{\cos\theta_2}\left[(\dot{\theta}_2 - \omega_o)K_1 - \dot{\theta}_2 - \omega_o\right]\right\}\dot{\theta}_3 \\
&+ \left[\omega_o \sin\theta_2(\dot{\theta}_2 - \omega_o)(-2K_2 + 1 - K_1)\right]\theta_3 \\
&+ \left[\tan\theta_2(\dot{\theta}_2 - \omega_o)(K_1 + 1)\right]\dot{\theta}_1 \\
&+ \left\{\tan\theta_2\left(\ddot{\theta}_2 + 3\omega_o^2 K_1 \sin\theta_2 \cos\theta_2\right)\right. \\
&\qquad \left. + (1 - 2K_2)\left[\left(\dot{\theta}_2 - \omega_o\right)^2 + 3\omega_o^2 \cos^2\theta_2\right]\right\}\theta_1 \\
&+ (\zeta\omega_n\omega_o)\dot{a} + \left[\frac{\omega_n^2\omega_o^2}{2} - \frac{\tan\theta_2}{2}\left(\frac{1 + K_1}{1 - K_2}\right)\ddot{\theta}_2 + 3\omega_o^2 \sin\theta_2 \cos\theta_2\right]a
\end{aligned} \tag{B-12a}$$

$$\ddot{\theta}_2 + 3\omega_o^2\left(\frac{K_1 + K_2}{1 + K_1K_2}\right)\sin\theta_2 \cos\theta_2 = 0 \tag{B-12b}$$

$$\ddot{\theta}_3 = \left\{\tan\theta_2\left[\dot{\theta}_2 + \omega_o - K_1(\dot{\theta}_2 - \omega_o)\right]\right\}\dot{\theta}_3$$

$$+ \left\{\omega_o\left[\dot{\theta}_2 - (\dot{\theta}_2 - \omega_o)K_1\right]\right\}\theta_3 + \left[\frac{(\dot{\theta}_2 - \omega_o)(K_1 + 1)}{\cos\theta_2}\right]\dot{\theta}_1$$

$$+ \left[-\frac{K_2}{\cos\theta_2}\frac{(1 + K_1)}{(1 - K_2)}\left(\ddot{\theta}_2 + 3\omega_o^2 \sin\theta_2 \cos\theta_2\right)\right]\theta_1$$

$$+ \left[-\frac{1}{2\cos\theta_2}\left(\frac{1 + K_1}{1 - K_2}\right)\left(\ddot{\theta}_2 + 3\omega_o^2 \cos\theta_2 \sin\theta_2\right)\right]a \qquad \text{(B-12c)}$$

$$\ddot{a} = \left[2(\dot{\theta}_2 - \omega_o)(1 - K_2)\cos\theta_2\right]\dot{\theta}_3 + \left[2\omega_o \sin\theta_2(\dot{\theta}_2 - \omega_o)(K_2 - 1)\right]\theta_3$$

$$+ \left\{2(K_2 - 1)\left[(\dot{\theta}_2 - \omega_o)^2 + 3\omega_o^2 \cos^2\theta_2\right]\right\}\theta_1$$

$$+ (-2\zeta\omega_n\omega_o)\dot{a} + \left[-(\dot{\theta}_2 - \omega_o)^2 - 3\omega_o^2 \cos^2\theta_2 - \omega_n^2\omega_o^2\right]a \qquad \text{(B-12d)}$$

B.8 Final Forms

Equations (B-12) can be recast in various forms depending on their use in the text.

B.8.1 Linearized Dimensionless Form

By considering θ_2 as a small angle and neglecting its products with θ_1, θ_3 and derivations in Equations (B-12), and introducing $\tau = \omega_o t$ as a new variable, we obtain the linearized dimensionless form given in Equations (3.2-1) and (3.2-2) of the text.

B.8.2 Linearized Symmetric Form

A more symmetric form is obtained by re-eliminating the K-parameters from Equations (3.2-1) and (3.2-2) and introducing the new variable

$$\beta = \theta_1 + \alpha$$

(the roll angle of B^*) to replace α. The result is Equations (3.2-18) of the text, in which the time variable is again t rather than $\omega_o t$.

B.8.3 Form for Floquet Analysis

For numerical work using Kane's Floquet theory technique (Appendix C) we define a column vector ($\underset{\sim}{x}$) by

$$x_1 = \theta_1 \qquad x_4 = \dot{\theta}_1$$

$$x_2 = \theta_3 \qquad x_5 = \dot{\theta}_3$$

$$x_3 = \alpha \qquad x_6 = \dot{\alpha}$$

Then Equations (B-11) can be rewritten in first-order form as

$$\frac{d(\underset{\sim}{x})}{dt} = \left[W(y, z, K_1, K_2, \zeta, \omega_n)\right](\underset{\sim}{x}) \qquad \text{(B-13)}$$

with the auxiliary equations

$$\dot{y} = z$$

$$\dot{z} = -3\left(\frac{K_1 + K_2}{1 + K_1 K_2}\right)\omega_o^2 \sin y$$

$$y = 2\theta_2 \qquad \text{(B-14)}$$

Equations (B-12) and (B-13) are in the form required for the Floquet theory technique. Terms involving θ_2 can be eliminated from the matrix $[W]$ by using Equations (B-14).

B.8.4 Equations for a Single Rigid Body

The equations for a single rigid body are most readily obtained by putting $k = c = 0$ in the symmetric form, Equations (3.2-18).

This yields Equations (3.1-4) of the text. To derive equations in which the gravity torque is represented explicitly, we substitute Equations (B-3) into Equations (B-1), neglect high-order terms, and set the constraint moment to zero, yielding Equation (3.1-1) of the text.

Appendix C. Results from Floquet Theory

In this appendix we summarize some of the well-known properties of linear differential equations with periodic coefficients, drawing principally from References C.1 and C.2. Such systems have the form

$$(\dot{\underset{\sim}{x}}) = [A(t)](\underset{\sim}{x}) \tag{C-1}$$

where

$(\dot{\underset{\sim}{x}})$ is a coordinate vector of n dimensions

$[A(t)]$ is an n-dimensional square matrix whose coefficients are periodic in t, with period T

Equations (B-11) of Appendix B, after the modifications indicated in Section B.8.3, have the form of Equation (C-1).

C.1 Basis of Floquet Theory Technique

It is well known that Equations (C-1) have n linearly independent solutions. A square matrix $[X]$ whose columns are linearly independent solutions of Equation (C-1) is called a fundamental matrix for Equation (C-1) and satisfies

$$[\dot{X}] = [A(t)][X] \tag{C-2}$$

Since the columns are linearly independent, the determinant

$$\det\left([X]\right) \neq 0 \tag{C-3}$$

Conversely, any matrix satisfying Equations (C-2) and (C-3) is a fundamental matrix whose columns are independent solutions.

Premultiplication of Equation (C-2) by a nonsingular constant matrix $[L]$ yields

$$[\dot{Y}] = [A(t)][Y] \tag{C-4}$$

$$[Y] = [X][L] \tag{C-5}$$

$$\det\left([Y]\right) \neq 0$$

So $[Y]$ is also a fundamental matrix and any two fundamental matrices $[X]$, $[Y]$ are related through Equation (C-5), for some $[L]$.

If $[X(t)]$ is a fundamental matrix of Equation (C-1), then so is

$$[X_1(t)] \stackrel{\text{Def}}{=} [X(t + T)] \tag{C-6}$$

because

$$[\dot{X}_1(t)] = [\dot{X}(t + T)] = [A(t + T)][X(t + T)] = [A(t)][X_1(t)] \tag{C-7}$$

using Equation (C-1). The fact that

$$\det\left([X_1]\right) \neq 0$$

can be proved easily but also follows from the obvious fact that a set of independent solutions of Equation (C-1) are still independent after a translation in time.

Equation (C-5) says that the fundamental matrix $[X_1]$ is related to the fundamental matrix $[X]$ through

$$[X_1] = [X][M] \tag{C-8}$$

$$[X(t + T)] = [X][M] \tag{C-9}$$

for some nonsingular constant $[M]$, and that

$$[X] = [Y][L]^{-1}$$

for another nonsingular constant $[L]$ and an arbitrary fundamental matrix $[Y]$. Thus we have, from Equation (C-9),

$$[Y(t + T)][L]^{-1} = [Y(t)][L]^{-1}[M]$$

$$[Y(t + T)] = [Y(t)][L]^{-1}[M][L] \qquad (C-10)$$

Where $[L]$ can be chosen arbitrarily as long as it is nonsingular.

If $[L]$ can be chosen to make

$$[L]^{-1}[M][L]$$

a diagonal matrix, the solution columns ($\underset{\sim}{y}_i$) of $[Y]$ will have the useful property

$$[\underset{\sim}{y}_i(t + T)] = \lambda_i[\underset{\sim}{y}(t)] \qquad (C-11)$$

where the λ_i (called characteristic multipliers) are eigenvalues of $[M]$. The ($\underset{\sim}{y}_i$) are then called <u>normal solutions</u>.

$$|\lambda_i| > 1$$

then means there is a solution of Equation (C-1) which grows with time and is therefore unstable. An arbitrary set of initial conditions on Equation (C-1) will, in general, lead to a nonzero initial condition on the unstable solution and the whole system will grow without bound.

The constant matrix $[M]$ is nonsingular by hypothesis and can always be diagonalized as long as its eigenvalues are distinct, which is invariably the case in practice. In the very special case of repeated eigenvalues, it may be shown (Reference C. 2) that the system is stable if, for the repeated roots λ_j, either $|\lambda_j| < 1$ or if $|\lambda_j| = 1$, $m = n - r$ where m is the multiplicity of the eigenvalue, n is the order of $[M]$, and r is the rank of $[M]$.

C. 2 Kane's Numerical Implementation of Floquet Theory

Equation (C-11) shows that the stability behavior of Equation (C-1) for all time can be determined from its behavior over a single period of the coefficients. Analytical determination of the λ_i is difficult even for systems of order as low as two. Kane's procedure is to integrate each column of Equations (C-1) over time T, starting with initial con-condition

$$[X(0)] = [I] \qquad (C-12)$$

The unit matrix. Then

$$[X(T)] = [X_1(0)] = [X(0)][M] = [M]$$

using Equations (C-8) and (C-12). The eigenvalues of $[X(T)]$ are then the characteristic multipliers. The determination of λ_i for the problem of Equations (B-11) and Section 3. 3 involves six numerical integrations of the six scalar equations (C-1), and determination of six eigenvalues. In the present problem, the integrations were performed on the IBM 7094* using the fourth-order Runge-Kutta integration formula.

In the case of interest, the elements of A(t) are not known explicitly but must be generated from the solutions of the pitch equation

$$\ddot{\theta}_2 + \frac{\omega_p^2}{2} \sin 2\theta_2 = 0$$

*The assistance of the Computing Facility of the University of California, Los Angeles, is gratefully acknowledged.

Rather than use the known elliptic-integral solution, it is convenient to integrate this equation numerically, generating the coefficients for Equation (C-1) in the same computer program.

C.3 Relation to Constant-Coefficient Solution

In the special case where $[A(t)]$ is constant, the solution of Equation (C-1) has the form

$$(\underset{\sim}{x}) = \sum_i (\underset{\sim}{C}_i) e^{s_i t} \quad , \quad (\underset{\sim}{C}_i) \text{ constants}$$

s_i are the characteristic roots of the system. The special normal solutions which repeat themselves in the sense of Equation (C-11) are then

$$(\underset{\sim}{y}_i) = (\underset{\sim}{C}_i') e^{s_i t}$$

and the characteristic multipliers are

$$\lambda_i = e^{s_i T} \tag{C-13}$$

where T, the period, can be any positive number. $|\lambda_i| > 1$ implies the familiar constant coefficient instability condition

$$\text{Real } (s_i) > 0$$

so that the Floquet theory procedure is a useful generalization of familiar constant-coefficient techniques to the case of periodic coefficients.